DETERMINATION OF RADIOLOGICAL HAZARD LEVELS OF GAMMMA RAYS FROM RADIONUCLIDES IN WATER FROM SELECTED BOREHOLES IN MOROTO DISTRICT, UGANDA

BY

OKELLO SAM

A DISSERTATION SUBMITED TO THE GRADUATE SCHOOL IN PARTIAL FULFILMENT OF THE REQUIREMENTS FOR THE AWARD OF THE DEGREE OF MASTER OF SCIENCE IN PHYSICS OF KYAMBOGO UNIVERSITY

MARCH 2021

DECLARATION

I Okello Sam do hereby declare that this Dissertation contains my own original research work and has not been submitted to any academic institution for an academic award.

Signed: ……..

Date: ……

APPROVAL

This dissertation by Okello Sam was carried out under our close supervision and guidance. The dissertation is hereby cleared to be presented to the Board of Examiners and Senate for the award of the degree of Master of Science in Physics of Kyambogo University with our due approval.

Signed: ……..

Supervisor 1: Oriada Richard

Date ……

Signed: ……

Supervisor 2: Enjiku Ben D.D

Date ……

DEDICATION

This dissertation is dedicated to my wife Mrs. Okello Esther.

ACKNOWLEDGEMENT

I would like to thank a number of people for the support that they rendered to me.

My sincere gratitude first goes to my supervisors Mr. Oriada Richard and Mr. Enjiku Ben D.D for their advice, encouragement and guidance that was instrumental and kept me on the right track from the start to the end. The lecturers in the Department of Physics deserve my sincere thanks for their support especially Associate Professor Edward Jurua who introduced me to Radiation Physics upon which my dissertation is based.

I am grateful to the Management of Radioisotope Laboratory, Makerere University for allowing me to use the facilities in the laboratory and above all to the staff for teaching me how to operate the NaI(Tl) gamma ray spectrometer. My special thanks goes to Dr. Kisolo for always being readily available to assist me whenever I would find challenges with the equipment.

I thank the retired Head Teacher of Teso College Aloet, Mr. Ocaatum Silvester for his kindness in granting me time to concentrate on my research. The staff members of Teso College Aloet especially my colleagues in the Department of Physics Mr. Ojangole George Francis, Mr. Atung Dominic, Mr. Kipruto Moses and Mr. Ejopu Enock deserve special mention for their support.

The Assistant District Water Engineer of Moroto District Local Government, Eng. Ayamo Judith for allowing me use their water sources for carrying out my research.

To the members of my family, my father Mr. Okello Nelson; my mother Mrs. Okello Martha, my brothers Mr. Omongin John Micheal, Mr. Omera Sam and Mr. Oluka Solomon, I express my gratitude for their financial, moral and spiritual guidance.

My wife Mrs. Okello Esther and my children Grace and Joseph certainly deserve my gratitude for their spiritual guidance and financial support from the start to the end of the study.

I would also like to thank my course mates, Mr. Aguma Patrick and Mr. Kigundu Javira for their academic and spiritual advice during the course of my work.

TABLE OF CONTENTS

LIST OF FIGURES

PAGE

LIST OF TABLES

PAGE

ABSTRACT

This study was designed to identify gamma ray emitting radionuclides using the GDM 20 NaI(Tl) detector and to determine and compare the activity concentrations, absorbed dose rates, annual effective dose equivalent and the internal and external radiological hazard levels of gamma rays from radionuclides in water from boreholes in four sub counties of Rupa, Katikekile, Nadunget and Northern Division of Moroto District.

The radionuclides of ^{226}Ra and ^{232}Th were found in water samples from all the boreholes of the four sub counties. The radionuclide of ^{40}K was only found in two boreholes, three boreholes and five boreholes of Rupa, Katikekile and Nadunget respectively. None was found in the boreholes from Northern Division. The activity concentration of ^{226}Ra exceeded the world average value of 35 Bql^{-1} in three boreholes of Rupa and Northern Division; in four boreholes of Katikekile and in all the seven boreholes of Nadunget. The activity concentration of ^{232}Th was found to be less than the world average of 30 Bql^{-1} in all the water samples from all the regions. The activity concentration of ^{40}K was found to exceed the world average of 400 Bql^{-1} in all the water samples from all the regions. The absorbed dose rates was found to be greater than the world average of 84 $nGyh^{-1}$ for water samples from two boreholes of Rupa and Northern Division; in five boreholes of Katikekile and in six boreholes of Nadunget. The annual effective dose equivalent was found to be lower than the world internal exposure limit of 0.41 $mSvy^{-1}$ in all the water samples analyzed. The internal radiological hazard level was found to exceed the permissible value of 1.00 (unity) only in one borehole and three boreholes in Katikekile and Nadunget respectively. The external radiological hazard level was found to exceeded the permissible limit in one borehole from Nadunget; and equal to 1.00 the permissible limit in one borehole from Katikekile.

However activity concentration of ^{226}Ra and ^{40}K exceeded the world average value in seventeen boreholes and ten boreholes respectively. While ^{232}Th activity concentrations in all boreholes were below the world average value. It is recommended that a similar study should be carried out to check the results of this study and to find the excess life time cancer risk on the populace that use the water especially those that show high activity and hazard levels. The scope of the study for later studies should be extended to more boreholes.

CHAPTER ONE: INTRODUCTION

1.1 Background of the Study

Uganda as a landlocked country occupies 241,550.7 km^2 of land of which open water and swamps occupy an area of 41,743.2 km^2 (United Nations World Water Agency Program; UN WWAP, 2006). The main sources of water in Uganda include lakes, rivers, swamps, springs, wells and rainfall, (Rugumayo et al., 2006). Water sources in Uganda are unevenly distributed in terms of size and type. Some districts lack large water bodies while others have large water bodies for various uses (Nsubuga et al., 2014). However there are regions in Uganda that are endowed with open water sources. Most parts of Central, Southern and South Eastern Uganda are endowed with open water bodies such as river Nile, lake Victoria, lake Albert, lake Edward and lake George. All these lakes are fresh water lakes (WWAP, 1999). The crater lakes of the rift valley namely lake Albert, lake Edward and lake George are alkaline lakes and have a pH of 8.5 (Mungoma, 1990). The volumes of water in the open sources of water in Uganda depend on rainfall (Nsubuga, 2014) and has been affected by climate change. The annual rainfall varies from over 2000 mm in areas around lake Victoria and Mt. Elgon, to less than 700 mm in the Northern parts of Uganda. In Northern parts of the country, the rainy seasons are less well defined (Government of Uganda, Ministry of Water and Environment, 2010; GOU, 2010). South Eastern parts of Uganda and areas around lake Victoria has two distinct rainy seasons (December- February and June- August). The national safe drinking water coverage in rural areas is estimated at 67% while urban areas stand at 71% (Uganda Water and Environment Sector Performance report, 2016).

There are two distinct categories of water sources and are influenced by climatic, physiographic and geological factors. These categories include surface and underground water sources which are part of the earth's hydrologic cycle (Asaba et al., 2014). Underground water sources are mainly from boreholes, springs and hand dug wells (Uganda National Bureau of Standards; UNBS, 2016). Underground water is one of the sources of fresh water for drinking and irrigation worldwide (World Health Organization; WHO/United Nations International Children's Emergency Fund; UNICEF, 2014). In

Uganda 61 % of water is from underground sources and is accessed from boreholes, shallow wells and protected springs. They are the major source of water supply in semi arid and arid areas in Uganda (Kabonesa et al., 2015, Government of Uganda; GOU, 2010).

The underground water sources provide water for municipal or public water supply, domestic and commercial (industrial), mining and agriculture (Asaba et al., 2015). Municipal or public water use includes water for street cleaning, fire fighting, municipal parks and public swimming pools. Domestic water use includes water used in residential homes for drinking and cooking, bathing, toilet flushing, washing clothes and dishes, watering lawns and gardens and swimming pool maintenance (Rugumayo et al., 2006). Water for commercial use is mainly in industries/ factories, hotels, restaurants, large civilian and military institutions and public and private golf courses. Water use in industrial is majorly for cooling of engine parts, processing and production in factories. Some of the industries and factories that use water include mining, textile, steel and paper rolling, chemical and associated products (Luo et al., 2017). Agricultural water use applies to water used for irrigation and livestock such as water applied to farms or horticultural crops, diaries, fish farms and other farm needs (Nakalembe et al., 2017). Water is thus one of the unique renewable resources essential for all forms of life, food production, promoting economic development and for general well being (UNBS, 2016). The availability of fresh water, the nature's gift controls the major part of the country's economy (Elimelech and Montgomery, 2006). The availability of water resources determines the land use and population distribution (UN WWAP, 2006).

The largest portion of Northern, North West and North Eastern parts of Uganda are semi arid with limited surface water bodies and these include the districts of Moroto, Kabong, Napak, Kotido, Nakapiripirit, Amudat and Abim among others (Kabonesa et al., 2015, GOU, 2010). In Moroto district the rural and urban domestic water provision is mainly from the underground water sources where water is pumped from deep and shallow underground sources using borehole pumps or engine pumps. In semi arid areas water from valley dams and surface runoff is mainly used for livestock watering and is easily contaminated with human and animal wastes (UNBS, 2009). The contaminated water

sources can expose the human population to diseases such as diarrhea, cholera among others (UNICEF, 2012).

Underground water is vulnerable to contamination by non biological and soluble materials in the rocks through which water flows before they reach the ground water surface. These contaminants may include radioactive compounds, heavy metals and their compounds that are soluble in water (Tchokossa et al., 2011). The radioactive materials may contain isotopes that emit gamma radiations as they decay. Underground water obtained from this region may be contaminated by minerals which include radionuclide isotopes which are soluble in water (Abbady, 2005).The underground water sources are supplemented by gravitation flow schemes and rain water harvesting technologies (Asingwire, 2011; Government of Uganda, Ministry of water and Environment, 2010). The underground water source provides water for most of the rural and urban population in Moroto district. The access rate to water in Moroto district varies from 58% in Tapac Sub county to 95% in Katikekile sub- county. The district has a total of 300 water points which serve a total population of 89,209 people (Directorate of water development, Ministry of water and Environment, 2017). The number of functional boreholes in Moroto District are as shown in Table 1.1.

Table 1.1: Number of boreholes per sub-county in Moroto District (Source: Directorate of Water Development, Ministry of Water and Environment Republic of Uganda, 2017).

Sub- county	**Functional boreholes**
Katikekile	40
Nadunget	85
Northern Division	33
Rupa	97
Southern Division	19
Tapac	26
Total	**300**

The boreholes in Uganda are generally located in areas where the geology is dominated by crystalline rocks (including granites), which constitute around 70% of the land area (Nagudi, 2011). These Archean and Proterozoic rocks of high grade metamorphism are commonly referred to as “Gneissic-Granulitic Complex”. The crystalline rocks of Uganda are mostly covered by ‘regolith’ or ‘overburden', a layer of weathered material which

varies from rock fragments near the interface with the bedrock, to well-weathered soil and hardened laterite at the ground surface (Nagudi, 2011). The regolith layers vary in thickness but are often around 30 meters thick. The thickness and condition of the regolith and the degree of fracturing of the crystalline rocks typically determine the depth of the water sources (Ruettinger et al., 2011). This is true for Moroto District.

Gamma radiations from radionuclides such as Potassium-40, Uranium-238 and Thorium-232 and their decay products are the major source of internal radiation exposure to the human body. High levels of the naturally occurring radionuclides are associated with igneous rocks such as granite rocks and their distribution depends on the rock types from which they originate and the process which concentrates them (Pring, 2006).

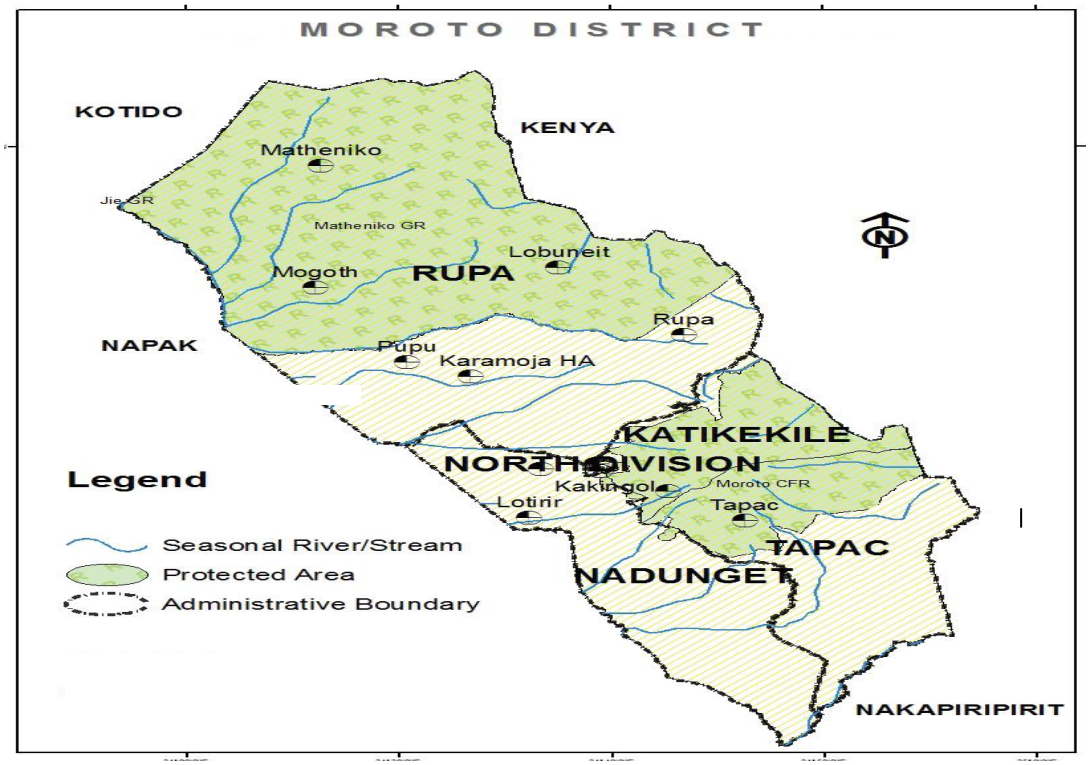

Figure 1.1: Map of Moroto District indicating the area under study (Ngoya, 2008).

Radionuclides in soils and rocks emit ionizing radiations namely, beta radiations, alpha radiations and gamma radiations. Rock phosphate and carbonate contain high levels of Uranium-235 and Radium-226 which are radioactive while phosphate ores contain higher

levels of Uranium-238 which is also radioactive (Xiang et al., 2011). Compounds of Uranium such as uranyl nitrate hexahydrate, uranyl fluoride, uranyl tetrachloride readily dissolve in water (Faanu et al., 2011). The compounds of Thorium that readily dissolve in water include chlorides, fluorides, nitrates, and sulfates (Filippelli, 2011). The mobility and vertical transport of these soluble compounds depend on the soil and rock properties such as Potential of Hydrogen (pH), redox potential, soil matrix porosity and particle size. When underground water moves through fractures in the bedrock that contains soluble deposits of these radioactive nuclides (Tchokossa et al., 2011), the water can get contaminated. High proportions of these soluble compounds in soils and rocks results into their higher activity concentrations thus contaminating underground water through leaching, weathering and dissolution (Abbady, 2005).

The natural sources of Gamma radiations (ionizing radiations) are naturally occurring radioactive minerals in the environment and cosmic radiations. Cosmic radiations originate from space (Nicolet et al., 2003). Secondary cosmic rays are produced by interactions of primary rays. Terrestrial radiation is the major source of ionizing radiations. It arises from terrestrial or primordial radionuclides in the earth crust. Soils, rocks and building materials (UNSCEAR, 2008) are the major sources of ionizing radiations in underground water. The soils and rocks contain primordial radioactive isotopes from which ionizing radiations originate. They are mainly Uranium-238, Thorium-232, radionuclides in their decay series and Potassium-40 (IAEA-TECDOC-2003). Primordial radionuclide's have half-lives of order of 100 million years, comparable to the age of the earth. Uranium and Thorium can initiate a chain of radioactive decay into daughter radionuclides (Matolin et al., 2003). Although the daughter radionuclides are short lived they are distributed in the environment because they are continually being emitted by the long lived parent radionuclide. Radioactive isotopes are chemically bound to the earth's crust and can be a source of radiation exposure (Matolin et al., 2003). Potassium-40, Uranium- 235, Uranium- 238, Caesium- 137 and Thorium-232 and their decay products are among the radio-isotopes that produce high energy gamma rays when they get dissolved in underground water sources (UNSCEAR, 2008).

If large proportions of soluble compounds of the radionuclides do exist in different soils and rock types it is probable that underground water will get contaminated, (Lesikar et al.,

2006). When these radionuclides are taken in by people through ingestion, they emit ionizing radiations that can damage internal body tissues. These radiations are of high energy and are thus more penetrating. Drinking water contaminated with radionuclides for a long time may lead to associated health problems such as radiation poisoning, cancer, anaemia, osteoporosis, cataracts, skin burn, bone growth, destruction of hair follicles, impaired immune system, kidney and liver diseases since the radiation causes damage to the deoxyribonucleic acid (DNA) (Little, 2003).

A study was done outside Uganda on underground water samples from Ondo and Ekiti states in Nigeria for gamma ray emitting radionuclides (Ayodele et al., 2017). The water samples were found to be contaminated with radionuclides of ^{226}Ra, ^{232}Th and ^{40} K with varying activity concentrations. A study was also done on the distribution and activity concentration of radionuclides in borehole water from Akure and Ondo states in Nigeria (Ibikunle et al., 2013). It was found out that the water samples were contaminated with radionuclides of ^{226}Ra, ^{232}Th and ^{40} K that are the daughters and parent emitters of gamma rays. The rock geology of these areas was dominated by igneous and sedimentary rocks. In Uganda a study was done on radiological hazard levels by gamma emitting radionuclides in natural water bodies in selected sub-counties of Mubende District (Candia, 2015). He found out that the natural water bodies were contaminated by radionuclides of ^{226}Ra, ^{232}Th and ^{40} K. The district was also dominated by igneous and sedimentary rocks. This study still leaves room for studies to be done in Moroto in particular with regards to underground borehole water sources.

The geology of Karamoja Region and Moroto District in particular is dominated by igneous and sedimentary rocks that are enriched with minerals such as Gold, Chromite, Copper, Gemstones, Limestone, Marble, Tin, Uranium, Gypsum, Nickel, Lithium, Mica, Talc, Caesium and Zircon (Ministry of Energy and Mineral Development; Department of Geological survey and Mines, 2011). These radioactive minerals when they dissolve in water could contaminate underground water sources. A study done on the mineral distribution in Karamoja (Kabongo et al., 2014) found out that the rock geology of karamoja and Moroto in particular was endowed with different minerals.

1.2 Statement of the problem of study

The geology of Moroto district is endowed with minerals (Kabongo et al., 2014). It is probable that the soils and rocks in Moroto contain radioactive nuclides such as Uranium, Potassium and Thorium.

When such high activity concentration radioactive nuclides found in the rocks dissolve in water, it can be a health hazard or danger to the people who consume it.

1.3 Purpose of the study

This study was therefore designed to identify radionuclides and determine the radiological hazard levels of gamma rays from radionuclides that have dissolved in water from some selected boreholes in Moroto District.

1.4 Objectives of the study

The objectives of the study were to:-

(i) Identify the gamma ray emitting radionuclides present in the borehole water from selected boreholes in Moroto District.

(ii) Measure the activity concentrations of gamma ray emitting radionuclides in water samples from the selected borehole water.

(iii) Determine the absorbed dose rates of gamma rays emitted from radionuclides in the water samples.

(iv) Calculate the annual effective dose equivalent of the gamma rays emitted from radionuclides in the water samples.

(v) Find the internal and external radiological hazard levels by gamma rays in the water samples.

1.5 Scope of the study

The study was dealing with the determination of the radiological hazard levels of gamma rays from radionuclides in water from boreholes. Theses underground water from boreholes is more prone to contamination by radionuclides from underground rocks. The study was carried out in four different sub counties of Moroto District. The district is

located in North-Eastern Uganda. It is approximately 210000 metres by road, North East of Mbale town.

The sub counties in Moroto under study are Rupa, Katikekile**,** Nadunget and Northern division. The four sub-counties were selected because they had the rock geology associated to igneous and sedimentary rocks that hosts several radioactive minerals that could contaminate underground water sources. Also the sub counties had many borehole and the boreholes were easily accessible. Unlike in Tapac sub- county where the boreholes could not easily be accessed due to the hostile nature of the communities. Southern division on the other hand had very few boreholes and as a result was left out during the study. The study was carried out to investigate underground water sources from boreholes not any other source of water because there was needed to find out the level of contamination of underground borehole water sources by the dissolved radionuclides that are contained in the soils and rocks in the area.

The study was carried out by analyzing a total of twenty eight (28) samples of water from the selected boreholes. Seven (7) boreholes were sampled from each of the four regions. The seven boreholes were selected from several boreholes in order to give a good variety of boreholes. The selection of boreholes in each region was done using random sampling. The boreholes that were sampled were at distances greater than 500 m away from each other. The study was restricted to identification of the gamma ray emitting radionuclides in the water samples, determination of variables such as activity concentrations, absorbed dose rates, annual effective dose equivalent, internal and external radiological hazard levels by the gamma rays in terms of the effects. The study was also restricted to borehole water samples and not any other source of water because the interaction of water and the rocks that contain soluble radionuclides could lead to contamination of underground water sources.

1.6 Significance of the study

The results of the study may be of benefit to the Ministry of Water and Environment, UNICEF, and the Ministry of Health with regard to borehole water safety in Moroto District. This information would be used for sensitizing the local population that consumes water in areas where the radiological hazard levels have been found to be high. The results

also provide information to the Atomic Energy Council to develop relevant radiation safety standards for the general population in the country with regards to radionuclide water contamination.

CHAPTER TWO: REVIEW OF RELATED LITERATURE

2.1 Introduction

The review of related literature of the study has covered the concepts related to radioactivity and materials which contain radioisotopes.

The review has also described nature and properties of naturally occurring ionizing radiations such as terrestrial sources as in soils and rocks, medical exposures; nuclear weapon testing and radioactive decay have been covered.

The review further describes the rock types and mineral composition in igneous rocks that contain mineral ores with abundant radioactive nuclides such as Potassium, Uranium, Thorium and Caesium.

The review has also described the nature and disintegration of radioactive nuclides. This also includes the decay series of radionuclides.

Biological effects of ionizing radiations in the body such as ionization and excitation of the body tissues, molecules and its damage to the DNA have also been described.

The radiological dosimetric quantities and the parameters of ionizing radiations such as absorbed dose rate, annual effective dose equivalent and radiological hazard index have also been covered.

The review has covered detection and measurement of ionizing radiations using scintillation detectors and gas filled detectors. Gamma ray spectrometry has also been covered in the review of related literature. Water contamination by radionuclides has also been described.

2.2 Nature and properties of naturally occurring ionizing radiations

All matter is made up of atoms. Atoms may be stable or unstable. Atoms with excess energy and nucleons are unstable and thus decay by emitting ionizing radiations. Such ionizing radiations are alpha (α), beta (β) and gamma (γ) radiations. An alpha radiation is positively charged and has the least penetrating power but the greatest ionizing power of all the three kinds of ionizing radiations. When they get into the body they can cause serious damage since they are ionizing and are thus capable of ionizing human cells. Beta radiations are highly energetic electrons which are released from inside the nucleus of an atom. Beta radiations have greater penetrating power than alpha radiations and can easily

travel through the skin. They have the least ionizing power than alpha radiations but are still dangerous.

Gamma radiations are the most energetic electromagnetic waves of very high frequency. They have the greatest penetrating power of all the three kinds of ionizing radiations. They are the least ionizing, but have huge amounts of energy and can travel through thin lead and thick concrete. They carry no charge hence not deflected by electric and magnetic fields.

The natural sources of Gamma radiations (ionizing radiations) are naturally occurring radioactive minerals in the environment and cosmic radiations. Cosmic radiations originate from space, (Nicolet et al., 2003). Cosmic radiation is the minor source of external exposure to gamma radiation, the major source of natural exposure is from terrestrial sources. Cosmic radiation is composed of subatomic particles from outer space, mostly energetic protons, electrons, gamma rays, X-rays (Bleise et al., 2003). Cosmic rays are categorized into two types, primary and secondary cosmic rays. Cosmic rays are said to be primary cosmic rays if they have not interacted with matter in the earth's atmosphere, lithosphere or hydrosphere. Primary cosmic rays are composed of protons (about 85%) and alpha particles (about 14%) with much smaller fluxes (< 1%) of heavier nuclei. Secondary cosmic rays are produced by interactions of primary rays with the atmosphere and consist largely of subatomic particles such as pions, muons, and electrons. At sea level, the most detected cosmic radiation consists of secondary cosmic rays, with some 68% of the flux accounted for by muons and 30% by electrons (Bleise et al., 2003). Less than 1% of the flux consists of protons. Primary cosmic rays are mainly positively charged and usually carry large kinetic energy of order of 2 to 30 GeV. These large energies of primary cosmic rays enable them to literally blast apart atoms in the earth's atmosphere upon collision. The intensity of cosmic rays increases with altitude, latitude and solar flare activities (Biological Effects of Ionizing Radiations; BEIR VII, 2006). When cosmic radiations interact with the earth's atmosphere a variety of radionuclide's such as Sodium- 22 (half life of 2.605 years) and Carbon-14 (half life of 5715 years) are produced. The contributions of radionuclide's to radiation absorbed dose rate is not significant (International Atomic Energy Agency Technical Document; IAEA-TECDOC-1363, 2003). At sea level, the average absorbed dose rate arising from exposure to directly

ionizing radiations is 31 $nGyh^{-1}$ which is equivalent to an annual effective dose equivalent rate of 0.270 $mSvy^{-1}$ (United Nations Scientific Committee on Effects of Atomic Radiation; UNSCEAR, 2000, 2008).

Terrestrial radiation is the major source of ionizing radiations. It arises from terrestrial or primordial radionuclides in the earth crust. Soils, rocks, air, water, food and building materials (UNSCEAR, 2008) contain primordial radioactive isotopes from which ionizing radiations originate. They are mainly Uranium-238, Thorium-232, radionuclides in their decay series and Potassium-40 (IAEA-TECDOC-2003). Primordial radionuclide's have half-lives of order of 100 million years, comparable to the age of the earth. Uranium and Thorium can initiate a chain of radioactive decay into daughter radionuclides. Although the daughter radionuclides are short lived they are distributed in the environment because they are continually being emitted by the long lived parent radionuclide. Radioactive isotopes are chemically bound to the earth's crust and can be a source of radiation exposure if exposed to the earth surface or released by natural processes such as earthquake, volcanic and human activities such as mining and construction (Matolin et al., 2003).

Other gamma radiations were derived from radio isotopes synthesized during creation of solar system. The isotopes are present till today due to their long half lives (Focazio et al., 1998*)*. Potassium-40, Uranium- 235, Uranium- 238, Caesium- 137 and Thorium-232 and their decay products are among the radio-isotopes that produce high energy gamma rays (Nicolet et al., 2003).

Several activities, practices such as use of fertilizers, use of radioisotopes in medical diagnosis, nuclear accidents, processing industries that use large volumes of raw materials containing natural radionuclides exposes people and other radiation workers in nuclear establishments and hospitals to ionizing radiations (UNSCEAR, 2000).

2.3 Rock types and minerals composition

The igneous rocks are subdivided into intrusive and extrusive igneous rocks that were formed as a result of cooling and or crystallization of molten magma within the earth crust or at the surface of the earth crust. They can be coarse or fine grained. The coarse grained igneous rocks include granite, delorite, gabbro and peridotites (Mibei, 2014). They contain

mineral ores with abundant radioactive nuclides such as Potassium, Uranium, Caesium and Thorium that have been present since the formation of the earth 4.5 billion years ago (Alnour et al., 2012). Granite and sedimentary rocks in Uganda contain ^{238}U, ^{232}Th and ^{40}K radionuclides in addition to the heavy accessory minerals such as Monazite, and Zircon (Baguma, 2009). Karamoja region and Moroto district in particular is dominated by igneous and sedimentary rocks that hosts mineral ores with abundant radioactive nuclides. Uranium in form of euxenite, microlite, and kasolite exists in pegmatite rocks and were detected in spring waters in the Western rift valley (Nagudi, 2011). Thorium exists in monazite formed by weathering of granite rocks containing quartz-rutile ilmenite nodules in the biotite gneisis. The mineral varies in colour from typically honey yellow to almost black and contains up to 11% ThO_2. In Uganda the rocks of granite and pegmatite nature that are weathered contain 0.5% ThO_2 (Nagudi, 2011).

Traces of these radioactive nuclides are always present in the bedrock. Natural radioactivity occurs at varying proportions in all forms of rocks and soils around the world and accounts for external gamma dose rates that humans receive from the environment. Due to weathering and other physical and chemical processes radionuclides in rocks and soils accumulate in sediments and dissolve into ground water leading to human exposure (Isinkaye et al., 2015). The consumption of this water contaminated by radionuclides of high activity concentrations can be a health hazard to the consuming population. Since borehole water is obtained from underground water there is likelihood that the borehole water can contain the radionuclides found in the underground rocks. In Uganda limited areas of research have been done about water. A study was carried out on radiological hazard levels by gamma emitting radionuclides in natural water bodies in selected sub-counties of Mubende District (Candia, 2015). He found out that the natural water bodies were contaminated by radionuclides of ^{226}Ra, ^{232}Th and ^{40}K. This study still leaves room for studies to be done in Moroto in particular with regards to underground borehole water.

2.4 Nature and disintegration of radioactive nuclides

An unstable nucleus of an atom undergoes radioactivity and emits ionizing radiations like alpha, beta and gamma rays. The unstable atoms decay by emitting a particle transforming the nucleus to another nucleus or into a lower energy state and the chain of decay continues until the nucleus attains the state of stability. Ionizing radiation has enough

energy to ionize matter either directly or indirectly when their energy exceeds the ionizing potential of matter.

Radioactive decay is a spontaneous transition of an atomic nucleus into a different nuclide by emitting particles only, photons only or particles followed by photons (Lieser, 1991). The decay of a radioactive nuclide is a random process and is subject to the laws of statistics. The decay rate or activity of a radioactive source is described by a simple linear differential equation (2.1) called decay law where the number of decaying atoms per unit time is proportional to the number of atoms N that persisted decay at the moment, t (Lieser, 1991).

$$A(t) = \frac{dN}{dt} = -\lambda N(t). \tag{2.1}$$

Where

$A(t)$ *is the activity* $(decay\ per\ unit\ time)$ *and* λ is the decay constant

The SI unit of activity is the Becquerel (Bq) defined as one disintegration per second

The integration of the decay equation with respect to time provides the equation

$$N(t) = N_0 . e^{-\lambda t}. \tag{2.2}$$

The decay constant for a particular radionuclide is expressed as

$$\lambda = \frac{In2}{T_{\frac{1}{2}}}. \tag{2.3}$$

Statistically $\lambda -$ refers to the probability of the number of nuclei that undergoes radioactive transformations in time t and is characteristic for each radioactive isotope. $T_{\frac{1}{2}}$ is the half-life of a radioactive material.

$$A = \lambda . N. \tag{2.4}$$

Specific activity of a radioactive source is defined as the activity per unit mass of a radioisotope sample. The daughter nuclides produced by $\alpha-$decay and especially $\beta-$ decay are often obtained in an excited energy state. The energy associated with this excited state is released when the nucleus emits a photon of high energy. Most frequently the $\gamma-$ray is emitted within 10^{-12} seconds after particle emission. The emission of a gamma ray photon has no effect on the mass and atomic numbers of the radionuclide.

There are three naturally occurring radioactive decay series namely; Uranium decay series, Actinium decay series and Thorium decay series (IAEA-TECDOC-1363, 2003; Shirley, 1978). The Uranium decay series (Figure 2.1) starts from Uranium-238 which decays by alpha emission to Thorium-234 which is itself unstable, it further decays by beta emission to produce Protactinium -234 (^{234}Pa) and this process goes on until stable Lead (^{206}Pb) is produced. The Actinium decay series (Figure 2.2) starts from Uranium (^{235}U) and decays by emission of alpha particle to Thorium (^{231}Th). Thorium -231 is also unstable and further decays to produce Protactinium (^{231}Pa) by beta emission. The process goes on until stable Lead (^{207}Pb) is produced. Thorium decay series (Figure 2.3) begins from Thorium-232 (^{232}Th). It decays by alpha emission to produce Radium (^{228}Ra). Radium-228 decays by emission of beta particles to produce Actinium (^{228}Ac) and this process goes on until stable Lead (^{208}Pb) is obtained.

The three natural radioactive decay series contains a radioactive daughter nuclide which is in gaseous state, that is Radon ^{222}Rn (Radon in ^{238} U decay series), ^{219}Rn (Actinon in the ^{235}U decay series) and ^{220}Rn (Thoron in the ^{232}Th decay series). Radium-226 decays by alpha emission to Radon, ^{222}Rn which is a radioactive inert gas. Radon decays by alpha emission to give a progeny of radioactive daughters (UNSCEAR, 2000). The existence of Radon and Thoron in the chain is the main reason for the public health concerns about the naturally occurring environmental radioactivity. The gas diffuses from the soils and the rocks into the air and can concentrate in the poorly ventilated homes, public buildings and underground water (Bartram et al., 2014). The concentration of Radon gas depends on the concentration of Uranium and Thorium in soils, rocks and building materials.

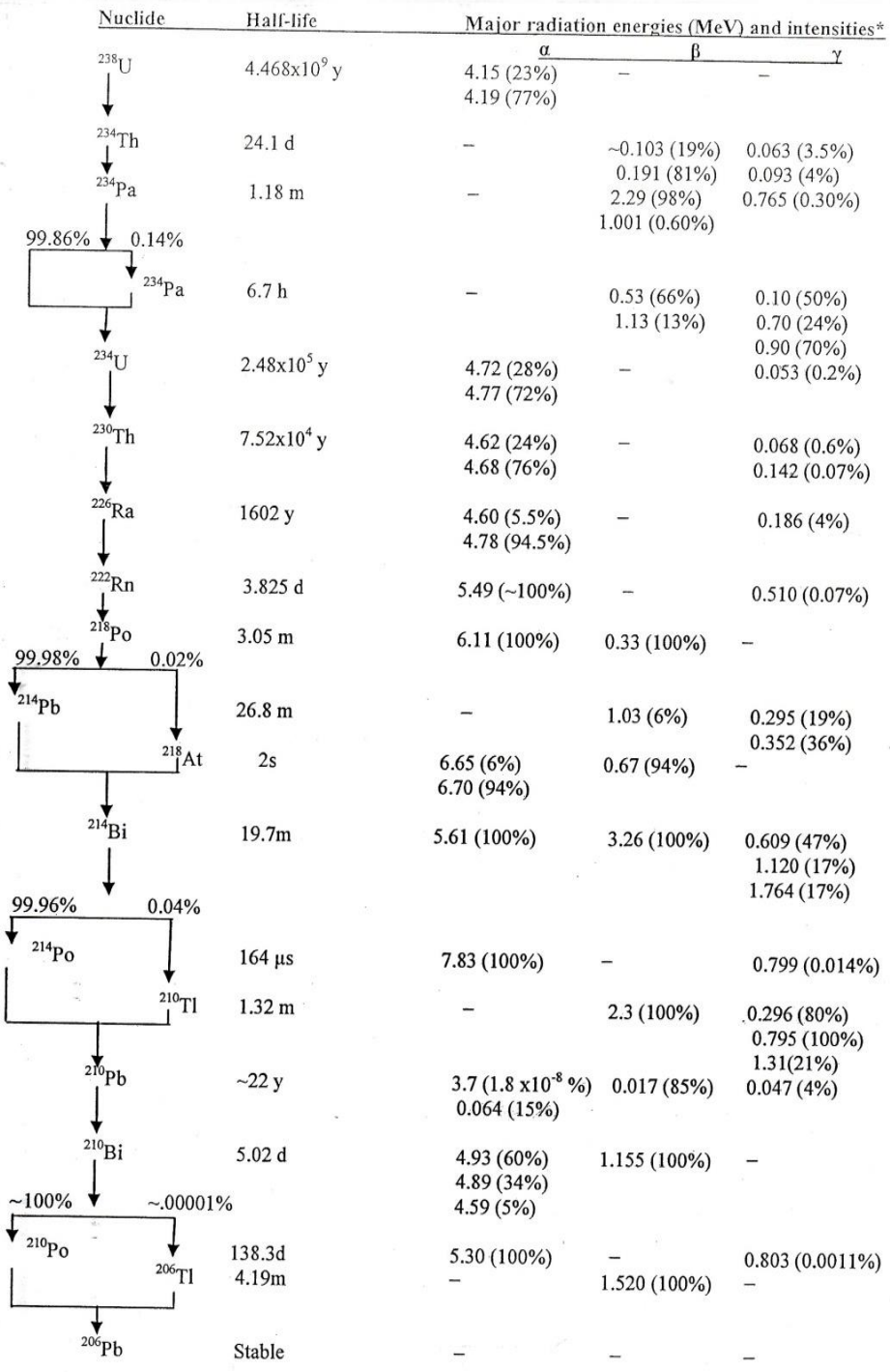

Figure 2.1: Diagram of Uranium decay series (Kölbel et al., 2020).

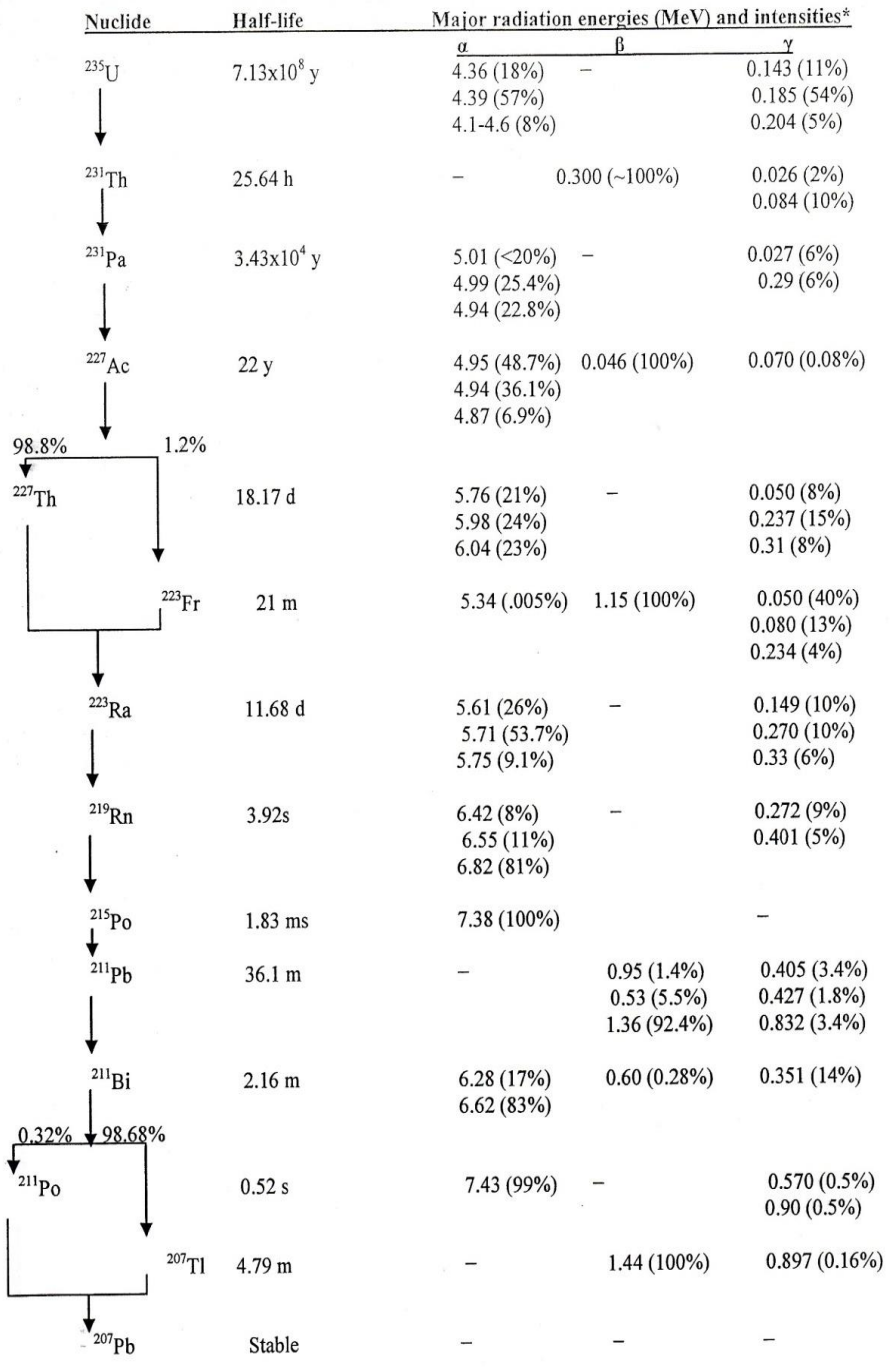

Figure 2.2: Diagram of Actinium decay series (Ishimori et al., 2013).

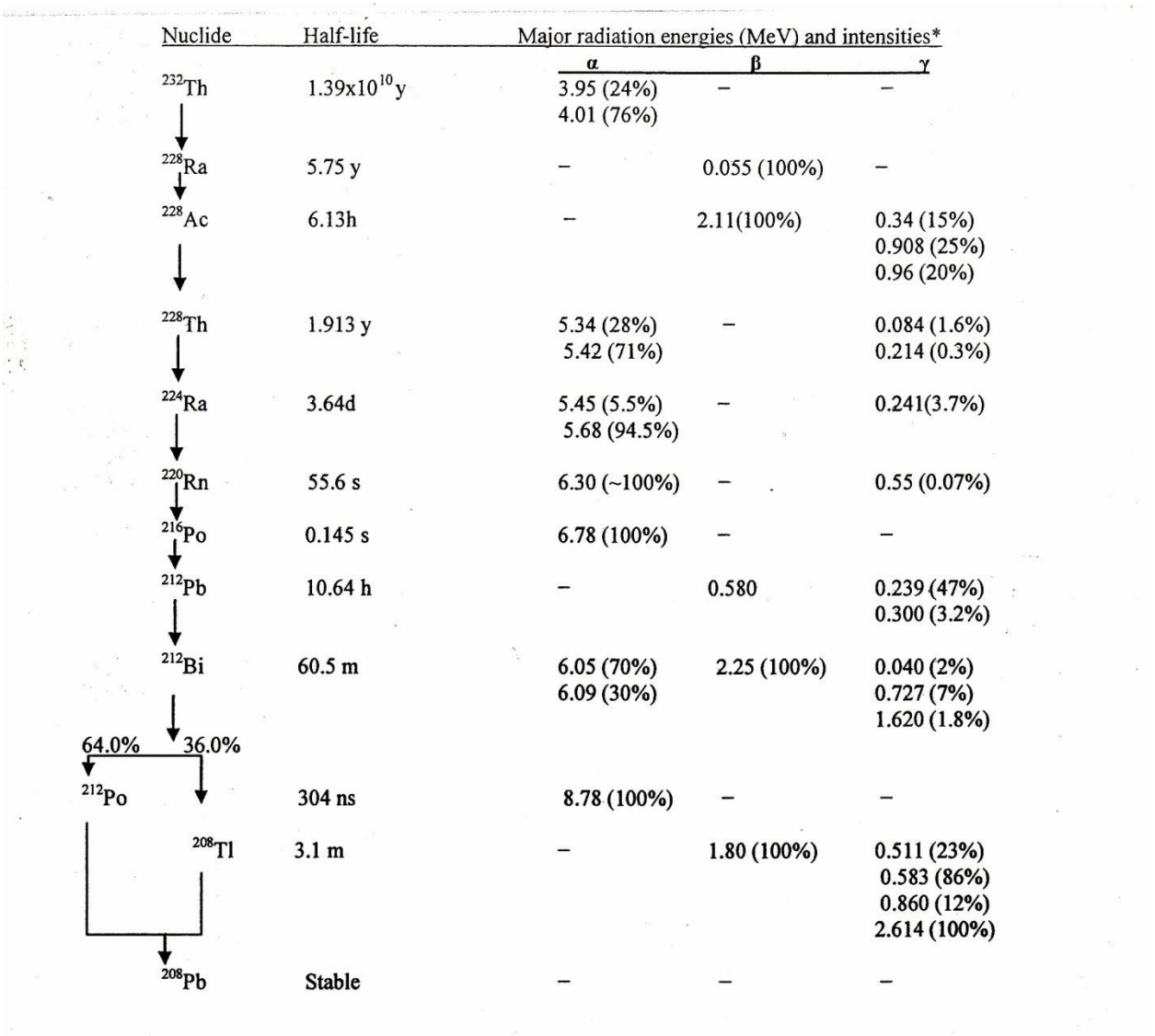

Figure 2.3: Diagram of Thorium decay series (Yusoff and Mohamed, 2016).

The decay scheme of ^{226}Ra shown in Figure 2.4 (Turner, 2007) shows how Radon gas is produced by alpha emission from ^{226}Ra. The two modes of alpha decay of ^{226}Ra along with the alpha particle energies and frequencies are shown by the two slanting arrows. Either changes the nucleus from that of ^{226}Ra to that of ^{222}Rn. When the lower energy particle is emitted Radon nucleus is left in excited state with energy of 186 keV above the ground state.

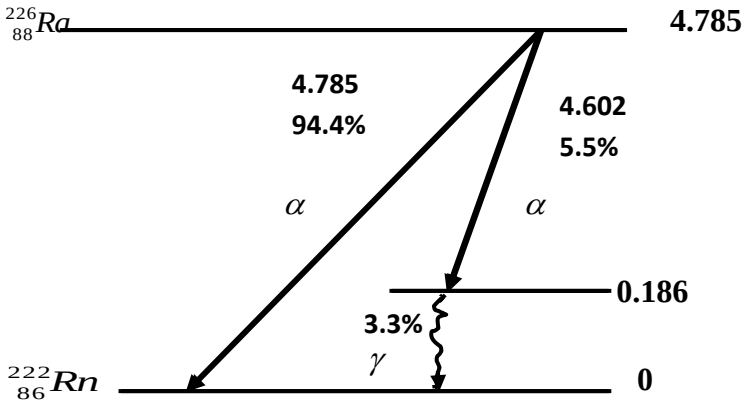

Figure 2.4: Diagram of decay scheme of ^{226}Ra (Turner, 2007)**.**

The frequency of 3.3% associated with this photon emission implies that internal conversion electron is emitted in the order of 2.2% of the total number of disintegrations. When an internal conversion electron is emitted, it leaves a vacancy in the K or L shells of the ^{222}Rn. This results in emission of characteristic X-rays (Turner, 2007). There are also non-series naturally occurring radioisotope that are alpha, beta and gamma radiation emitters. They include Potassium, (^{40}K, 89% β and 11% γ), Lanthanum (^{138}La, 100% β, 30% α and 70% γ) Lutetium (^{176}Lu, 100% β, 95% γ) (Firestone et al., 1996). Potassium-40 is found in the soils and rocks within an isotopic abundance of 0.0118% in the earth's crust (IAEA-TECDOC, 2003).

2.5 Biological effects of ionizing radiations

The interaction of ionizing radiation with the human body produces ionization and excitation of the body tissues and as a result it impairs the normal function of the cell. This is because ionizing radiations have sufficient energy to strip off electrons from atoms and break up their chemical bonds. This subjects the human body to harm and the severity of this harm depends on the nature and the energy of radiation, total dose and dose rates, the extent and part of the body exposed, age of the person exposed to the radiation, and the radiation sensitivity of the organ exposed. During interaction, part or whole of the energy may be absorbed by the cell and since the water content in the human tissues is more than 70%, most of the energy will be deposited in the water molecule and only a small part is

taken up directly by the other biomolecules (UNSCEAR, 2006). A series of reactions is undergone by the excited and ionized water molecule producing free radicals which react with biomolecules of the cell. This may result in the damage of the deoxyribonucleic acid (DNA) and proteins leading to inhabition of cell division, chromosome aberrations, gene mutation and cell death (Grasty et al., 2014). This thus may produces acute health effects such as skin burn, hair loss, radiation poisoning, cancer and genetic damage (UNSCEAR, 2010). The health effects range from minor to severe depending on the dose of radiation received. The health effects are divided into stochastic and non-stochastic effects (Herbst, 2014).

Stochastic effects are associated with low level, long term exposure to ionizing radiations (Herbst, 2014). When an irradiated cell is modified rather than killed, stochastic effect occurs. The modified cell may become cancerous after prolonged time. The body's repair and defense mechanism makes this a very improbable outcome at small doses without a threshold below which cancer cannot result. The probability of cancer occurrence is high at higher dose rates. When radiation damage to a germ cell occurs whose function is to transmit genetic information to the progeny, it is conceivable that hereditary effects of various types may develop in the descendants of the individuals exposed (IAEA-TECDOC 379, 2009). The likely hood of stochastic effects is directly proportional to the dose received without a dose threshold. The cancer risk is higher in children and adolescents as they are significantly more sensitive to the ionizing radiation exposure than adults (UNSCEAR, 2000). The decay of naturally occurring radionuclide's that are ingested into the body may lead to health effects and account for internal human exposure when incorporated as part of the food chain (Uosif et al., 2012).

The non-stochastic or deterministic effects are the result of various processes mainly cell death and delayed cell division. This is caused by exposure to high levels of ionizing radiations. At very high energy these can impair the normal functioning of the affected tissue. The severity of the effect on the affected person increases with the dose. The non-cancerous health effects of exposure to ionizing radiation such as radiation burn and radiation sickness are non-stochastic. The short term and high level exposure to ionizing radiations is referred to as acute exposure. Unlike cancer, health effects from acute exposure to ionizing radiations usually appear within minutes, days, or months after

exposure. Acute effects such as radiation burn and sickness (radiation poisoning) may cause permanent aging and or death. The symptoms of radiation sickness include; nausea, weakness, hair loss, skin burn and diminished organ function (Herbst, 2014).

Large and acute doses of radiations produces injuries such as skin burn, cataracts and destruction of hair follicles to the exposed persons. Ionizing radiation damage starts at the cellular level and when it is absorbed in the cell, it impacts on a variety of critical targets in the cell most importantly the deoxyribonucleic acid (DNA) (Luckey, 2011). When the DNA gets damaged it causes cell death, mutation and carcinogenesis (UNSCEAR, 2000). Damage to the DNA can either be by direct or indirect action. Direct action according to (Luckey, 2011) occurs when ionizing radiation impacts on the DNA directly causing ionization of the atoms of the DNA molecule and is a fairly uncommon occurrence due to the small size of the target. Indirect action occurs when ionizing radiation interacts with non-critical target atom or molecules, usually water resulting in the production of free radicals (Mallya et al., 2012). Free radicals attack the critical target such as DNA since the radicals are able to diffuse some distance in the cell. Damage through indirect action is much more common than direct action. The daily intake of Uranium is estimated to be 1-2 μg in food and 1.5 μg in drinking water (Bleise et al., 2003). The average human body (70 kg) contains approximately 56 μg of Uranium, more than 50% of this amount accumulates in the skeleton (Bleise et al., 2003). A higher level of Uranium intake leads to its accumulation in the kidneys and as a result it produces chemical damage to the proximal renal tubes and renal gromeruli (Zamora et al., 1998). Radium on the other hand is one of the most hazardous chemical with respect to internal radiation exposure and is known to be carcinogenic (Herbst, 2014). As an alkaline earth metal Radium may substitute Calcium and Strontium in the human bone cells and it remains intact and thus causing radiation damage by emitting ionizing radiations.

2.6 Radiological dosimetric quantities

Radiological dosimetric quantities are expressed in three ways: absorbed dose, equivalent dose and effective dose. Absorbed dose is the amount of energy absorbed in a specified mass. Absorbed dose is measured in Gray. Equivalent dose signifies the different effects that different radiation types have on biological materials. Each radiation type is assigned

a weighting factor. Effective dose is the sum of the product of equivalent dose and tissue weighting factor. When ionizing radiation penetrates the human body and is absorbed by tissues and organs, it deposits energy (Mettler et al., 2009) and the energy is called absorbed dose measured in gray (Gy). A dose of one gray is equivalent to a unit of energy (joule) deposited in a kilogram of a substance (Ndontchueng et al., 2014*)*. The absorbed dose rates is determined from the mean activity concentrations of the gamma emitting radionuclide's such as ^{226}Ra of the ^{238}U series, ^{232}Th *and* $^{40}K\left(Bq\,l^{-1}\right)$ using the formula provided by the UNSCEAR in equation (2.5).

$$D\left(nGy\,h^{-1}\right)=0.92\,A_{Ra}+1.10\,A_{Th}+0.08\,A_{K}\,. \tag{2.5}$$

Where

$D-$*is the absorbed dose rate in* $nGy\,h^{-1}$ *and* A_{Ra}, A_{Th} *and* A_{K} *are the activity concentrations of* ^{226}Ra, ^{232}Th *and* ^{40}K *respectively*.

The dose coefficients of 0.92, 1.10 and 0.08 due to ^{226}Ra, ^{232}Th and ^{40}K are in units of $nGy\,h^{-1}$ *per* $Bq\,l^{-1}$ (UNSCEAR, 2000). They are used for converting the activity concentrations of the three radionuclides in to dose. The values of absorbed dose rate obtained were compared with the world wide average limit of 84 nGyh^{-1} as per the UNSCEAR. The mean activity concentrations of the radionuclides are obtained from statistical mean of the data. The maximum permissible activity concentrations of ^{226}Ra, ^{232}Th and ^{40}K as per the UNSCEAR are 370 Bql^{-1}, 259 Bql^{-1} and 4810 Bql^{-1} respectively. The activity concentrations obtained during the study were compared with the world average values of 35 Bql^{-1}, 30 Bql^{-1} and 400 Bql^{-1} for ^{226}Ra, ^{232}Th and ^{40}K respectively.

Biological effects always result when ionizing radiations is absorbed by living matter but the effects depend on the absorbed doses and the type of radiation (Grasty et al., 2014). A certain specified weighting factor $\left(W_R\right)$ is multiplied with absorbed dose to obtain equivalent dose measured in sievert $\left(Sv\right)$. Different tissues and organs have different radiation sensitivities; bone marrow is much more sensitive to radiation than muscle or nerve tissue (UNSCEAR, 2000). Equivalent effective dose is obtained by multiplying the tissue weighting factor $\left(W_T\right)$ by equivalent dose because different tissues have different

weighting factors as in Figure 2.5 (Radiation Protection Regulations, 2000) and is also measured in sievert (Sv).

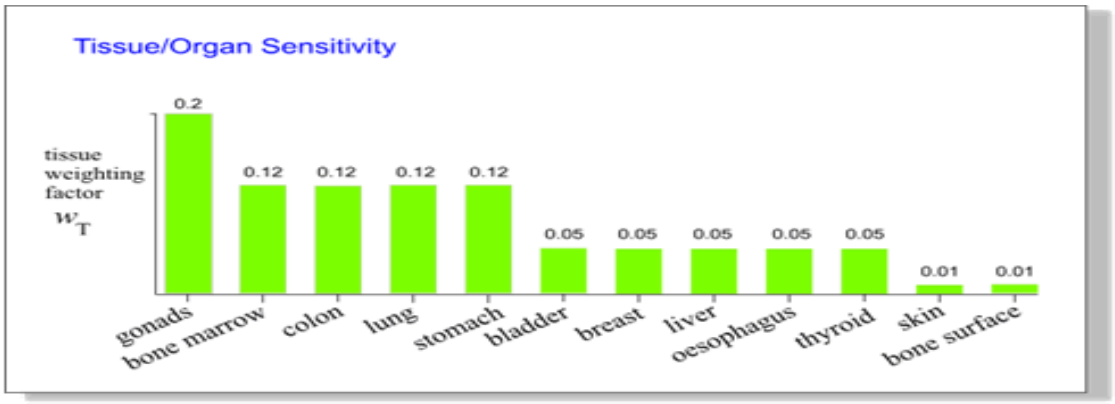

Figure 2.5: Bar chart of tissue weighting factor for different organs (Markinson, 2009).

The annual effective dose equivalent is the sum of dose absorbed by the body due to exposure to radiations over a period of one year. It is calculated according to the equation (2.6).

$$AEDE = \sum A_i . R_i . D_F . \qquad (2.6)$$

Where

$AEDE$ *was the annual effective dose equivalent*,
A_i *was the activity concentration of the radionuclide* (Bql^{-1})
R_i *was the* int*ake of water for a person in one year*
D_F *was the effective dose equivalent conversion factor* $(mSv\,Bq^{-1})$

The conversion factors vary depending on the radionuclide intake according to the ICRP and WHO. The values of the annual effective dose equivalent that are obtained in the study are compared with the world average value of 0.41 $mSvy^{-1}$ as per the UNSCEAR.

A number of radionuclides occur naturally in terrestrial soils and rocks and upon their decay the radionuclides produce external radiation field to which all humans are exposed leading to external radiological hazard levels. The value of the radiological hazard level is set to be less than 1 in order to keep the radiation hazard insignificant (Ndontchueng et al.,

2014). External radiological hazard level or index is determined based on the criterion introduced using a proposed model (Krieger et al., 1981) as given in equation (2.7).

$$H_{ex} = \frac{A_{Ra}}{370} + \frac{A_{Th}}{259} + \frac{A_K}{4810} \tag{2.7}$$

Internal radiological hazard index was obtained by reducing the maximum permissible concentration of Radium of 370 $Bq\,l^{-1}$ by a half to 185 $Bq\,l^{-1}$, and was determined from the formula given in the equation (2.8) (Hamzah et al., 2008).

$$H_{in} = \frac{A_{Ra}}{185} + \frac{A_{Th}}{259} + \frac{A_K}{4810} \tag{2.8}$$

Where A_{Ra}, A_{Th} *and* A_K *are the activity concentrations of* ^{226}Ra, ^{232}Th *and* ^{40}K *respectively*.

2.7 Detection and measurement of ionizing radiations

Measurement of ionizing radiations may be done by utilizing its physical and chemical effects on matter. The detection of ionizing radiations in the field and laboratory are mainly based on the ionizing properties of the radiations. Detection and measurement of radiations are taken in two different modes; namely pulse counting and spectrometry. In pulse counting the number of pulses are recorded not their heights. In spectrometry both the number of pulses and the heights are measured. The pulses are sorted to the channels of the multichannel analyzer according to their heights. Pulse counting can only be used for samples containing one single radionuclide. Spectrometry is used for samples that contain several radionuclides. The main radiation detection and measuring devices are gas filled, semiconductors and scintillation detectors (Westfall, 2019; Parks, 2009; Turner, 2007).

Low energy gamma rays and X-rays are usually detected using gas-filled detectors. Gas filled detectors include ionization chambers, proportional counters and Geiger Muller counters. An ionization detector consists of a metal tube with an end window filled with argon gas. A metal wire in the middle of the tube acts as an anode while the tube wall is the cathode. A voltage potential is applied across the electrodes and this creates an electric field inside the tube. When an ionizing radiation enters the chamber through the window,

neutral gas atoms in the chamber are ionized. The electric field created by the high voltage applied in the chamber causes electrons and positive ions to drift towards the anode and cathode respectively. An ionizing current pulse is thus generated which can be measured using electrometer (Turner, 2007). The schematic illustration of gas filled ionization chamber is as shown in Figure 2.6.

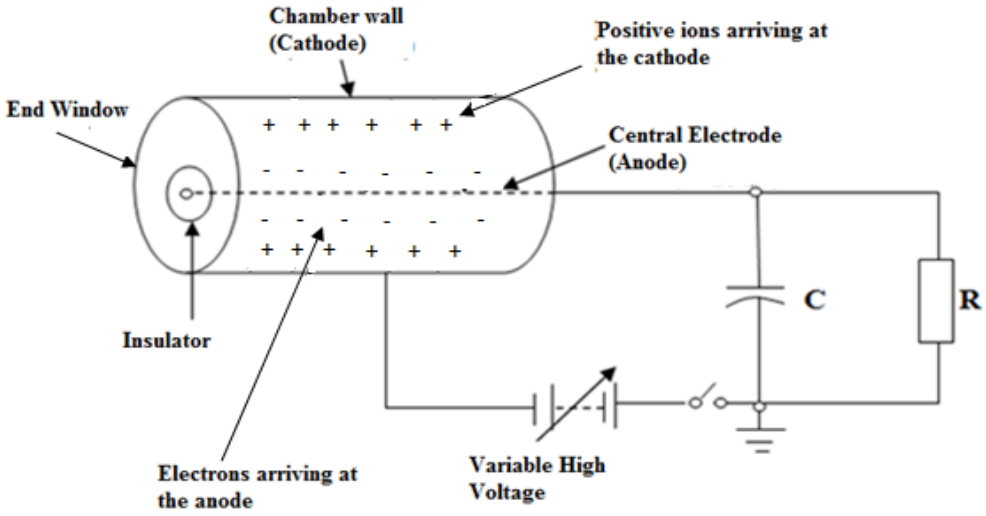

Figure 2.6: Diagram of gas ionization chamber (Kimura et al., 2005).

Semiconductor detectors are always made of Silicon and Germanium and are widely used in gamma and alpha spectrometry. Silicon semiconductor detectors are mainly used in alpha spectrometry while Germanium detectors are used in gamma spectrometry. In a semiconductor detector, two semiconducting parts are attached together. One part is an n-type semiconductor with mobile electrons, while the other part is a p-type semiconductor with positive holes. When an electric field is applied across the p-n in a reverse bias mode, a region depleted of holes and electrons is formed at the interface of the n and p type semiconductors. When a gamma ray or alpha particle hits this depleted region, electron-hole pairs are formed in the region making conduction possible. The electric field then produces an electric pulse which can be recorded in the external circuit.

Germanium semiconductor detectors use electronic charge carriers (electron-ion and electron-hole pairs) created by the absorption of gamma ray photons in the Germanium

detector. These charge carriers form directly on the detector electrodes, causing a flow of electric current through the semiconductor and produce an output voltage pulse of amplitude proportional to the energy of the incident gamma ray photon. The detector consists of a Germanium crystal mounted in a vacuum cryostat cooled to -196 °C. Cooling is achieved by insertion of the cryostat into a Dewar vessel filled with liquid nitrogen, or by electrically powered cryogenic refrigerators. Germanium detectors, generally of small volume, are used in in-situ gamma ray spectrometry and have superior energy resolution (0.5% at 122 keV) as compared to scintillation detectors. Scintillation detectors are widely used in gamma ray spectrometry. Thallium-activated Sodium Iodide [NaI(Tl)] crystals are used as detectors in field gamma ray surveys (Okeyode et al., 2015). Sodium Iodide detector crystals are transparent, with a high density (3660 kgm^{-3}), and can be manufactured in large volumes. They have a detection efficiency of up to 13% (Turner, 2007). The dead time is of the order of 10^{-7} s and the energy resolution for Cs-137 at 662 keV ranges from 7 – 10%, depending on the volume of the detector.

The NaI(Tl) detectors are hygroscopic, they can age and are fragile, and the photomultiplier tube function is dependent on temperature (Nasiru, 2013). Their large crystal volumes are an advantage in applications such as airborne gamma ray surveying where measurement times are short. Thallium-activated Caesium-Iodide CsI(Tl) crystals are neither hygroscopic nor fragile i.e. do not break easily. They usually have a density of 4510 kgm^{-3}, and a dead time of the order 10^{-9} s (IAEA-TECDOC-1363, 2003).

A scintillation detector consists of a scintillator such as Sodium Iodide and a photomultiplier. A scintillator is a substance which emits light when struck by an ionizing particle (Nasiru, 2013; Dirk, 2011; Parks, 2009; Turner, 2007). As in Figure 2.7, the incident gamma ray photon interacts with the material of the scintillation crystal to produce scintillations. The scintillation photons induce the ejection of electrons from the photocathode of the Photomultiplier Tube (PMT). The ejected electrons are multiplied in the Photomultiplier Tube with ten or more dynodes, each multiplying the number of electrons by a certain factor. This is accomplished by an electric field of about one thousand volts applied at the end of the tube, achieving an electron multiplication factor in the range of 10^7 - 10^{10} (Turner, 2007).

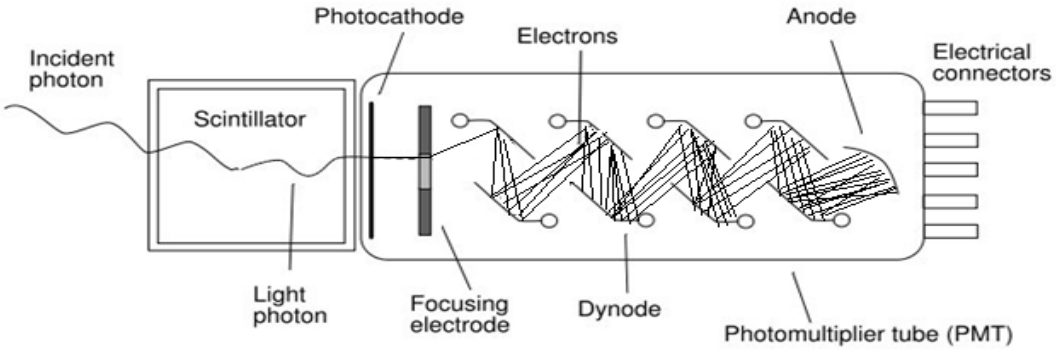

Figure 2.7: Schematic diagram of a Photo Multiplier Tube (Paredes et al., 2018).

Materials in scintillators emit and absorb photons of the same wavelength and as a result impurities are usually added to the scintillators to act as wavelength shifters, such that the wavelength of the emitted light photon does not fall into a self-absorption region (Turner, 2007). This is why thallium is added to sodium iodide crystals so that the designation is always NaI (Tl). At the end of the tube, the electrons generate an electric current signal whose magnitude is directly proportional to the scintillation light photon output, which is also directly proportional to the energy of the incident ionizing particle (Parks, 2009; Turner, 2007). This is accomplished by an electric field of about one thousand volts applied at the end of the tube, achieving an electron multiplication factor in the range of 10^7 - 10^{10} (Turner, 2007). Electronic block of NaI(Tl) detector is shown in Figure 2.8.

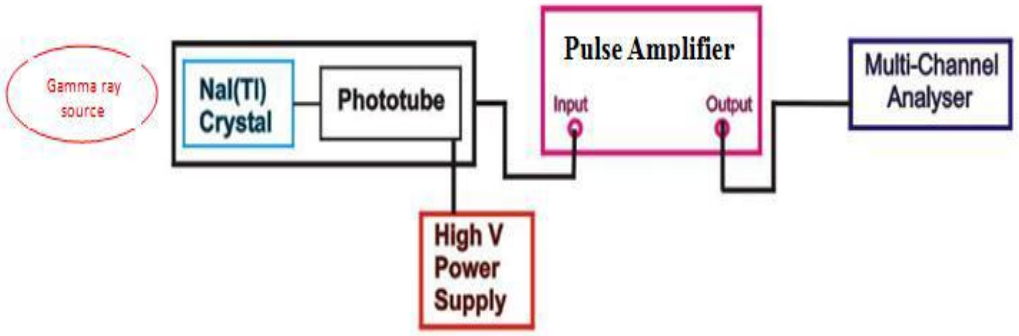

Figure 2.8: Electronic block diagram of NaI(Tl) detector (Beghian et al., 1958).

2.8 Gamma ray spectrometry

Gamma ray spectroscopy is one of the most developed and important techniques used in experimental nuclear physics because gamma ray detection and its energy measurement form an essential part of experimental nuclear physics research. Gamma ray spectroscopy is used in the quantitative study of the energy spectra of gamma ray sources. It is an analytical method that allows the identification and quantification of gamma ray emitting isotopes in a variety of matrices. In one single measurement and with little sample preparation, gamma ray spectrometry allows detection of several gamma ray emitting radionuclides in the sample. The measurement gives a spectrum of gamma lines which can be used to measure the intensity and energy of the emitted gamma rays (IAEA-TECDOC-1363, 2003).

There are different factors that determine the choice of a suitable gamma ray spectroscopy system for ionizing radiation detection and measurement. These are: the resolution which determines the complexity of the spectrum that can conveniently be analyzed; the detection efficiency which dictates the source strength necessary for the measurement of a spectrum; the simplicity of the arrangement and the ease of data accumulation; and secondary factors such as, the response linearity, the stability, the photoelectric interactions to Compton interactions ratio and the timing accuracy as well as detector availability.

Two of the major gamma spectroscopy devices used in gamma spectroscopy are; High purity Germanium (HpGe) spectrometer and Sodium Iodide (NaI) spectrometer (IAEA-TECDOC-1363, 2003). The Sodium Iodide (NaI) scintillator detector provides high efficiency gamma ray detection at moderate energy resolution. The high-purity

germanium (HpGe) semiconductor detector gives high resolution energy spectra at low efficiency. One disadvantage of NaI detector is that NaI absorbs water from the atmosphere which destroys the crystal and for this reason the crystal must be kept sealed. Another disadvantage of any scintillation counter is that the scintillation photons are detected using a photomultiplier tube (PMT).

In gamma ray spectroscopy using NaI(Tl) detector, the gamma rays interact with the detector atoms by three principal mechanisms: the photoelectric absorption, the Compton scattering and pair production (Parks, 2009; Turner, 2007). The interaction mechanisms are illustrated in Figure 2.9.

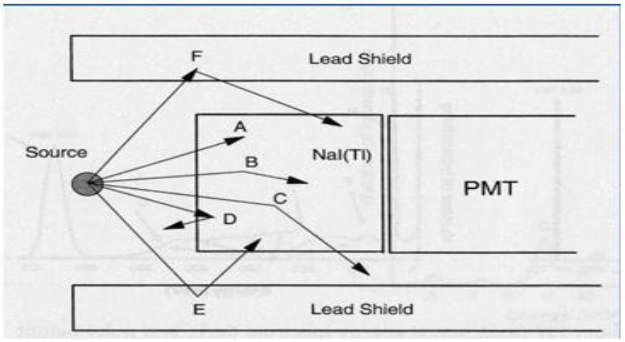

Figure 2.9: Diagram of Interaction of Gamma Rays with the detector material (Reilly and Grasty, 2009).

Photoelectric absorption is the main mode of interaction of low energy gamma rays with the detector. In the photoelectric absorption process, a gamma photon, incident on an absorber atom, is completely absorbed. In its place, an energetic photoelectron is ejected by the atom from one of its bound shells. For gamma photons of sufficient energy, the most probable origin of the photoelectron is the most tightly bound or K shell of the atom. The photoelectron appears with kinetic energy given by equation (2.9).

$$E_{e^-} = E - E_b \,. \qquad (2.9)$$

Where E_{e^-} *is* the kinetic energy of the ejected photoelectron, E is the energy of the incident gamma ray and E_b is the binding energy of the photoelectron in its original shell. Since the energy of the incident gamma ray (typically about 0.5 MeV) is much greater than the binding energy of the electron of the ion (typically 10 - 100 eV), the energy of the freed electron may be considered to be equal to that of the incoming gamma ray. Thus

photoelectric effect results in a peak, called the photo peak, in the photomultiplier spectrum at energy equal to that of the incident gamma ray. Photoelectric effect increases with atomic numbers of the absorber atoms. This interaction leaves the absorber atoms in an ionized state with a vacancy in one of the bound electron shells (Knoll, 1999). A free electron may then be captured from the medium or an electron from the higher (outer) shell /orbital of the absorber atom may make a transition to fill the vacancy left. In this case characteristic X-rays are produced. The X-rays may be re-absorbed in the detector through photoelectric absorption involving electrons from less tightly bound shells and auger electrons may be produced (Turner, 2007). Compton scattering occurs when the incoming gamma ray photon is deflected through an angle θ with respect to its original direction. The photon transfers a portion of its energy to the electron known as the recoil electron. Since all the angles of scattering are possible the energy transferred to the recoil electron varies from zero and has a maximum value when the scattering angle reaches 180^0 (Tuner, 2007; Knoll, 1999). The electron recoils with a speed, v, at some angle, ϕ, with the initial direction of the photon. The probability of Compton scattering per atom of the absorber depends on the number of electrons in the atom and so it linearly increases with atomic number. The gamma rays initial wavelength is given by $\lambda = \frac{hc}{E}\ nm,$ where E is the energy of the incident gamma ray in joules. The change in wavelength due to reduction in energy of the gamma ray increases with the scattering angle θ according to the Compton formula given by equation (2.10).

$$\Delta\lambda = \frac{h}{mc}(1-\cos\theta). \tag{2.10}$$

Where $h = 6.63x10^{-34}$ Js is the Planck's constant, $m = 9.11x10^{-31}\,kg,$ the mass of the electron and $c = 3.0x10^{8}\,ms^{-1}$, the speed of light (Parks, 2009).

The effect of Compton scattering is illustrated in Figure 2.10.

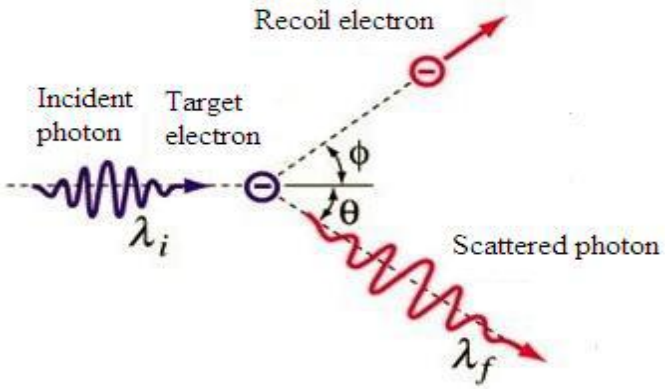

Figure 2.10: Diagram of compton scattering of photons (Bergstrom et al., 1993).

The energy of the scattered electron varies from zero to a maximum value, the Compton edge, due to a wavelength shift of 0.00486 nm. The energy distribution of Compton scattered electrons is essentially constant. The Compton spectrum produced by a photomultiplier tube is a flat plateau from zero energy up to the Compton edge where it drops off sharply at a rate limited by the energy resolution of the tube.

2.9 Radionuclide contamination of water sources

Underground water is vulnerable to contamination by soluble minerals in the rocks that they flow through before they reach the ground surface. These contaminants may include radioactive materials and as a result emit gamma radiations. A study on underground water sources of Iraqi Kurdistan region-Erbil found out that water was contaminated by radionuclides such as ^{238}U, ^{232}Th, ^{137}Cs and ^{40}K (Saman et al., 2016). Maximum activity concentrations for ^{238}U, were found in some water samples. The annual effective dose equivalent was found to be lower than the WHO safe limit of 0.1 $mSvy^{-1}$. Hence underground water from Erbil was found to be safe to be used for drinking and domestic purposes. Fakeha et al. (2014) found out that water samples from Western province of Saudi Arabia were contaminated with radionuclides such as ^{226}Ra, ^{232}Th and ^{40}K among others. The activity concentrations of ^{226}Ra ranged from Low Detectable Limit (LDL) to 2.5 Bql^{-1}, ^{232}Th ranged from LDL to 3.3 Bql^{-1} and ^{40}K ranged from LDL to 339.2 Bql^{-1}. The results showed that most of the estimated annual effective dose from samples exceeded the maximum permissible annual dose allowed by WHO of 0.1 $mSvy^{-1}$. A study was done on the concentration of radionuclide series by chemical analysis of bottled water

used in Italy and also estimated the absorbed dose for categories less than I year old to adults (Desideri et al., 2007). The activity concentrations of ^{226}Ra was found to range from 10.00 Bql^{-1} to 52.50 Bql^{-1}. Tchokossa et al. (2011) also analyzed water samples from oil and gas producing areas in Delta state Nigeria to assess radionuclide concentrations and absorbed dose from consumption of community water supplies. It was found that water samples were contaminated with radionuclides namely, ^{226}Ra, ^{232}Th and ^{40}K among others. The mean activity concentrations of ^{226}Ra, ^{232}Th and ^{40}K were (3.61 ± 1.78) Bql^{-1}, (2.26 ± 1.58) Bql^{-1} and (66.84 ± 21.00) Bql^{-1} for well water respectively. The annual effective dose equivalent was found to be (0.37 ± 0.18) mSvy^{-1} which was higher than the WHO limit hence it did show a significant health impact.

Ayodele et al. (2017) also analyzed water samples from Ondo and Ekiti states for gamma ray emitting radionuclides. It was found that the water samples contained radionuclides such as ^{226}Ra, ^{232}Th and ^{40}K among others. The mean activity concentrations of ^{232}Th, ^{40}K and ^{226}Ra were (8.43 ± 1.47) Bql^{-1}, (129.67 ± 8.27) Bql^{-1}, (15.83 ± 3.39) Bql^{-1} and (7.25 ± 1.69) Bql^{-1}, (156.57 ± 9.05) Bql^{-1}, (15.92 ± 3.68) Bql^{-1} for Ondo and Ekiti states respectively. The mean annual effective dose for children was found to be (6.52 ± 1.25) mSvy^{-1} and (5.90 ± 1.24) mSvy^{-1} for Ondo and Ekiti states respectively. For adults the values were found to be (6.56 ± 1.29) mSvy^{-1} and (5.18 ± 1.08) mSvy^{-1}. These values were above the WHO recommended limits of 0.1 mSvy^{-1}.

A study was also carried out on the distribution and activity concentrations of radionuclides in borehole water from Akure and Ondo states in Nigeria (Ibikunle et al., 2013). He found out that water samples contained ^{40}K, ^{226}Ra, and ^{232}Th that are emitters of gamma rays. The mean activity concentrations of ^{40}K, ^{226}Ra and ^{232}Th were (76.16 ± 18.97) Bql^{-1}, (9.51 ± 3.62) Bql^{-1} and (8.33 ± 3.79) Bql^{-1} respectively. The mean annual effective dose for infants was (6.72 ± 2.51) mSvy^{-1} which was extremely higher than the 0.1 mSvy^{-1} recommended by the WHO.

A study was also carried out on radionuclide concentration in water from boreholes in selected areas of Ogbomosoland (Awodugba and Tchokossa, 2008). All the water samples were found to contain gamma ray emitting radionuclides of ^{238}U, ^{232}Th and ^{40}K among others. The mean activity concentrations of values of ^{40}K, ^{232}Th and ^{238}U were found to be (3.98 ± 0.26) Bql^{-1}, (11.00 ± 2.58) Bql^{-1} and (17.73 ± 5.04) Bql^{-1} respectively. The mean

annual effective dose was found to be 0.123 $mSvy^{-1}$ which was high when compared with the recommended limit of 0.1 $mSvy^{-1}$ by the WHO.

Candia (2015) also carried out a study on radiological hazard levels by gamma emitting radionuclides in natural water bodies in selected sub counties of Mubende District in Uganda. He found out that all water samples contained radionuclides of ^{226}Ra, ^{232}Th and ^{40}K. The activity concentrations of ^{226}Ra, ^{232}Th and ^{40}K were found to range from (107.53 $\pm$ 2.60) Bql^{-1} to (97.41 $\pm$ 2.54) Bql^{-1}; (115.46 $\pm$ 1.56) Bql^{-1} to (69.76 $\pm$ 1.20) Bql^{-1} and (18.03 $\pm$ 1.37) Bql^{-1} to (14.24 $\pm$ 1.25) Bql^{-1} respectively. The activity concentrations of ^{226}Ra and ^{232}Th were found to exceed the world average values of 35 Bql^{-1} and 30 Bql^{-1} respectively. The mean absorbed dose rate was found to be 120.17 $nGyh^{-1}$ and 87.76 $nGyh^{-1}$ in Bukuya and Kassanda sub counties respectively which was higher than the world average value of 84 $nGyh^{-1}$. The mean annual effective dose equivalent was found to be 0.3 $mSvy^{-1}$ which was higher when compared with the recommended limit of 0.1 $mSvy^{-1}$ by the WHO. The mean internal and external hazard levels were found to be less than unity according to the ICRP recommendations.

CHAPTER THREE: METHODOLOGY OF THE STUDY

3.1 Introduction

This study was based on the use of sodium iodide detector to identify the gamma ray emitting radionuclides. The raw data collected was then used to determine activity concentrations of gamma ray emitting radionuclides. The activity concentrations obtained were then used to determine absorbed dose rates, annual effective dose equivalent, internal and external radiological hazard levels. The detailed procedures that were followed for determining activity concentrations, absorbed dose rates, annual effective dose equivalent, internal and external radiological hazard levels by gamma rays have also been discussed. The research designs that were followed in the study together with sampling and sample preparation that was carried out on the samples have also been described in this chapter.

3.2 Research design

The research involved exploratory and descriptive research designs. The Exploratory research design was first carried out to find the number and distribution of boreholes in Moroto District. This was done by reviewing the literature from the Directorate of Water Development, Ministry of Water and Environment about the distribution of boreholes in Moroto District. Further exploratory study was done by reviewing the literature from the department of geological survey and mines, Ministry of Energy and Mineral Development, on the kind of minerals contained in soils and rocks in the area under study. Further exploratory study was done by reviewing literature from a study that was done on mineral distribution in Karamoja region (Kabongo et al., 2014). The exploratory research design was to support the descriptive research design and the descriptive research design was based on the use of radioactive nuclide NaI(Tl) detector to measure activity concentrations of the possible radioactive materials that were present in the water samples. The descriptive research was also used for finding the mean, range, activity concentrations, absorbed dose rates, annual effective dose equivalent and the radiological hazard levels in the four different regions. The major focus of the research design was to measure the activity concentrations of the gamma ray emitting radionuclides using Sodium Iodide detector in the radio isotope laboratory.

3.3 Sampling and preparation of samples

The study was carried out in Moroto district which has six sub counties. Basing on the information on the distribution of boreholes, only four sub counties of Rupa, Katikekil, Nadunget and Norther Division were considered for the study. This was because the sub counties had the rock geology associated to igneous and sedimentary rocks that hosts several radioactive minerals that could contaminate underground water sources. They also had many boreholes and are easily accessible unlike Tapac sub county that has hostile communities. In order not to confuse the samples collected for analysis, Rupa sub county was designated region A and any sample picked from Rupa was lebelled A_1, A_2, A_3, A_4, A_5, A_6, and A_7. Katikekile sub-county was designated region B and any sample picked from Katikekile was lebelled B_1, B_2, B_3, B_4, B_5, B_6, and B_7. Nadunget sub-county was designated region C and any sample picked from Nadunget was lebelled C_1, C_2, C_3, C_4, C_5, C_6, and C_7. Northern division was designated region D and any sample picked from Northern division was lebelled D_1, D_2, D_3, D_4, D_5, D_6, and D_7. The study was designed to cater for seven (7) boreholes in each of the four regions. The seven boreholes were selected from several boreholes in order to give a good variety of the boreholes and this was done by random sampling. The boreholes sampled were at a distance greater than 500 m away from each other.

Based on the research design names of boreholes were written on pieces of paper, shaken and only seven (7) boreholes were randomly selected from each of the four regions of Rupa, Katikekile, Nadunget and Northern Division. A total of twenty eight (28) water samples were collected from the selected boreholes and taken for analysis. The water samples were collected directly using clean half (0.5) litre mineral water bottles and were labeled according to the regions. The water samples were then transferred in to a standard polyethylene marinelli beaker in the laboratory for analysis.

3.4 Identification of radionuclides in water samples

The water samples were analyzed for the existence of gamma ray emitting radionuclides and the activity concentrations of the radionuclides determined using Sodium Iodide (NaI) detector, GDM 20 series that is Thallium activated. The system made use of an IBM compatible personal computer. The detector operated using a cylindrical NaI(Tl) crystal of

height 7.62 cm and diameter 7.62 cm. The calibration of the detector for energy and efficiency was first done before the detector was used for any experimental work.

The energy calibration was done using ^{152}Eu solution over the energy range of 0.344 MeV to 1.41 MeV. The ^{152}Eu radioisotope was selected because it emits gamma rays of known energies and sufficient intensity. The 0.344 MeV gamma ray energy indicates the beginning and 1.41 MeV energy indicates the end of the energy range. These two gamma energy peaks were analysed using AutoDAS 3.16 to calibrate the energy axis of the detector. The energy calibration was stored in the computer with code BKGM17. The efficiency calibration of the detector was done at different gamma ray energies. The Eu-152 solution emits gamma quanta per second of energy 0.244 MeV. The activity was measured for a live time, t, and the area, A, of the corresponding photo peak was determined to Y pulses and the efficiency of the detector was then calculated using the equation (3.1).

$$\eta = \frac{Y}{At}. \tag{3.1}$$

Equation (3.1) was then used to obtain efficiency of the detector at other gamma ray energy peaks from ^{152}Eu. The energies used were 0.122 MeV, 0.245 MeV, 0.344 MeV, 0.780 MeV, 0.964 MeV, and 1.41 MeV (IAEA-PUB-1287, 2007). The efficiency was then plotted against the gamma ray energy to obtain an efficiency calibration curve of degree two given by the equation (3.2)

$$\eta = 6.3128E^2 - 15.857E + 11.834. \tag{3.2}$$

Where η is the efficiency for gamma rays with energy *E*.

The efficiency curve was then used to calculate the efficiency of the detector for gamma rays emitted by ^{238}U, ^{232}Th decay products and ^{40}K radionuclides in the sample. After the efficiency calibration of the GDM20 NaI(Tl) detector, the correction detector efficiency, c for each radionuclide detected in each sample is determined using equation (3.3).

$$c = k\eta. \tag{3.3}$$

Where k is the branching ratio of the radionuclide and η is the detector efficiency. The branching ratios (gamma ray emission probabilities) were obtained in the standard

radionuclide data tables from International Atomic Energy Agency Publication (IAEA-PUB- 1287, 2007).

The GDM 20 NaI(Tl) detector system and its photomultiplier tube was mounted in a box. The detector was surrounded by a silvered lead cylinder containing lead shots in order to shield it from back ground radiations. The hermetic seal protects the hydroscopic NaI from moisture absorption and other radiological influence. To reduce the effect of background radiations a cylindrical lead (10 cm) thick with a fixed bottom and a movable copper envelopes the detector. The lead shield contains an inner concentric cylinder of copper (0.3 mm) thick in order to absorb characteristic X- rays generated in the lead shield. The detector was connected to the computer with a multichannel analyzer (MCA) card and AutoDAS version 3.16. The detector system used in the experimental analysis is shown in the Figure 3.1

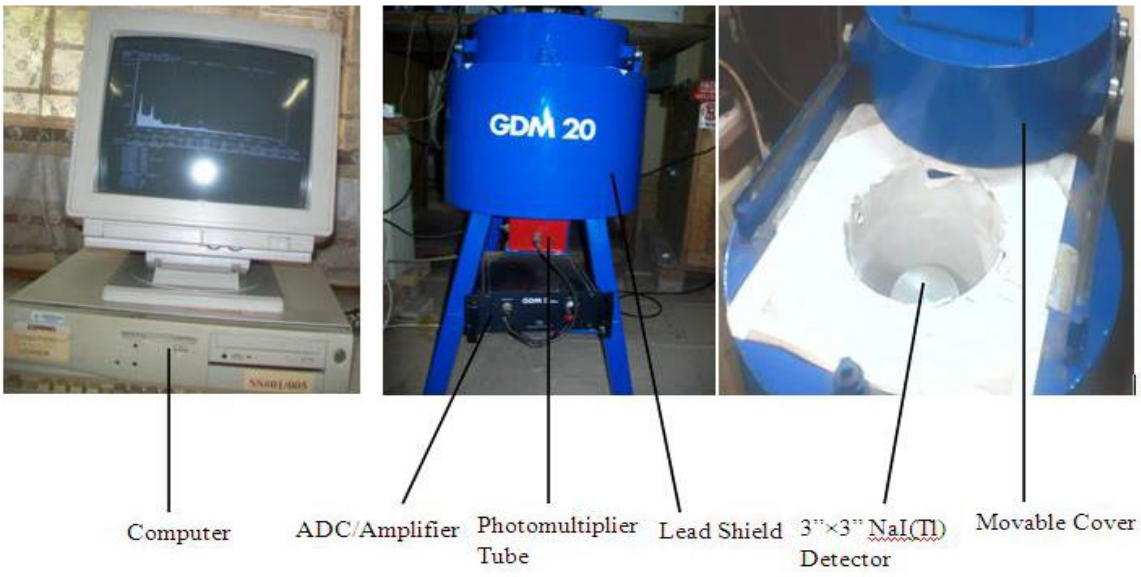

Figure 3.1: GDM 20 NaI(Tl) gamma ray detector.

The detector has an A/D converter which has 1024 channels and an amplifier time constant of 2 μs. The sample was mounted on the surface of the NaI(Tl) detector. When the gamma rays interact with the NaI crystal it creates a weak light. The light was collected and converted into electrical signals/ pulses in the photo multiplier tube (PMT).

The pulses are amplified and converted into digital information by the A/D converter. The information was then processed by the computer which presents it on the monitor as a frequency diagram or photo peaks of the distribution of the energy of the gamma quanta. The photo peaks were then analyzed in order to determine the activity concentrations of the radionuclides present in the water samples. Experimental peak energies were then determined from the computer software and were related to the theoretical energies of the different radionuclides.

The peak experimental energy of 85.92 keV corresponds to the theoretical energy of 84 keV for ^{228}Th radionuclide. The presence of ^{228}Th confirms the presence of ^{232}Th which is the parent radionuclide of ^{228}Th. The gamma rays at experimental energies in the range of 366.26 keV- 503.13 keV correspond to theoretical energy of 580 keV for ^{208}Tl radionuclide. This radionuclide is a daughter product of ^{232}Th radionuclide. This confirmed the presence of ^{232}Th in the samples. The gamma rays at experimental energies in the range of 191.70 keV- 238.27 keV detected in the samples corresponded to theoretical energy of 238 keV for ^{212}Pb a daughter product of ^{232}Th. This confirmed presence of ^{232}Th in the samples. The gamma rays at experimental energies in the range of 88.29 keV- 188.33 keV detected in the water samples corresponded to theoretical energy of 185 keV for ^{226}Ra which is a decay daughter radionuclide of ^{238}U radionuclide. Hence ^{238}U was present in the sample. Gamma rays at experimental energies in the range of 1188.83 keV- 1574.42 keV corresponded to theoretical energy of 1460 keV for ^{40}K radionuclide. This confirmed the presence of ^{40}K in the water samples. The photo peaks with experimental energies of less than 84 keV corresponded to the characteristic X- rays. The correction efficiencies for the GDM 20 Sodium Iodide gamma spectrometer are shown in the Table 3.1 (Technical Data for GDM 20, Makerere University Radioisotope Laboratory).

Table 3.1: Correction efficiencies for the detected radionuclides.

Energy/keV	Radionuclide	Series	Correction efficiency (c)
84	^{228}Th	^{232}Th	0.0286
185	^{226}Ra	^{238}U	0.0043
238	^{212}Pb	^{232}Th	0.0608
242	^{214}Pb	^{238}U	0.0104
295	^{214}Pb	^{238}U	0.0237
352	^{214}Pb	^{238}U	0.0300
580	^{208}Tl	^{232}Th	0.0101
610	^{214}Bi	^{235}U	0.0210
780	^{152}Eu	None	0.0296
1170	^{60}Co	None	0.0200
1460	^{40}K	None	$2.34x10^{-6}$

The values of the correction efficiency, basic data as in appendix A and the mass of the water samples as in appendix B were used in calculating the activity concentrations of the corresponding radionuclides for each sample.

The background radiation due to radiations from the external environment or impurity radionuclides in the detector was also measured with the movable cover of the detector open. The spectrum of the background radiation was stored in the computer with a file code of BK220219. The background spectrum was always subtracted from the spectrum obtained when the sample was run for a given live time. This was to obtain the net energy spectrum of only the radionuclides present in the water samples. During the analysis of the water samples, the polythene marinelli beaker was cleaned and its mass (MB) obtained from the weighing scale. The mass of the beaker and water sample (MBW) was also obtained. This was then used to determine the mass of the water sample (MW) that was used during the analysis by subtraction. The sample in the marinelli beaker to be analyzed was placed on the detector. The analysis was run for a live time of 1511 seconds. The spectrum obtained for the test water sample was stored with a specific file name for example OKRUPA1. This procedure was followed for all the other water samples that were analyzed. The water samples from each borehole from all the regions were analyzed once and the spectrum obtained used for identifying the radionuclides present in the sample. The net photo peak count / spectrum obtained after subtracting the background radiation spectrum was used for computing the basic data that included; centriod energy,

the standard deviation, Full Width at Half Maximum (FWHM), net area (sum between markers) and the count rate for each sample.

3.5 Radiological parameters

The radiological parameters that were measured and determined in the study included; activity concentration, absorbed dose rates, annual effective dose equivalents and the internal and external hazard levels.

3.5.1 Measurement of activity concentration

The activity concentrations, A, of the radionuclide present in each photo peak was determined from the basic data using the equation (3.4).

$$A = \frac{N}{tmc}. \tag{3.4}$$

Where A *is the activity concentration*

N – *Net photo peak count*
m – *mass of water sample under analysis*
c – *correction coefficient for the radionuclide*
t – *counting time*

But $\frac{N}{t} = Rate\ of\ acquisition\ of\ net\ photo\ peak\ count.$

The rate of acquisition of the net photo peak count as in appendix A and the mass of the water samples as in appendix B were used for determining the activity concentration. The values of activity concentrations obtained were used for finding the radiological parameters of; absorbed dose rate, annual effective dose equivalent and internal and external radiological hazard levels by the gamma rays in the water samples.

3.5.2 Absorbed dose rates

The absorbed dose rates were obtained from the activity concentrations of the radionuclides and the corresponding dose coefficients for three radionuclides of ^{40}K, ^{226}Ra and ^{232}Th using the equation (3.5).

$$D\left(nGy\,h^{-1}\right) = 0.92\,A_{Ra} + 1.10\,A_{Th} + 0.08\,A_{K}\,. \tag{3.5}$$

Where

D – *is the absorbed dose rate in* $nGy\,h^{-1}$ *and* A_{Ra}, A_{Th} *and* A_{K} *are the activity concentrations of* ^{226}Ra, ^{232}Th *and* ^{40}K *respectively*.

The dose coefficients of 0.92, 1.10 and 0.08 are for the radionuclides of Radium, Thorium and Potassium respectively and are in units of $nGy\,h^{-1}$ *per* $Bq\,l^{-1}$ (UNSCEAR, 2000). The activity concentrations of the radionuclides are obtained from the basic data.

3.5.3 Annual effective dose equivalent

The annual effective dose equivalent from the radionuclides was obtained from the activity concentrations of the radionuclides, intake of water for a person in one year and the effective dose equivalent conversion factor as per equation (3.6).

$$AEDE = \sum A_i\,.\,R_i\,.\,D_F\,. \tag{3.6}$$

Where

AEDE is the annual effective dose equivalent,
A_i *is the activity concentration of the radionuclide* $\left(Bql^{-1}\right)$
R_i *is the* int*ake of water for a person in one year*
D_F *is the effective dose equivalent conversion factor* $\left(mSv\,Bq^{-1}\right)$

The annual effective dose equivalent was determined for children and adults. This was obtained by assuming that children (5- 15 years) take on average a minimum of 1.2 litres and an adult person (18- 60 years) takes on average a minimum of two (2.0) litres of water a day basing on ICRP and WHO. In one year a minimum of 438 litres and 730 litres of water would be consumed by children and adults respectively. The effective dose equivalent conversion factors vary depending on the radionuclide intake and the age group according to the ICRP and WHO as in appendix B.

3.5.4 Internal and external hazard levels

The internal and external radiological hazard levels from the radionuclides were obtained from the activity concentrations and the maximum permissible concentrations of the radionuclides using equations below. The maximum permissible concentrations of Radium, Thorium and Potassium are 370 Bql^{-1}, 259 Bql^{-1} and 4810 Bql^{-1} respectively. Internal radiological hazard index was obtained by reducing the maximum permissible concentration of radium of 370 Bql^{-1} by a half to 185 Bql^{-1}, and was determined from the formula given by equation (3.7).

$$H_{in} = \frac{A_{Ra}}{185} + \frac{A_{Th}}{259} + \frac{A_K}{4810} \tag{3.7}$$

Where A_{Ra}, A_{Th} *and* A_K *are the activity concentrations of* ^{226}Ra, ^{232}Th *and* ^{40}K *respectively*.

External radiological hazard level or index was determined based on the criterion introduced using a proposed model (Krieger, 1981) as given in equation (3.8).

$$H_{ex} = \frac{A_{Ra}}{370} + \frac{A_{Th}}{259} + \frac{A_K}{4810} \tag{3.8}$$

3.6 Analysis of data

The major prominent photo peaks that were displayed were used for finding the basic data. The basic data included the centroid energy, standard deviation, Full Width at Half Maximum (FWHM), sum between markers or the net photo peak count, acquisition time and the rate. The centroid energy was used in the identification of the radionuclide and the rate was used for finding the activity concentrations of the radionuclides present in the water samples. The radionuclides of interest were ^{226}Ra, ^{232}Th and ^{40}K because they are the daughter and parent radionuclide emitters of gamma rays. Data that was obtained about activity concentrations of the radionuclides, absorbed dose rates, annual effective dose equivalent, external and internal radiological hazard levels were analyzed using statistical mean and range. Excel windows software was used to plot the column bar graphs.

CHAPTER FOUR: RESULTS OF THE STUDY

4.1 Introduction

The study focused on detecting radionuclides in water samples and determination of their activity concentrations, absorbed dose rates, annual effective dose equivalent and internal and external radiological hazard levels. The radionuclides detected, activity concentrations, absorbed dose rates, annual effective dose equivalent, internal and external radiological hazard levels in the water samples were compared for the four regions in Moroto District.

4.2 Gamma ray emitting radionuclides detected in water samples

The detection of gamma ray emitting radionuclides in the water samples was based on the identification of the presence of prominent photo energy peaks of the spectra that were generated by gamma rays from each radionuclide present in the samples. The radionuclides detected from the water samples in the four different regions are shown in Table 4.1.

Table 4.1: Radionuclides detected in the water samples from the four regions.

Regions	**Rupa**	**Katikekile**	**Nadunget**	**Northern Division**
Radionuclides	^{232}Th (^{228}Th)	^{232}Th (^{228}Th)	^{232}Th (^{228}Th)	^{232}Th (^{228}Th)
	^{238}U (^{226}Ra)	^{238}U (^{226}Ra)	^{238}U (^{226}Ra)	^{238}U (^{226}Ra)
	^{232}Th(^{212}Pb)	^{232}Th(^{212}Pb)	^{232}Th(^{212}Pb)	^{232}Th(^{212}Pb)
	^{238}U(^{214}Pb)	^{238}U(^{214}Pb)	^{238}U(^{214}Pb)	^{238}U(^{214}Pb)
	^{232}Th (^{208}Tl)	^{232}Th (^{208}Tl)	^{232}Th (^{208}Tl)	^{232}Th (^{208}Tl)
	^{235}U (^{214}Bi)	-	^{235}U (^{214}Bi)	-
	^{60}Co	^{60}Co	^{60}Co	-
	^{40}K	^{40}K	^{40}K	-
	-	-	-	^{152}Eu

In the detection of gamma ray emitting radionuclides, the prominent photo peak counts were identified and their experimental energies determined. The radionuclides of ^{226}Ra,

^{232}Th were detected in all the four regions of Rupa, Katikekile, Nadunget and Northern Division. The radionuclide of ^{40}K was detected in some boreholes in Rupa, Katikekile and Nadunget sub-counties whereas in Northern Division it was not detected.

4.3 Activity concentrations of radionuclides in the water samples

The activity concentrations of the three identified gamma ray emitting radionuclides of; ^{232}Th, ^{226}Ra and ^{40}K in each sample were determined using the equation (4.1).

$$\text{Activity concentration, A, } = \frac{N}{mct} \quad \text{in } Bql^{-1} \tag{4.1}$$

where N is the net photo peak count, m is the mass of the water sample that was under analysis, c is the detector correction coefficient for the radionuclide and t is the counting time. But $\frac{N}{t} = Rate\ of\ acquisition\ of\ net\ photo\ peak\ count$. The activity concentration of ^{226}Ra was calculated from the gamma ray photo peak corresponding to ^{226}Ra a decay daughter nuclide of ^{238}U at the gamma ray energy of 185 keV. The activity concentration of ^{232}Th was determined from the gamma ray spectra of ^{228}Th, ^{212}Pb, ^{208}Tl at the energies of 84 keV, 238 keV and 580 keV respectively. The activity concentration of ^{40}K was determined through its own gamma ray spectrum at the energy of 1460 keV. The activity concentrations of ^{226}Ra, ^{232}Th, and ^{40}K obtained in each borehole during the study were compared with the world population average activity concentrations of 35 Bql^{-1}, 30 Bql^{-1} and 400 Bql^{-1} (UNSCEAR, 2000) for ^{226}Ra, ^{232}Th and ^{40}K respectively.

4.3.1 Gamma ray emitting radionuclides activity concentrations in Rupa, Katikekile, Nadunget and Northern Division

The values of activity concentrations of ^{226}Ra, ^{232}Th, and ^{40}K from borehole water samples in the four sub counties of Rupa, Katikekile, Nadunget and Northern Division are shown in Table 4.2. The activity concentrations in each sub county was plotted in form of a bar graph to show how the concentrations were varying from one borehole to another. The radiological parameters were also compared to show their variation across regions. The values of activity concentrations of ^{226}Ra, ^{232}Th, and ^{40}K that are the daughter and parent gamma ray emitting radionuclides were compared with the world average values of 35 Bql^{-1}, 30 Bql^{-1} and 400 Bql^{-1} for ^{226}Ra, ^{232}Th and ^{40}K respectively.

Table 4.2: Activity concentrations of the three radionuclides in water from the four regions.

BH	Activity Concentration/Bql^{-1}											
	^{226}Ra				^{232}Th				^{40}K			
	A	**B**	**C**	**D**	**A**	**B**	**C**	**D**	**A**	**B**	**C**	**D**
1	72.64	88.94	37.95	55.51	26.45	8.20	1.43	8.91	2170.0	0.0	3670.0	0.0
2	32.41	36.18	75.25	21.14	2.48	5.90	16.22	3.24	0.0	1210.0	4120.0	0.0
3	29.29	26.33	57.11	18.89	5.28	5.11	9.11	3.47	0.0	4360.0	3610.0	0.0
4	68.81	60.58	86.58	14.94	14.65	7.63	24.31	2.79	1460.0	1260.0	3110.0	0.0
5	18.99	27.68	92.34	80.63	2.91	6.66	18.48	27.54	0.0	0.0	0.0	0.0
6	55.06	108.04	62.34	73.09	5.95	25.29	20.35	16.66	0.0	0.0	0.0	0.0
7	34.41	20.80	55.60	30.33	7.31	5.37	13.23	4.29	0.0	0.0	863.0	0.0
Average	**44.52**	**52.65**	**66.74**	**42.08**	**9.29**	**9.17**	**14.73**	**9.56**	**1815.0**	**2276.7**	**3074.6**	**0.0**

BH: Boreholes A: Rupa B: Katikekile C: Nadunget D: Northern Division

The activity concentrations of the radionuclides were found to vary from one region to another. The activity concentrations of ^{226}Ra in Rupa was found to vary from one borehole to another. The average activity concentrations of ^{226}Ra was also found to different across regions. The variation in the activity concentration of ^{226}Ra in the Rupa was plotted in form of a bar graph as shown in Figure 4.1.

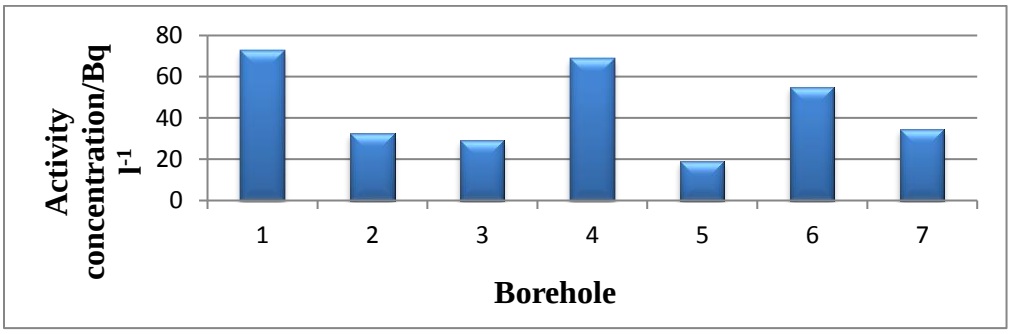

Figure 4.1: Bar graph of activity concentrations of ^{226}Ra in Rupa water samples.

The activity concentrations of ^{226}Ra in Rupa ranged from 72.64 Bql^{-1} to 18.99 Bql^{-1}. The concentrations of ^{226}Ra in water samples obtained from Rupa were compared with the

world average value of 35 Bql^{-1}. Water samples from boreholes 1, 4 and 6 located at Rupa Primary School, Musupo Primary School and Namogorat respectively exceeded the world average value of 35 Bql^{-1}. These boreholes were located on the slopes of the mount Moroto. The rocks in those areas had large deposits of radium that had dissolved in water. It was also found out that the average activity concentration of ^{226}Ra varied from one region to the other. The average activity concentration of ^{226}Ra from each of the four regions exceeded the world average value of 35 Bql^{-1}.

The activity concentrations of ^{232}Th in Rupa was found to vary from one borehole to another and its variation was plotted in form of a bar graph shown in Figure 4.2.

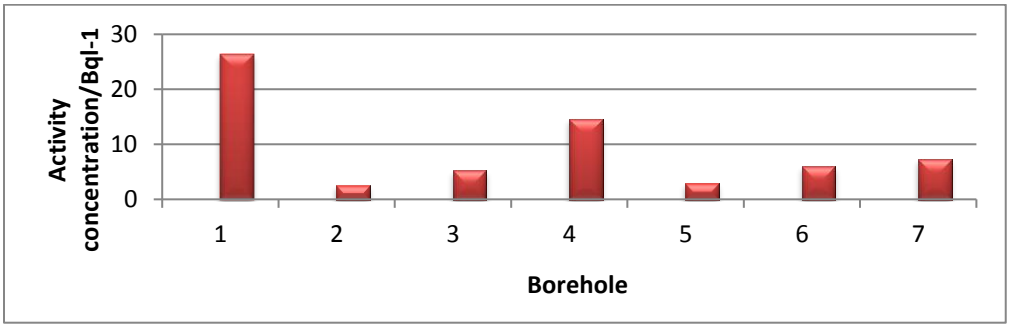

Figure 4.2: Bar graph of activity concentrations of ^{232}Th in Rupa water samples.

The activity concentration of ^{232}Th was found to range from 26.45 Bql^{-1} to 2.48 Bql^{-1}. The activity concentrations of ^{232}Th from boreholes in Rupa were compared with the world average activity concentration of 30 Bql^{-1}. It was found out that water samples from all selected boreholes in this region were below the world average value. It was noted that boreholes 1 and 4 located at Rupa and Musupo primary schools had the highest activity concentrations compared to the other five boreholes although it was below the world average value. The boreholes 1 and 4 are located on the slopes of mount Moroto while the other boreholes were on the flat land. The slopes of mount Moroto had more dissolved compounds of ^{232}Th in underground water. The average activity concentration of ^{232}Th was also found to vary from one region to another. It was also found to be below the world average value of 30 Bql^{-1} in all the four regions.

The activity concentrations of ^{40}K in Rupa was detected in only two boreholes while the other boreholes were below detectable limits. In borehole 1 located at Rupa Primary School the activity concentration of ^{40}K was found to be 2170.00 Bql^{-1} while in borehole 4 located at Musupo Primary School the activity concentration determined was found to be 1460.00 Bql^{-1}. The activity concentration was compared with the world average value of 400 Bql^{-1}. The activity concentration of ^{40}K in these boreholes exceeded the world average value. The soils and rocks in areas around Rupa and Musupo Primary schools found at the slopes of mount Moroto were rich in ^{40}K that had dissolved in the underground water compared to other areas in the region (Kabongo et al., 2014).

The activity concentrations of ^{40}K in Rupa was found to vary from one borehole to another and its variation was plotted in form of a bar graph shown in Figure 4.3.

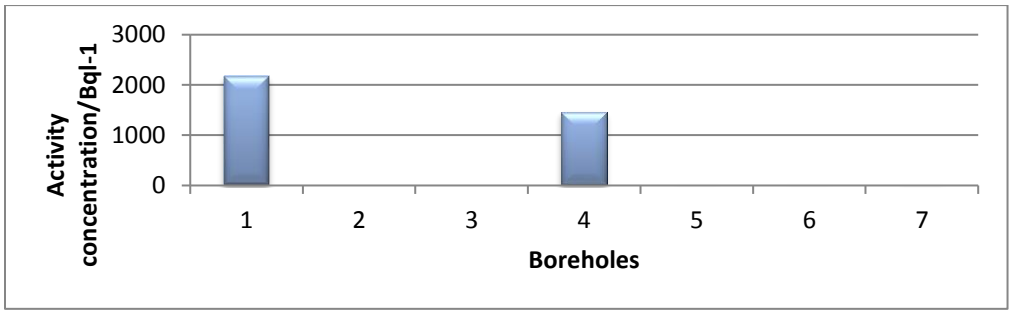

Figure 4.3: Bar graph of activity concentrations of ^{40}K in Rupa water samples.

The concentration of ^{226}Ra in Katikekile was found to vary from one borehole to another. The variation in the activity concentration of ^{226}Ra in Katikekile was plotted in form of a bar graph shown in Figure 4.4.

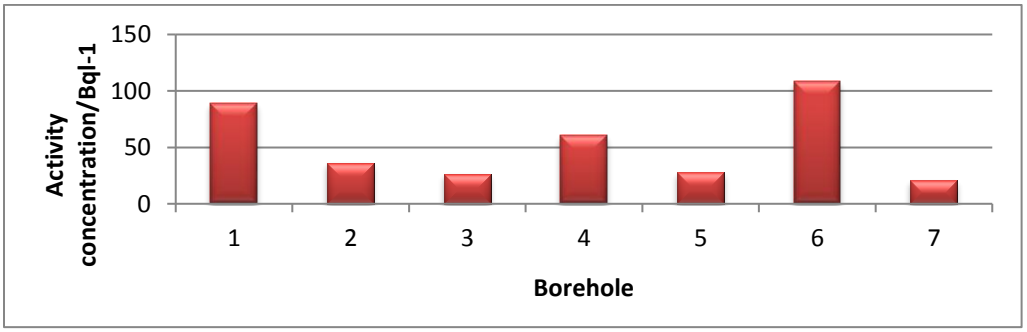

Figure 4.4: Bar graph of activity concentrations of ^{226}Ra in Katikekile water samples.

The activity concentrations of ^{226}Ra in Katikekile ranged from 108.04 Bql^{-1} to 20.80 Bql^{-1}. It was found out that the activity concentrations of ^{226}Ra in boreholes 1, 2, 4 and 6 located at Makalas, Morutomei, Lomuyembe and Lomunyen exceeded the world average value. These boreholes were located on the slopes of mount Moroto where rocks had high accumulation of radioactive minerals. The activity concentration of ^{226}Ra was found to be higher in borehole 6 and 1 located at Lomunyen and Makalas.

The activity concentrations of ^{232}Th in Katikekile was found to vary from one borehole to another. The variation in the activity concentration of ^{232}Th in Katikekile was plotted in form of a bar graph as shown in Figure 4.5.

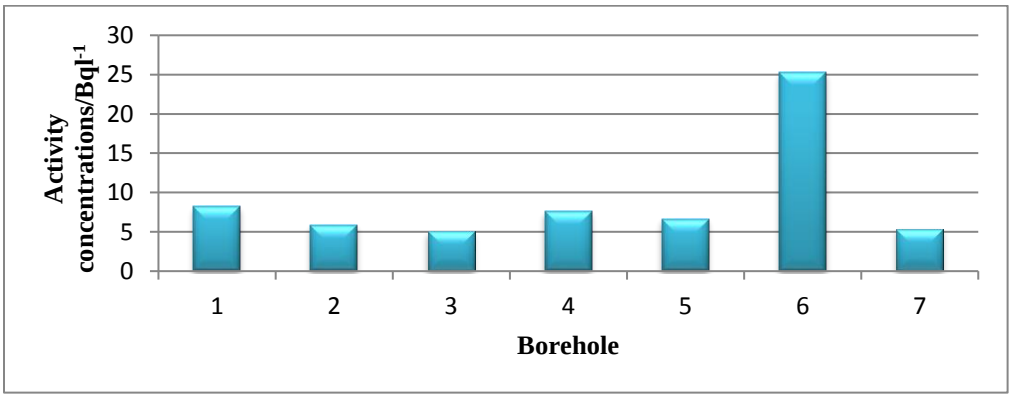

Figure 4.5: Bar graph of activity concentrations of ^{232}Th in Katikekile water samples.

The activity concentration of ^{232}Th in Katikekile was found to range from 25.29 Bql^{-1} to 5.11 Bql^{-1}. All the boreholes selected in the region did not exceed the world average value of 30 Bql^{-1}. Although the activity concentration of ^{232}Th in Katikekile was found to be lower than the world average value, the highest activity concentration was found in borehole 6 located at Lomunyen. This implies that the soils and rocks around Lomunyen were rich in ^{232}Th that had dissolved in water.

The activity concentrations of ^{40}K in Katikekile was found to vary from one borehole to another. It was found that ^{40}K was detected in only three boreholes while the other four

boreholes were at low detectable limits. The variation in the activity concentration of ^{40}K in the region was plotted in form of a bar graph shown in Figure 4.6.

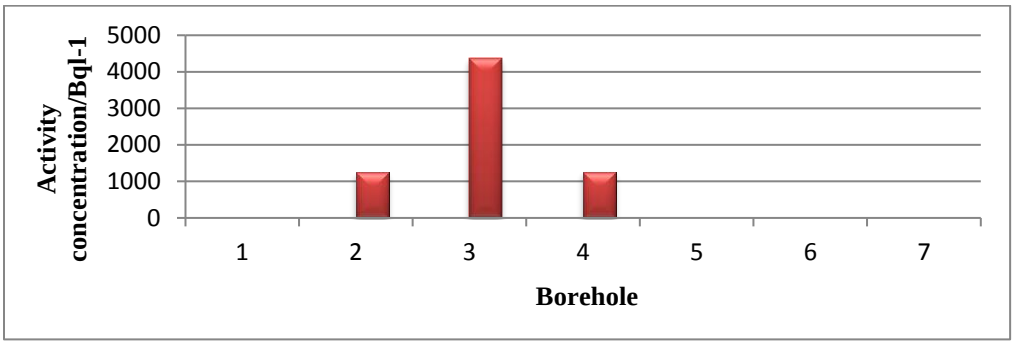

Figure 4.6: Bar graph of activity concentrations of ^{40}K in Katikekile water samples.

The activity concentrations of ^{40}K in Katikekile was found to range from 4360.00 Bql^{-1} to 1240.00 Bql^{-1}. The boreholes 2, 3 and 4 located at Morutomei, Lia Primary School and Lomuyembe where ^{40}K was detected exceeded the world average activity concentration of 400 Bql^{-1}. These boreholes were located on the slopes of the mount Moroto where rocks had high accumulation of radioactive minerals. Although the activity concentration of ^{40}K exceeded the world average value, it was found to be highest in borehole 3 located at Lia Primary School.

The concentration of ^{226}Ra in Nadunget was found to vary from one borehole to another. The bar graph was used to compare the activity concentration of ^{226}Ra in Nadunget as shown in Figure 4.7.

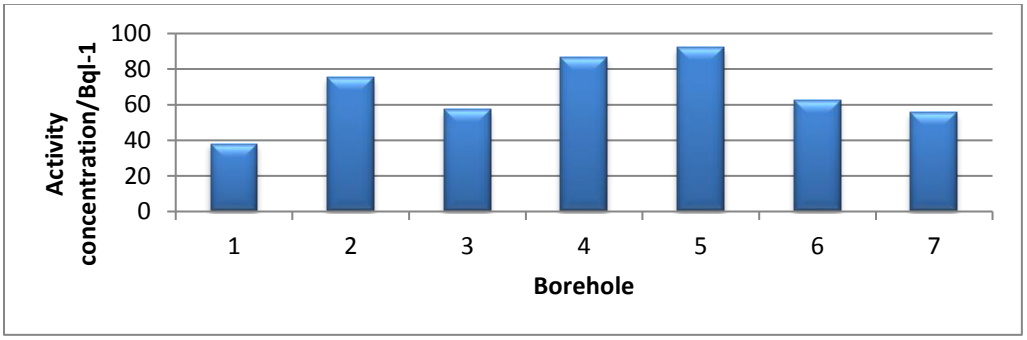

Figure 4.7: Bar graph of activity concentrations of ^{226}Ra in Nadunget water samples.

The activity concentrations of ^{226}Ra in water samples from Nadunget ranged from 92.34 Bql^{-1} to 37.95 Bql^{-1}. The activity concentrations of ^{226}Ra in all selected boreholes were found to exceed the world average value of 35 Bql^{-1}. Although the activity concentration of ^{226}Ra exceeded the world average value, it was found to be higher in boreholes 5, 4 and 2 located at Nabokat, Naitakwae Primary School and Kanakomol respectively compared to other boreholes. These boreholes were located on flat low land even though their activity concentrations were high compared to the other borehole water samples. The rock geology in the area had high accumulation of radioactive minerals.

The activity concentrations of ^{232}Th in Nadunget was also found to vary from one borehole to another. The variation in the activity concentration of ^{232}Th in Nadunget was plotted in form of a bar graph shown in Figure 4.8.

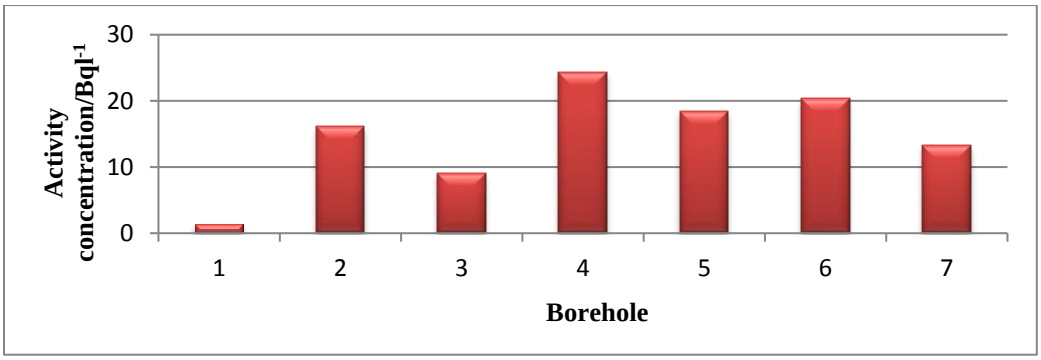

Figure 4.8: Bar graph of activity concentrations of ^{232}Th in Nadunget water samples.

The activity concentration of ^{232}Th was found to range from 24.31 Bql^{-1} to 1.43 Bql^{-1}. The activity concentration of ^{232}Th in all boreholes in the region did not exceed the world average value of 30 Bql^{-1}. Although the activity concentration of ^{232}Th in Nadunget was found not to exceed the world average value, the highest activity concentration was found in borehole 4 located at Naitakwae Primary School.

The activity concentrations of ^{40}K in Nadunget was found to vary from one borehole to another. It was found that ^{40}K was detected in only five boreholes, the two boreholes were at low detectable limits. The variation in the activity concentration of ^{40}K in the region was plotted in form of a bar graph shown in Figure 4.9.

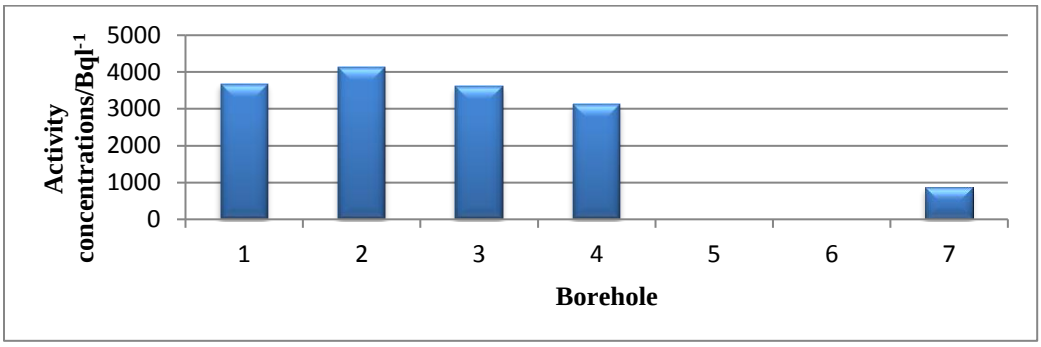

Figure 4.9: Bar graph of activity concentrations of ^{40}K in Nadunget water samples.

The activity concentrations of ^{40}K in Nadunget was found to range from 4120.00 Bql^{-1} to 863.00 Bql^{-1}. The boreholes 1, 2, 3, 4, and 7 located at Katanga, Kanakomol, Natinyonoit, Naitakwae and Nangorit where ^{40}K was detected in Nadunget exceeded the world average activity concentration of 400 Bql^{-1}. Although the activity concentration of ^{40}K detected in the boreholes exceeded the world average value, it was found to be highest in borehole 2 located at Kanakomol. However ^{40}K was not detected in the two boreholes 5 and 6 from Nabokat and Namijimij respectively.

The activity concentration of ^{40}K in Northern Division was not detected. The presence of ^{40}K was not as wide spread as was the case for ^{226}Ra and ^{232}Th in the four regions considered in the study. The concentration of ^{226}Ra in Northern Division was found to vary from one borehole to another. The variation of activity concentration of ^{226}Ra in Northern Division plotted in form of a bar graph as shown in Figure 4.10.

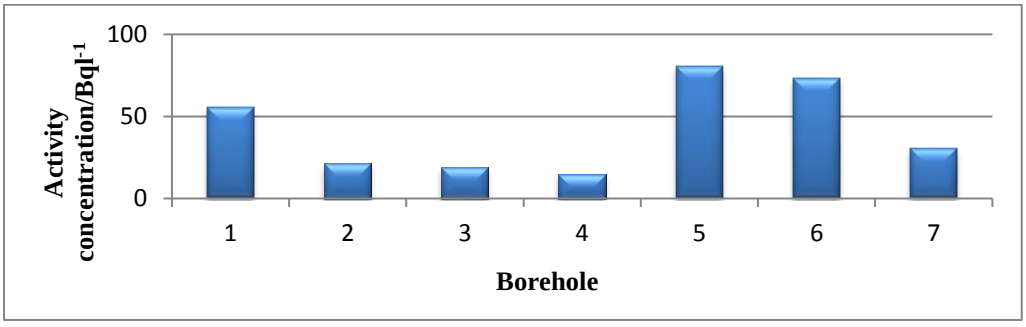

Figure 4.10: Bar graph of activity concentrations of ^{226}Ra in Northern Divisions samples.

The activity concentrations that were measured for ^{226}Ra in Northern Division ranged from 80.63 Bql^{-1} to 14.94 Bql^{-1}. The activity concentrations of ^{226}Ra in Northern Division was found to exceed the world average value of 35 Bql^{-1} in boreholes 1, 5 and 6 located at Moroto High School, Moroto Referral Hospital and Moroto Primary Teachers College. However the highest activity concentration was found in borehole 5 located at Moroto Referral Hospital as opposed to other boreholes. The bar graph of activity concentration of ^{232}Th in Northern Division is shown in Figure 4.11.

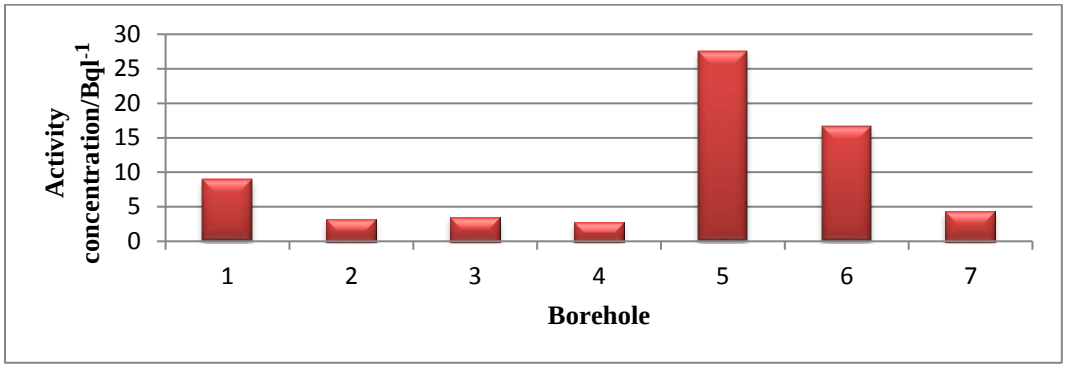

Figure 4.11: Bar graph of activity concentrations of ^{232}Th in Northern Division samples.

The activity concentration of ^{232}Th was found to range from 27.54 Bql^{-1} to 2.79 Bql^{-1}. The activity concentration of ^{232}Th determined in all boreholes did not exceed the world average value of 30 Bql^{-1}. Although the activity concentration of ^{232}Th was found to be below the world average value, high activity concentration was found in borehole 5 located at Moroto Referral Hospital.

The average activity concentration of ^{226}Ra was found to be different across the four regions. The variation of the average activity concentration across the regions was plotted in form of a bar graph as in Figure 4.12.

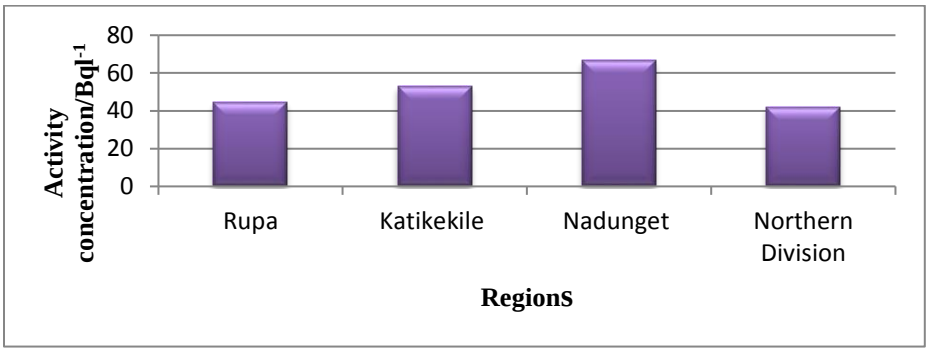

Figure 4.12: Bar graph of average activity concentration of ^{226}Ra in the four regions.

The results of the study found out that the average activity concentration of ^{226}Ra was high in Nadunget compared to the other three regions. This could be due to the fact that the rocks in Nadunget had high accumulation of compounds of ^{226}Ra that had dissolved in underground water.

The average activity concentration of ^{232}Th was also found to be different across the four regions. The variation of the average activity concentration across the regions was plotted in form of a bar graph as in Figure 4.13.

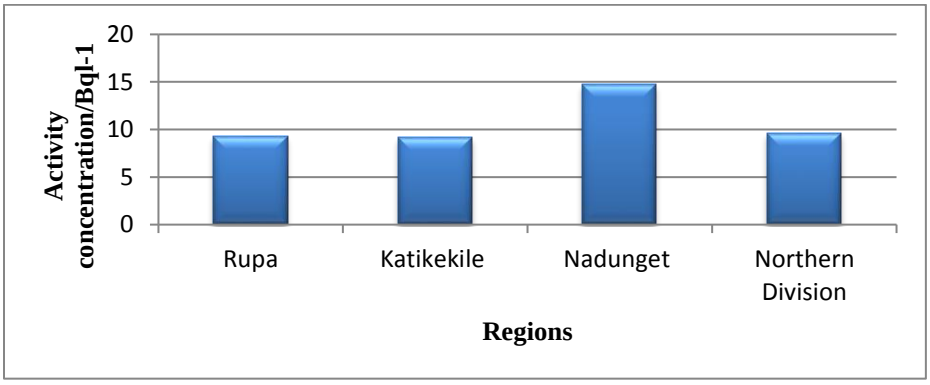

Figure 4.13: Bar graph of average activity concentration of ^{232}Th in the four regions.

The average activity concentration of ^{232}Th was found to be high in Nadunget compared to the other three regions. This could be due to the fact that the rocks in Nadunget had high accumulation of compounds of ^{232}Th that had dissolved in underground water.

The average activity concentration of ^{40}K was also found to be different across the four regions. The variation of the average activity concentration across the regions was plotted in form of a bar graph as in Figure 4.14.

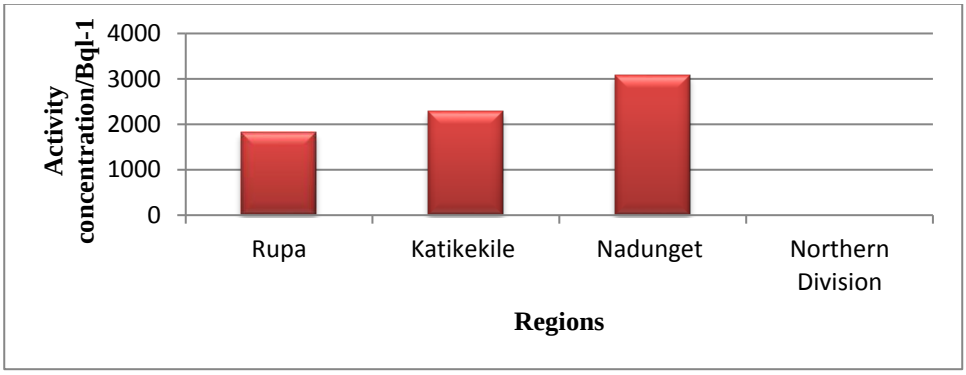

Figure 4.14: Bar graph of average activity concentration of ^{40}K in the four regions.

The average activity concentration of ^{40}K was also found to be high in Nadunget compared to the other three regions. This could be due to the fact that the rocks in Nadunget had high accumulation of compounds of ^{40}K that had dissolved in underground water. However ^{40}K was not as wide spread as ^{232}Th and ^{226}Ra in the four regions because at Northern Division it was at low detectable limits.

4.4 Gamma ray absorbed dose rates

The study was designed to determine the gamma radiation absorbed dose rates from radionuclides in water from the selected boreholes. The absorbed dose rates from the gamma ray emitting radionuclides in the water from different boreholes in the four regions are shown in Table 4.3. The absorbed dose rates in each of the boreholes obtained in the study from the four regions of Moroto district were compared with the world wide average value of 84 $nGyh^{-1}$ (UNSCEAR, 2000).

Table 4.3: Absorbed dose rates by gamma rays from water samples in the four regions.

Borehole	Absorbed dose rate/ $nGyh^{-1}$				World average value/$nGyh^{-1}$
	Rupa	Katikekile	Nadunget	Northern Division	
1	269.52	90.84	330.09	60.87	84.00
2	32.55	138.98	416.67	23.01	
3	32.75	378.64	351.37	21.20	
4	196.22	164.93	502.39	16.81	
5	20.67	32.79	105.28	104.47	
6	57.20	127.22	79.74	85.57	
7	36.70	25.04	134.77	32.62	
Average	**92.23**	**136.92**	**274.33**	**49.22**	

The study the absorbed dose rate was found to vary from one borehole to another. The average absorbed dose rate was also found to vary from one region to another. The absorbed dose rates determined in Rupa were found to vary from one borehole to another. The variation in the absorbed dose rates in Rupa was compared using a column bar chart shown in Figure 4.15.

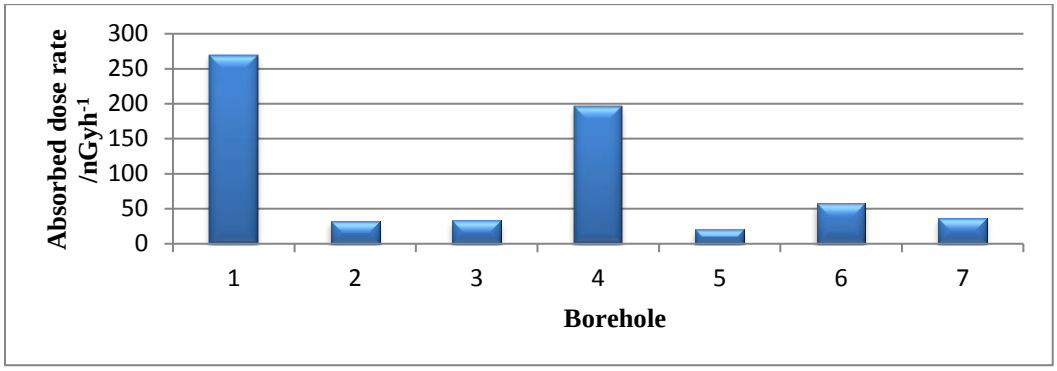

Figure 4.15: Bar graph of absorbed dose rates by gamma rays in Rupa.

The absorbed dose rates determined in Rupa ranged from 269.52 $nGyh^{-1}$ to 20.67 $nGyh^{-1}$. The absorbed dose rates were found to exceed the world average value of 84 $nGyh^{-1}$ in boreholes 1 and 4 located at Rupa Primary School and Musupo Primary School respectively. This was due to the high activity concentration of the three radionuclides of ^{226}Ra, ^{232}Th and ^{40}k in the water samples obtained from Rupa.

The absorbed dose rates in Katikekile was also found to vary from one borehole to another and its variation was also compared using a column bar chart shown in Figure 4.16.

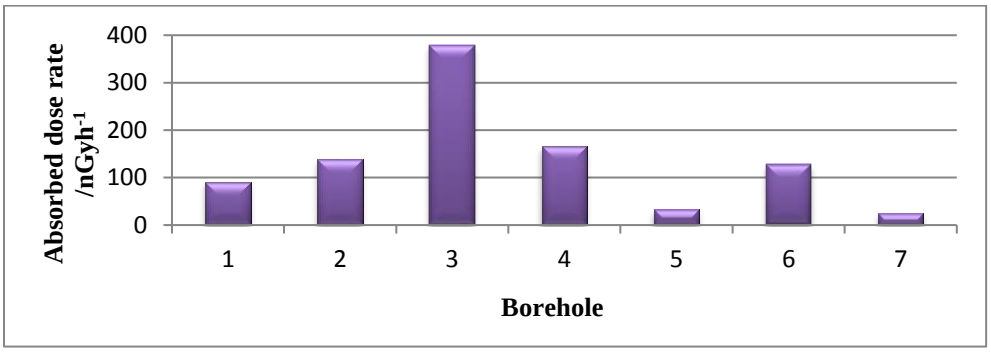

Figure 4.16: Bar graph of absorbed dose rates by gamma rays in Katikekile.

The absorbed dose rates that were determined in Katikekile ranged from 378.64 $nGyh^{-1}$ to 25.04 $nGyh^{-1}$. The absorbed dose rates were found to exceed the world average value of 84 $nGyh^{-1}$ except in boreholes 5 and 7 located at Lopeduru and Lokutakori respectively. This was due to the variation in the activity concentration of the three radionuclides of ^{226}Ra, ^{232}Th and ^{40}k in the water samples. However the absorbed dose rate in Katikekile was found to be high in borehole 3 located at Lia Primary School. The rocks found around Lia primary school had high accumulation of radioactive minerals. The water samples from boreholes that did not show presence of ^{40}K had low absorbed dose rates.

The absorbed dose rate in Nadunget was also found to vary from one borehole to another and its variation was compared using a bar graph as shown in Figure 4.17.

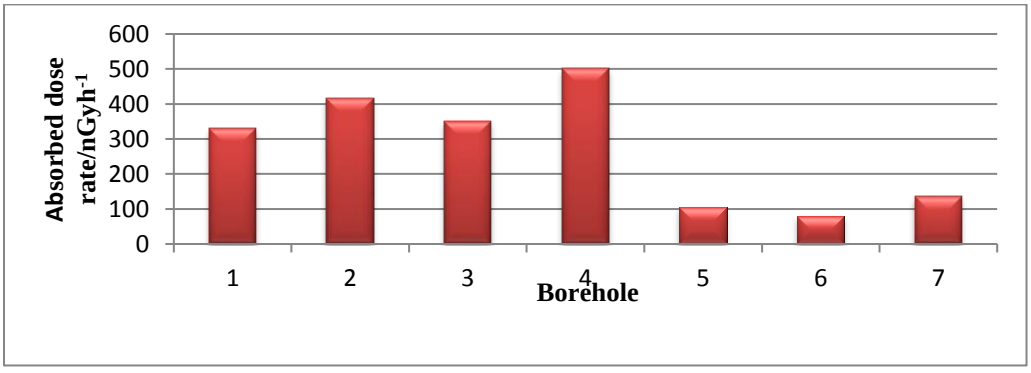

Figure 4.17: Bar graph of absorbed dose rates by gamma rays in Nadunget.

The absorbed dose rates that were determined in Nadunget ranged from 502.39 $nGyh^{-1}$ to 79.74 $nGyh^{-1}$. The absorbed dose rates were found to exceed the world average value of 84 $nGyh^{-1}$ except in boreholes 6 located at Namijimij. However the highest absorbed dose rate in the region was found in borehole 4 located at Naitakwae Primary School.

The absorbed dose rate in Northern Division was also found to vary from one borehole to another and its variation was compared using a column bar chart shown in Figure 4.18.

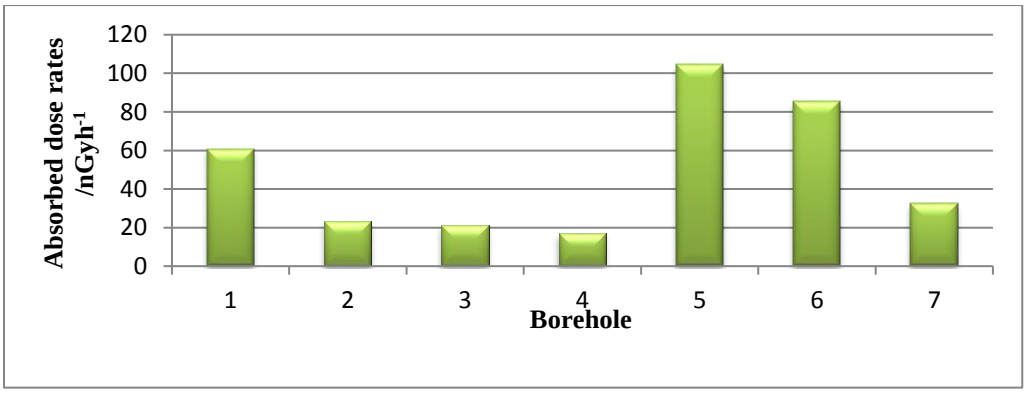

Figure 4.18: Bar graph of absorbed dose rate by gamma rays in Northern Division.

The absorbed dose rates determined in Northern Division ranged from 104.47 $nGyh^{-1}$ to 16.81 $nGyh^{-1}$. The absorbed dose rates were found to exceed the world average value of 84 $nGyh^{-1}$ in boreholes 5 and 6 located at Moroto Referral Hospital and Moroto Primary Teachers College. However the highest absorbed dose rate in the region was found in borehole 5 located at Moroto Referral Hospital.

The average absorbed dose rates was found to be different across the four regions. The variation of the average absorbed dose rate across the regions was plotted in form of a bar graph as in Figure 4.19.

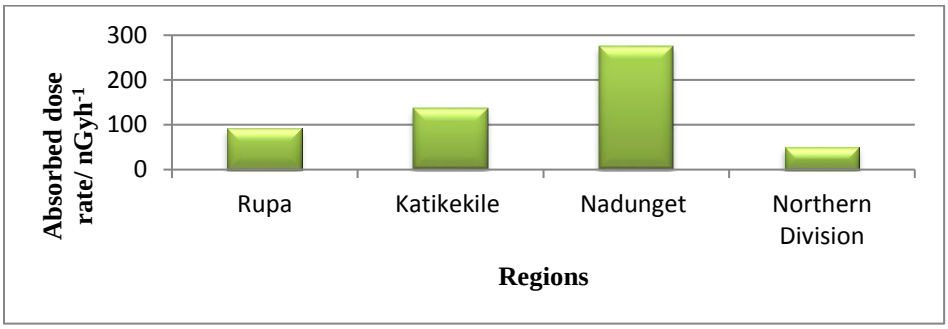

Figure 4.19: Bar graph of average absorbed dose rate in the four regions.

The average absorbed dose rate was found to be high in Nadunget compared to the other three regions. This could be due to the high activity concentration of the three radionuclides in this region. The high activity concentrations are as a result of high accumulation of dissolved radioactive minerals in underground water.

4.5 Annual effective dose equivalent by the gamma rays

The study was designed to determine the annual effective dose equivalent by gamma ray emitting radionuclides in water from selected boreholes in the four different regions and was determined for both children between the age of (5- 15) years and adults between the age of (18- 60) years. The effective dose equivalent conversion factors as in appendix B and daily intake of water for the children and adults (UNSCEAR, 2000) were used for determining the annual effective dose equivalent by gamma rays for children and adults. The annual effective dose equivalent determined in each borehole was compared with the world wide internal exposure limit of 0.41 $mSvy^{-1}$ (UNSCEAR, 2000).

4.5.1 Annual effective dose equivalent for children

The annual effective dose equivalent by gamma rays from the radionuclides in water samples from the four regions determined for children is as shown in Table 4.4.

Table 4.4: Annual effective dose equivalent by gamma rays for children.

Borehole	Annual effective dose equivalent/mSvy^{-1}				Worldwide internal exposure limit /mSvy^{-1}
	Rupa	Katikekile	Nadunget	Northern Division	
1	0.043	0.025	0.035	0.016	0.41
2	0.009	0.022	0.041	0.006	
3	0.009	0.048	0.050	0.006	
4	0.034	0.029	0.056	0.004	
5	0.005	0.009	0.028	0.026	
6	0.016	0.007	0.048	0.022	
7	0.010	0.001	0.025	0.009	
Average	**0.018**	**0.020**	**0.040**	**0.013**	

The annual effective dose equivalent by gamma rays in water samples determined for children in all the four regions were found to vary from one borehole to another. The average annual effective dose equivalent determined for children also varied from one region to another. The values of annual effective dose equivalent were found to be below the world wide internal exposure limit of 0.41 mSvy^{-1} in all the boreholes.

The average annual effective dose equivalent determined for the children was found to be different across the four regions. The variation of the average annual effective dose equivalent determined for the children across the four regions was plotted in form of a bar graph as in Figure 4.20.

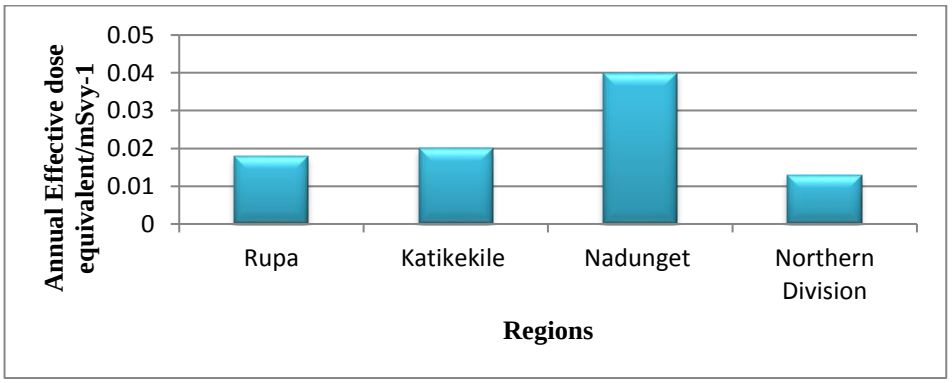

Figure 4.20: Bar graph of average annual effective dose equivalent for the children.

The average annual effective dose equivalent determined for children was found to be high in Nadunget compared to the other three regions. This could be due to the high

activity concentration of the three radionuclides in this region. The high activity concentrations are as a result of high accumulation of dissolved radioactive minerals in underground water.

4.5.2 Annual effective dose equivalent for adults

The Annual effective dose equivalent by gamma rays in each borehole as determined for adults are shown in Table 4.5.

Table 4.5: Annual effective dose equivalent by gamma rays for adults.

Borehole	**Annual effective dose equivalent/mSvy^{-1}**				**Worldwide internal exposure limit/msvy^{-1}**
	Rupa	**Katikekile**	**Nadunget**	**Northern Division**	
1	0.026	0.018	0.024	0.012	0.41
2	0.007	0.013	0.035	0.004	
3	0.006	0.025	0.029	0.004	
4	0.021	0.018	0.033	0.003	
5	0.004	0.006	0.020	0.018	
6	0.012	0.023	0.014	0.016	
7	0.007	0.005	0.016	0.006	
Average	**0.012**	**0.015**	**0.024**	**0.009**	

The annual effective dose equivalent by gamma rays in water samples determined for adults in all the four regions were found to vary from one borehole to another. The average annual effective dose equivalent determined for adults also varied from one region to another. The values of annual effective dose equivalent were found to be below the world wide internal exposure limit of 0.41 mSvy^{-1} in all the boreholes.

The average annual effective dose equivalent deternimed for the adults was found to be different across the four regions. The variation of the average annual effective dose equivalent deternimed for the adults across the four regions was plotted in form of a bar graph as in Figure 4.21.

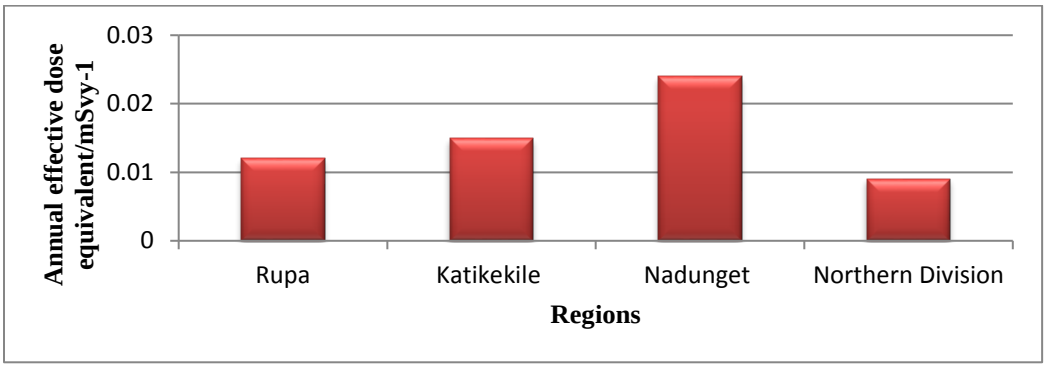

Figure 4.21: Bar graph of average annual effective dose equivalent for the adults.

The average annual effective dose equivalent determined for adults was found to be high in Nadunget compared to the other three regions.

4.6 Radiological hazard levels by gamma rays in water Samples

The radiological hazard levels by gamma rays in the water samples from selected boreholes involved in the study are internal and external hazard levels. The hazard levels were compared with the maximum permissible value of unity (1.00) as per the International Commission on Radiological Protection (ICRP).

4.6.1 Internal radiological hazard levels by gamma rays in water samples

The internal hazard level by gamma rays from radionuclides in each of the water samples from boreholes in the four regions were determined and shown in Table 4.6.

Table 4.6: The Internal hazard levels by gamma rays in the four Regions.

Borehole	**Internal hazard level;H_{in}**			
	Rupa	**Katikekile**	**Nadunget**	**Northern Division**
1	0.95	0.51	0.97	0.33
2	0.18	0.48	1.33	0.13
3	0.18	1.07	1.09	0.12
4	0.73	0.62	1.21	0.09
5	0.11	0.18	0.57	0.54
6	0.32	0.68	0.42	0.46
7	0.21	0.13	0.35	0.18
Average	**0.38**	**0.52**	**0.85**	**0.26**

The internal hazard level obtained in Rupa ranged from 0.95 to 0.11. The internal hazard levels varied from one borehole to another. The average internal hazard levels were also

found to vary from one region to another. The variation of internal hazard levels in Rupa was plotted in form of a column chart shown in Figure 4.22.

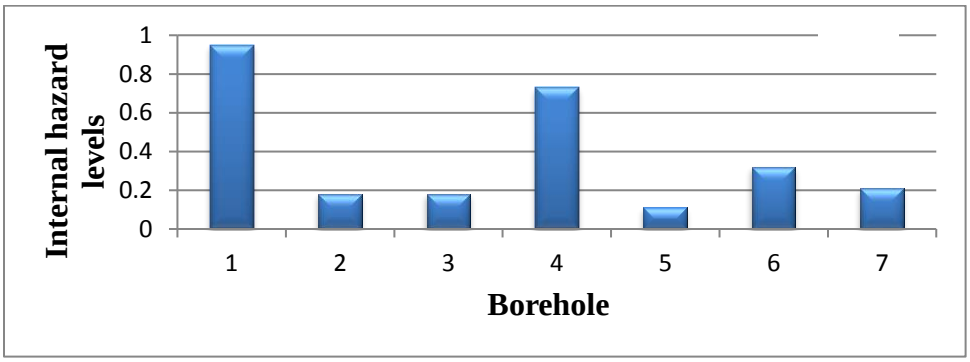

Figure 4.22: Bar graph of variation of internal hazard level by gamma rays in Rupa.

The internal hazard levels determined in Rupa were found to be below the maximum permissible value of unity as per the ICRP recommendations.

Although the internal radiological hazard levels obtained from each borehole was found to be below unity, the highest value was obtained in borehole 1 located at Rupa Primary School compared to other boreholes.

In Katikekile values varied from 1.07 to 0.13. The variation in the internal hazard level determined for each borehole was plotted in form of a bar graph as shown in Figure 4.23.

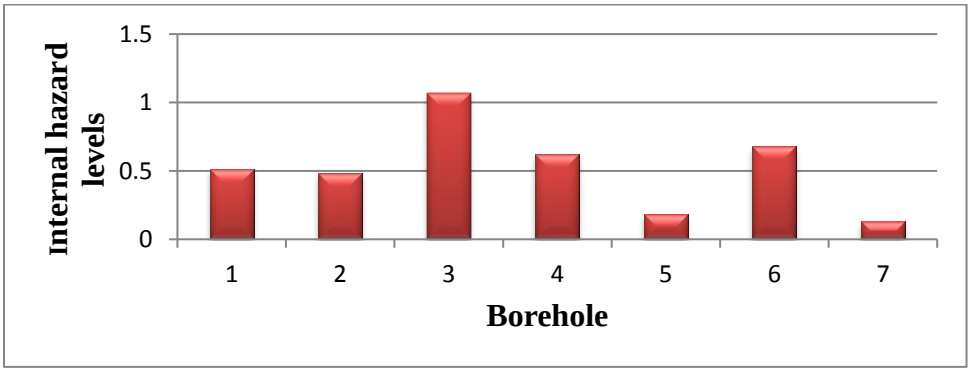

Figure 4.23: Bar graph of variation of internal hazard level by gamma rays in Katikekile.

The internal hazard levels determined in Katikekile were found to be below unity except in borehole 3 located at Lia Primary School that exceeded unity by 0.07.

Internal hazard levels in Nadunget varied from 1.33 to 0.35 and its variation was plotted in form of a bar graph as shown in Figure 4.24.

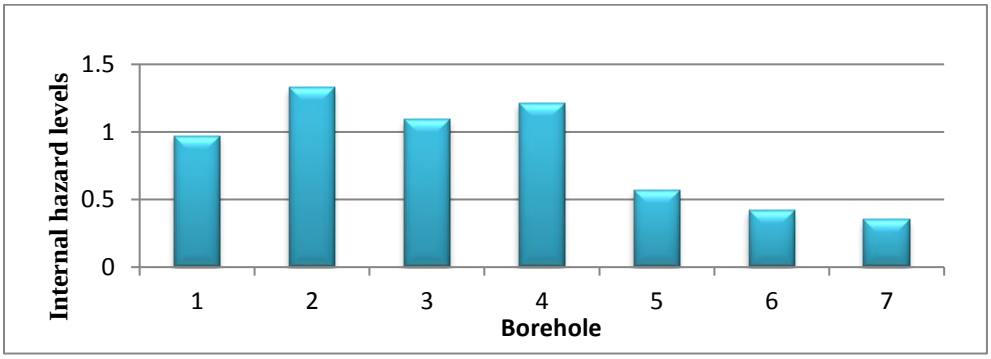

Figure 4.24: Bar graph of variation of internal hazard level by gamma rays in Nadunget.

From the graph above the internal radiological hazard levels were found to be above unity the maximum permissible value according to the ICRP recommendations in boreholes 2, 3 and 4 located at Kanakomol, Natinyonoit and Naitakwae Primary School. This means that the water samples from Kanakomol, Natinyonoit and Naitakwae are not radiologically safe for human consumption. Its consumption may cause any health risk to the populace.

In Northern Division internal hazard level ranged from 0.54 to 0.09. The variation of internal hazard level determined for each borehole was carried out using a column chart shown in Figure 4.25.

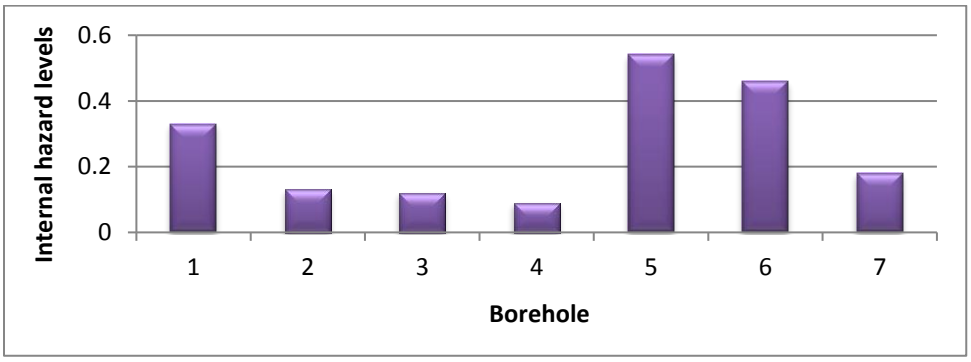

Figure 4.25: Bar graph of internal hazard level by gamma rays in Northern division.

The internal radiological hazard levels were found to be below unity the maximum permissible value as per the ICRP recommendations in all the boreholes. Although the internal radiological hazard levels were found to be below unity, it was found to be highest in boreholes 5 located at Moroto Referral Hospital.

The average internal hazard level was found to be different across the four regions. The variation of the average internal hazard level across the four regions was plotted in form of a bar graph as in Figure 4.26.

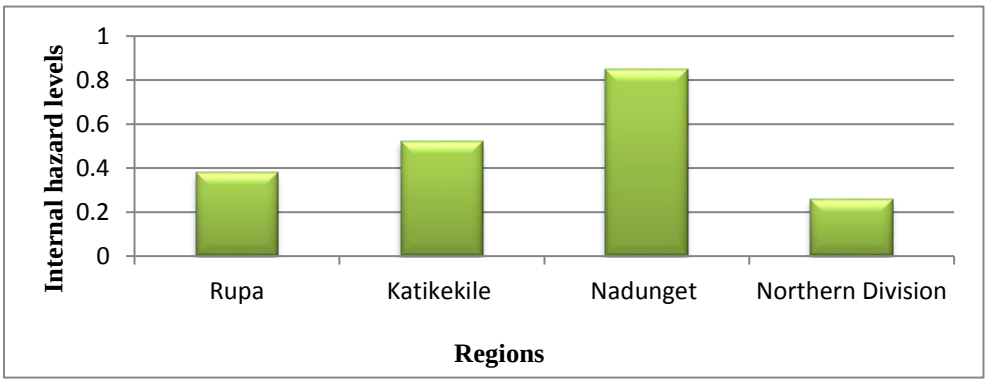

Figure 4.26: Bar graph of the average internal hazard level in the four regions.

The average internal hazard level was found to be high in Nadunget compared to the other three regions. This could be due to the high activity concentration of the radionuclides of

^{226}Ra, ^{232}Th and ^{40}K in this region. The high activity concentrations are as a result of high accumulation of dissolved radioactive minerals in underground water.

4.6.2 External radiological hazard levels by gamma rays in water samples

The external hazard levels by gamma rays determined from radionuclides detected in the water samples from each borehole in the four regions are shown in Table 4.7.

Table 4.7: External hazard levels by gamma rays in the four Regions.

Borehole	**External hazard level;H_{ex}**			
	Rupa	**Katikekile**	**Nadunget**	**Northern Division**
1	0.75	0.27	0.87	0.18
2	0.10	0.38	1.12	0.07
3	0.10	1.00	0.94	0.06
4	0.80	0.46	0.97	0.05
5	0.06	0.10	0.32	0.32
6	0.17	0.39	0.25	0.26
7	0.12	0.08	0.38	0.10
Average	**0.30**	**0.38**	**0.69**	**0.15**

The external hazard level obtained in Rupa for each borehole ranged from 0.80 to 0.06. The variation of the external hazard level determined for each borehole was plotted in form of a bar graph as shown in Figure 4.27.

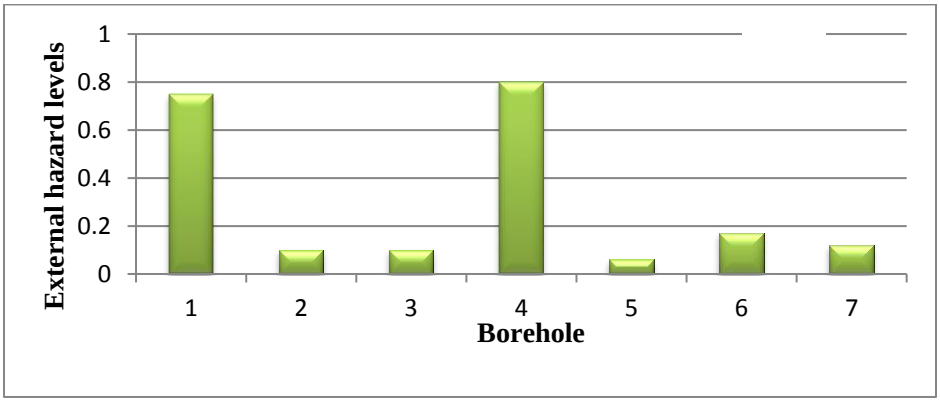

Figure 4.27: Bar graph of variation of external hazard level by gamma rays in Rupa.

The external radiological hazard levels obtained for each borehole was found to be below the maximum permissible value of unity according to the recommendations of the ICRP.

However high hazard levels were obtained from boreholes 4 and 1 located at Musupo and Rupa Primary Schools as compared to other boreholes.

In Katikekile external hazard levels varied from 1.00 to 0.08. The variation of the external hazard level determined for each borehole was carried out using a column chart shown in Figure 4.28.

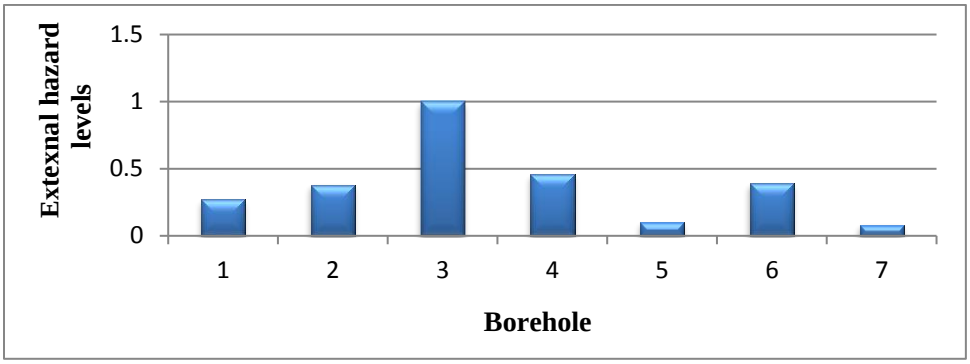

Figure 4.28: Bar graph of variation of external hazard level by gamma rays in Katikekile.

The external radiological hazard levels obtained for each borehole did not exceed the maximum permissible value of unity according to the recommendations of the ICRP.

External hazard levels obtained from each borehole in Nadundet was found to vary from 1.12 to 0.25. The variation of the internal hazard levels was plotted as a column bar chart shown in Figure 4.29

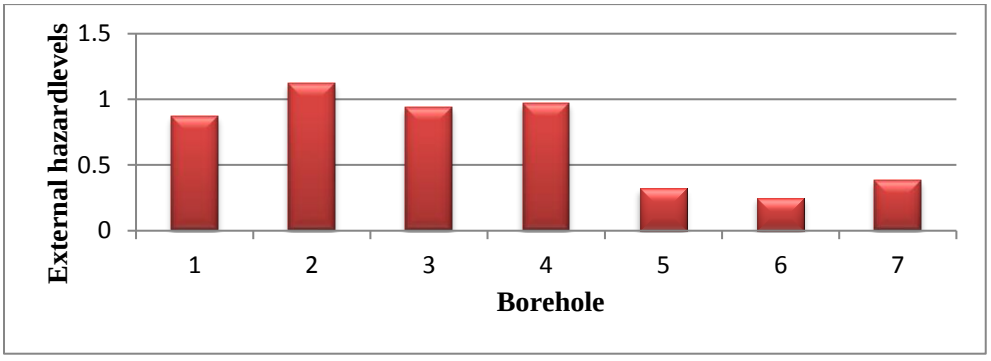

Figure 4.29: Bar graph of variation of external hazard level by gamma rays in Nadundet.

The external radiological hazard levels obtained for each borehole as in Figure 4.29 was found to be below unity the maximum permissible value according to the recommendations of the ICRP except in borehole 2 located at Kanakomol that exceeded unity by 0.12. This means that the water from Kanakomol obtained for the study in Nadunget was not radiologically safe for human consumption. Its consumption may cause any health risk to the populace.

In Northern Division external hazard level ranged from 0.32 to 0.05 as obtained in each borehole.

The variation of the external hazard level determined for each borehole in Northern Division was plotted in form of a bar graph as shown in Figure 4.30.

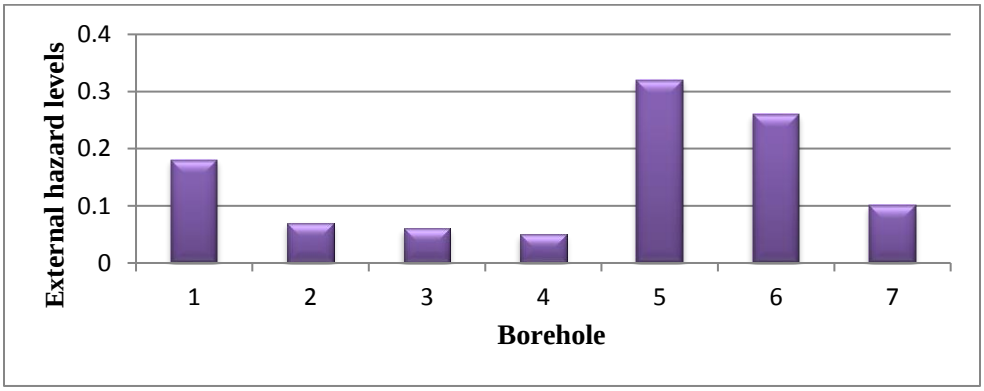

Figure 4.30: Bar graph of external hazard level by gamma rays in Northern Division.

The external radiological hazard levels were obtained for each sample and was found to be below unity in all boreholes water samples.

The average external hazard level was found to be different across the four regions. The variation of the average external hazard level across the four regions was plotted in form of a bar graph as in Figure 4.31.

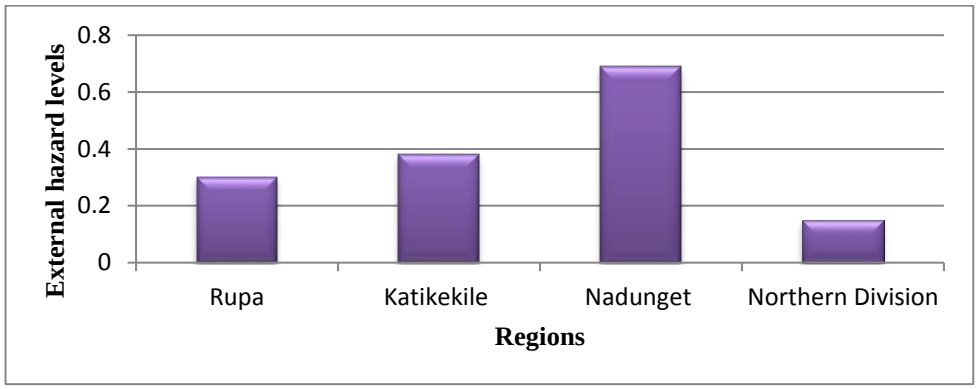

Figure 4.31: Bar graph of the average external hazard level in the four regions.

The average external hazard level was found to be high in Nadunget compared to the other three regions.

CHAPTER FIVE: DISCUSSION, CONCLUSIONS AND RECOMMENDATIONS

5.1 Introduction

The study has basically come up with findings about the gamma ray emitting radionuclides present in the water samples, activity concentrations of the radionuclides, absorbed dose rates, annual effective dose equivalent and internal and external radiological hazard levels. The findings of the study have also been compared with the world wide average activity concentrations of the radionuclides, worldwide average absorbed dose rates, worldwide internal exposure limits and maximum permissible value of unity. Possible conclusions and recommendations have also been drawn.

5.2 Discussion

The gamma ray emitting radionuclides detected in water samples includes ^{238}U (^{226}Ra; ^{214}Pb), ^{232}Th (^{228}Th; ^{212}Pb; ^{208}Tl), ^{60}Co; ^{40}K, ^{214}Bi and ^{152}Eu. In Rupa sub county ^{152}Eu was not detected in water samples from all the boreholes while the other radionuclides were detected. In Katikekile sub county ^{214}Bi and ^{152}Eu were not detected. In Nadunget sub county ^{152}Eu was not detected in all the boreholes while in Northern Division ^{214}Bi, ^{60}Co and ^{40}K was not detected in all boreholes. The rocks that host the different radioactive mineral ores were not uniformly distributed in the area under the study.

The activity concentrations of ^{226}Ra, ^{232}Th and ^{40}K detected in the water samples varied from one borehole to another. In Rupa the presence of ^{226}Ra was found in all the boreholes although the activity concentration was found to be varying. As from the results of the study the activity concentration of ^{226}Ra in Rupa for the seven boreholes were found to be different. This could probably be due to the fact that the boreholes 1, 4 and 6 located at Rupa Primary School, Musupo Primary School and Namogorat were found on the slopes of mount Moroto where the rocks had high accumulation of radioactive minerals that had dissolved in underground borehole water. The activity concentration of ^{226}Ra was found to exceed the world wide average value of 35 Bql^{-1} (UNSCEAR, 2000) in these boreholes. In Katikekile sub county the presence of ^{226}Ra was found in all the boreholes although the activity concentration was found to be varying. The activity concentration of ^{226}Ra was found to exceed the world average value of 35 Bql^{-1} in boreholes 1, 2, 4 and 6 located at

Makalas, Morutomei, Lomunyembe and Lomunyen. These boreholes were found on the slopes of the mountain which had high accumulation of dissolved radioactive minerals. Drilling of boreholes on the slopes of mount Moroto may not be safe since the activity concentrations of ^{226}Ra detected from water samples collected from boreholes on the slopes of the mountain are high. In Nadunget the presence of ^{226}Ra was found in all the boreholes although the activity concentration was varying. The activity concentration of ^{226}Ra was found to exceed the world wide average value of 35 Bql^{-1} in all boreholes that were selected for the study. The soils and rocks in the region contain more soluble deposits of ^{226}Ra when compared to other regions. The boreholes in this region are found on flat low lands. In Northern Division the presence of ^{226}Ra was found in all the boreholes although the activity concentration was found to be varying. The activity concentration of ^{226}Ra was found to exceed the world wide average value in boreholes 1, 5 and 6 located at Moroto High School, Moroto Referral Hospital and Moroto Primary Teachers College. The variation in the activity concentration of ^{226}Ra in water samples from selected boreholes in the four regions may be due to the differences in the geology of rocks and soils in the areas where the study was carried out.

The presence of ^{232}Th was found in all the boreholes selected for the study in Rupa, Katikekile, Nadunget and Northern Division although the activity concentration was found to be varying. The activity concentration of ^{232}Th that was detected in all the boreholes from the four regions under the study was found to be below the world wide average value of 30 Bql^{-1}. The soils and rocks found in the area under study did not have high accumulation of soluble compounds of ^{232}Th. The activity concentration of ^{232}Th in water samples was also found to be lower compared to ^{226}Ra because compounds of ^{226}Ra are more soluble than those of ^{232}Th (International Commission on Radiological Protection; ICRP, 1987). High values of activity concentrations of Thorium were detected in boreholes located at Rupa Primary School and Musupo Primary School in Rupa sub county and Lomunyen in Katikekile that are also found on the slopes of the mount Moroto. Drilling of boreholes on the slopes of mount Moroto may not be safe since the activity concentrations of ^{232}Th detected from water samples collected from boreholes on the slopes of the mountain are high. In Nadunget activity concentration of ^{232}Th was found to be high in boreholes located at Naitakwae Primary School and Namijimij even though it

was below the world wide average value. The rocks in these areas had high accumulation of ^{232}Th. These boreholes were located on flat low land. In Northern Division activity concentrations of ^{232}Th obtained did not exceed the world wide average values in all boreholes but was found to be high in the borehole located at Moroto Referral Hospital. This could be due to poor disposal of radioactive wastes used in the hospital that could leach in to underground water.

The presence of ^{40}K was not detected in all the boreholes that were selected for the study in Rupa, Katikekile, Nadunget and Northern Division. The activity concentration of ^{40}K measured in water samples from boreholes was found to exceed the world wide average value of 400 Bql^{-1} in the three sub counties of Rupa, Katikekile and Nadunget. This could probably be due to the fact that the rocks in the three regions had high accumulation of ^{40}K. In Rupa ^{40}K was detected in boreholes located at Rupa Primary School and Musupo Primary School. In Katikekile ^{40}K was detected in boreholes located at Morutomei, Lia Primary School and Lomunyembe. In Nadunget ^{40}K was detected in boreholes located at Katanga, Kanakomol, Naitakwae and Nangorit. In Northern Division ^{40}K was not detected in all the boreholes. The presence of ^{40}K was thus not as wide spread as was the case of ^{226}Ra and ^{232}Th in the water samples in the four different regions. However the activity concentrations of ^{226}Ra, ^{232}Th and ^{40}K were found to be below the maximum or critical permissible activity concentrations of 370 Bql^{-1}, 259 Bql^{-1} and 4810 Bql^{-1} respectively in all the boreholes.

The absorbed dose rates by gamma rays in the water samples from the four regions of Rupa, Katikekile, Nadunget and Northern Division were found to vary from one borehole to the other and the average absorbed dose rate was also found to be different across the regions. The world population mean absorbed dose rate is 84 nGyh^{-1} (UNSCEAR, 2000). In Rupa the boreholes located at Rupa Primary School and Musupo Primary School were found to exceed the world average value of 84 nGyh^{-1}. In Katikekile the boreholes located at Morutomei, Lia Primary School, Lomunyembe and Lomunyen were found to exceed the world average value of 84 nGyh^{-1}. In Nadunget the selected boreholes in the region were found to exceed the world average value of 84 nGyh^{-1} except the borehole located at Namijimij that did not exceed the world average value. In Northern Division the boreholes located at Moroto Referral Hospital and Moroto Primary Teachers College were found to

exceed the world average value. The high absorbed dose rates in these boreholes may be due to the presence of Radon a decay product of ^{238}U (^{226}Ra) emanating from underground (Tchokossa et al., 2011).

The annual effective dose equivalent by gamma rays obtained in the study for both children and adults in the water samples from selected boreholes in the four regions of Rupa, Katikekile, Nadunget and Northern Division were found to be below the world wide internal exposure limit of 0.41 $mSvy^{-1}$ and the maximum permissible limit of 1 $mSvy^{-1}$ (UNSCEAR, 2000) for the members of the public in all the boreholes. This could be due to the variation of activity concentrations of the three radionuclides that were detected.

The internal radiological hazard levels by gamma rays from water samples in Rupa and Northern Division were found to be below unity, the maximum permissible value as per the ICRP. In Katikekile and Nadunget the internal hazard levels were also found to be below unity except for the case of boreholes located at Lia Primary School, Kanakomol, Natinyonoit and Naitakwae Primary School that were found to be 1.07, 1.33, 1.09 and 1.21 respectively. This could be due to the high activity concentrations of the radionuclides detected in borehole water samples from these areas. This suggests that internal exposure from radionuclides detected from such water samples may pose serious radiological health hazard to the members of the general public. Hence consumption of water from boreholes located at Lia Primary School, Kanakomol, Natinyonoit and Naitakwae Primary School may cause a health risk to the populace compared to water from the other boreholes.

The external radiological hazard levels of gamma rays from water samples from Rupa, Katikekile and Northern Division were found to be lower than unity except borehole located at Lia Primary School where the external hazard level was exactly unity. This suggest that external exposure from radionuclides detected in water samples from the three regions of Rupa and Northern Division may not pose serious radiological hazards to the members of the general public. In Katikekile and Nadunget sub counties the external hazard levels in water samples from selected boreholes were found to be below unity except in the borehole located at Lia Primary School and Kanakomol where the external hazard levels were exactly unity and greater than unity by 0.12 respectively. The water

from boreholes located at Lia Primary School and Kanakomol may cause a health risk to the consuming populace.

5.3 Conclusions

The activity concentrations of ^{226}Ra, ^{232}Th and ^{40}K were found to exceed the world average values of 35 Bql^{-1}, 30 Bql^{-1} and 400 Bql^{-1} respectively in some boreholes. The areas where such boreholes are located should be classified as High Background Radiation areas.

The internal radiological hazard levels by gamma rays exceeded the maximum permissible limit of unity in boreholes located at Lia Primary School in Katikekile sub county; Kanakomol, Natinyonoit and Naitakwae Primary School in Nadunget sub county. The external radiological hazard levels exceeded unity in Kanakomol borehole and was exactly unity in the borehole located at Lia Primary School. The water from these particular boreholes may pose serious radiological health risks to the members of the general public. These boreholes are thus recommended to be closed and alternative water sources such as piped water and rain water harvesting technologies be provided. Although water obtain from some boreholes in Rupa sub county and Northern Division had high absorbed dose rates greater than 84 $nGyh^{-1}$ the world average value, internal and external radiological hazard levels were found to be below unity hence water from these two sub counties is thus safe. The radiological hazard levels of gamma radiations are different from one borehole to another. The pattern of the variation of the radiological hazard levels is also found to be different from one region to another.

5.4 Recommendations

Based on the results of this study it is recommended that, Ministry of Health should carry out an epidemiological study in this study area to determine the radiological excess life time cancer risk at a later stage of the populace that consume the water.

The scope of the study should be widened to more boreholes in order to obtain first level data of radionuclide water contamination in Moroto District.

A similar study should be carried out in the area to check the results obtained in this study about the radiological hazard levels of gamma ray emitting radionuclides to the populace

that consume the water especially in Katikekile and Nadunget where the radiological hazard levels were found to be greater than permissible limit of unity in some boreholes.

Atomic Energy Council should determine the background radiation emissions in the area where the study was carried out and develops relevant radiation safety guidelines and enforce these radiation safety guidelines.

REFERENCES

.

1. Abbady, A. G., Uosif, M. A. M., & El-Taher, A, (2005). Natural radioactivity and dose assessment for phosphate rocks from Wadi El-Mashash and El-Mahamid Mines, Egypt. *Journal of Environmental radioactivity, 65-78.*

2. Alnour, I. A., Wagiran, H., Ibrahim, N., Laili, Z., Omar, M., Hamzah, S., & Idi, B. Y, (2012). *Natural radioactivity measurements in the granite rock of quarry sites, Johor, Malaysia. Radiation Physics and Chemistry, 1842-1847.*

3. Asaba, R. B., Fagan, G., Kabonesa, C., & Mugumya, F, (2014). Women and Access to Water in Rural Uganda: A Review. *H_2O: The Journal of Gender and Water, 4-23.*

4. Awodugba, A. O., & Tchokossa, P, (2008). *Assessment of Radionuclide Concentrations in Water Supply from Bore-Holes in Ogbomosoland, Western Nigeria*. *Indoor and Built Environment, 183-186.*

5. Ayodele, A. E., Arogunjo, A. M., Ajisafe, J. I., & Arije, O. T, (2017). Radioactivity level of dug well water across selected cities in two states of Nigeria. *The Journal of Environmental forensics, 331-338.*

6. Baguma, Z, (2009). Status of Radioactive Elements in Uganda. Department of Geological Survey and Mines. *Technical Meeting on Uranium from Unconventional Resources, Vienna Austria, 11-17.*

7. Bartram, J., Brocklehurst, C., Fisher, M. B., Luyendijk, R., Hossain, R., Wardlaw, T., & Gordon, B, (2014). Global monitoring of water supply and sanitation: history, methods and future challenges. *International journal of environmental research and public health, 8137-8165.*

8. Beghian, L. E., Kegel, G. H. R., & Scharenberg, R. P, (1958). *Fast Sodium Iodide Spectrometer and Its Application to Mill microsecond Time Measurement*. *Review of Scientific Instruments, 753-757.*

9. Bergstrom Jr, P. M., Surić, T., Pisk, K., & Pratt, R. H, (1993). *Compton scattering of photons from bound electrons: full relativistic independent-particle-approximation calculations. Physical Review A, 1134-1141.*

10. Bleise, A., Danesi, P. R., & Burkart, W, (2003). Properties, use and health effects of depleted uranium (DU): a general overview. *Journal of environmental radioactivity, 93-112.*

11. Candia, J, (2015). *Radiological hazard levels by gamma ray emitting radionuclides in natural water bodies in selected sub counties of Mubende district in Uganda, 38-61.*

12. Desideri, D., Meli, M. A., Feduzi, L., Roselli, C., Rongoni, A., & Saetta, D, (2007). 238U, 234U, 226Ra, 210Po concentrations of bottled mineral waters in Italy and their dose contribution. *Journal of Environmental Radioactivity, 86-97.*

13. Directorate of Water Development, Ministry of Water and Environment, (2017). *Distribution of boreholes in Moroto District, 237-239.*

14. El-Gamal, H., & El-Mageed, A. I. A, (2014). Natural radioactivity in water samples from Assiut City, Egypt. *Journal of Environmental radioactivity, 44-49.*

15. El-Gamal, H., Sefelnasr, A., & Salaheldin, G, (2019). *Determination of Natural Radionuclides for Water Resources on the West Bank of the Nile River, Assiut Governorate, Egypt. Water, 311-328.*

16. Environmental Protection Agency, (1999). *Federal Guidance Report Number, 86-110.*

17. Faanu, A., Adukpo, O. K., Tettey-Larbi, L., Lawluvi, H., Kpeglo, D. O., Darko, E.O., & Efa, A. O, (2016). *Natural radioactivity levels in soils, rocks and water at a mining concession of Perseus gold mine and surrounding towns in Central Region of Ghana. SpringerPlus, 98-106.*

18. Faanu, A., Darko E. O., and Ephraim J. H, (2011). Determination of Natural Radioactivity and Hazard in Soil, Rock, waste and tailing samples in a mining area in Ghana. *West African Journal of Applied Ecology, 78-82.*

19. Fagan, G. Honor. Linnane, Suzanne, McGuigan, Kevin, G., and Rugumayo, Albert, I, (2002). *Water is life, Progress to secure safe water provision in rural Uganda, 1-14.*

20. Fakeha, F., Quadri, S. S., Ghouse, M., & Asia, T, (2014). *Radionuclide contamination of underground water sources in western province of Saudi Arabia, Case Report. International Journal of Pure and Applied Sciences and Technology, 44-59.*

21. Filippelli, G. M, (2011). *Phosphate rock formation and marine phosphorus geochemistry: the deep time perspective*. *Chemosphere, 759-766.*

22. Firestone, R. B., Shirley, V. S., CD, S. F. C., & Baglin, C. M, (1996). *Table of Isotopes, 263-272.*

23. Focazio, M. J., Szabo, Z., Kraemer, T. F., Mullin, A. H., Barringer, T. H., & DePaul, V. T, (2001). Occurrence of selected radionuclides in ground water used for drinking water in the United States: A targeted reconnaissance survey, 1998. *US Geological Survey Water-Resources Investigations Report 00-4273. Reston, VA: US Geological Survey, US Department of the Interior, 218-222.*

24. Government of Uganda, Ministry of water and Environment, (2010). *Sustaining Natural Resources in a Changing Environment, 68-82.*

25. Grasty, R. L., & LaMarre, J. R, (2004). The annual effective dose from natural sources of ionising radiation in Canada. *The Journal of Radiation Protection Dosimetry, 215-226.*

26. Hamzah, Z., Saat, A., Omar, M., Wood, A. K. & Alias, M, (2008). An assessment of absorbed dose and radiation hazard index from natural radioactivity. *Malaysian Journal of Analytical Sciences, 195-204.*

27. Herbst, C. M, (2014). Fact Sheet on Radiation and Radiation Therapy. *Cancer Association of South Africa. Journal of Medical physics, 61-63.*

28. Ibikunle, S. B., Ajayi, O. S., & Dada, O. R, (2013). Activity Concentration Assessment of Natural Radionuclides in Borehole Water and its Radiological Impact from Akure, Nigeria. *International Journal of science and research, 2875-2879.*

29. ICRP, 72, (1996). *Age-dependent doses to members of the public from intake of radionuclides: Part 5, Compilation of Ingestion and Inhalation Dose Coefficients, Annals of the ICRP, ICRP Publication 72, Pergamon Press, Oxford, 1-91.*

30. ICRP, A, (1987). *Statement from the 1987 Como Meeting of the International Commission on Radiological Protection. Radiation Protection Dosimetry, 189-192.*

31. Ishimori, Y., Lange, K., Martin, P., Mayya, Y. S., & Phaneuf, M, (2013). *Measurement and calculation of radon releases from NORM residues, 25-38.*

32. Isinkaye, O. M., Jibiri, N. N., & Olomide, A. A, (2015). Radiological health assessment of natural radioactivity in the vicinity of Obajana cement factory, North Central Nigeria. *Journal of Medical Physics/Association of Medical Physicists of India, 52-67.*

33. Kabonesa, C. Asaba, R. B., & Fagan, G. H, (2015). Women's access to safe water and participation in community management of supply. *Water is Life: Progress to secure safe water provision in rural Uganda, Practical Action Publishing, Rugby, United Kingdom, 15-29.*

34. Kabongo I., Hinton J., Kabiswa C., Okedi J, (2014). *The Mining and Mineral sector in Karamoja region. Development opportunities and constraints, 12-16.*

35. Kimura, K., Izumikawa, T., Koyama, R., Ohnishi, T., Ohtsubo, T., Ozawa, A. & Yamaguchi, Y, (2005). *High-rate particle identification of high-energy heavy ions using a tilted electrode gas ionization chamber. Nuclear Instruments and Methods in Physics Research Section A: Accelerators, Spectrometers, Detectors and Associated Equipment, 608-614.*

36. Knoll, G. F, (1999). *Radiation Detection and Measurements*. *Third Edition, New York: John Wiley and Sons, Inc, 33-34.*

37. Kölbel, L., Kölbel, T., Maier, U., Sauter, M., Schäfer, T., & Wiegand, B, (2020). *Water–rock interactions in the Bruchsal geothermal system by U–Th series radionuclides*. *Geothermal Energy, 1-33.*

38. Kreiger, N., Kelsey, J. L., Harris, C., & Pastides, H, (1981). *Injuries to the upper extremity: patterns of occurrence. Clinics in plastic surgery, 13-19.*

39. Lesikar, B. J., Melton, R., Hare, M., Hopkins, J., & Dozier, M, (2006). *Drinking Water Problems: Radionuclides (Spanish). Texas FARMER Collection. Journal of Medical physics, 71-83.*

40. Little, M. P, (2003). Risks associated with ionizing radiation: Environmental pollution and health. *British medical bulletin, 259-275.*

41. Luckey, T. D, (2011). *Biological effects of ionizing radiation: a perspective for Japan. J Am Phys Surg, 45-63.*

42. Luo, A., Fang, H., Xia, J., & Lin, B, (2017). Mapping potentials of low-grade industrial waste heat in Northern China. *Resources, Conservation and Recycling, 335-348.*

43. Makinson, K. A, (2009). *Tissue weighting factors for radiation protection: derivation and parametric analysis, 5-13.*

44. Mallya, S. M. White, S. C., & Elsaman, R, (2012). Update on the biological effects of ionizing radiation, relative dose factors and radiation hygiene. *Australian dental journal, 2-8.*

45. Mallya, S. M., Barghan, S., & Tetradis, S, (2012). Application of cone beam computed tomography for assessment of the temporomandibular joints. *Australian dental journal, 109-118.*

46. Matolin, M., Minty, B., Nicolet, J. P., Reford, W. S., & Schetselaar, E. M, (2003). Guidelines for radioelement mapping using gamma ray spectrometry data: also as open access e-book. *International Atomic Energy Agency (IAEA) -TECDOC-1363, 179-188.*

47. Mettler Jr, F. A., Bhargavan, M., Faulkner, K., Gilley, D. B., Gray, J. E., Ibbott, G. S., & Yoshizumi, T. T, (2009). *Radiologic and nuclear medicine studies in the United States and worldwide: frequency, radiation dose, and comparison with other radiation sources—1950–2007. Radiology, 520-531.*

48. Mibei, G, (2014). *Introduction to types and classification of rocks. Geothermal Development Company, 40-51.*

49. Ministry of Energy and Mineral Development, Directorate of geological survey and mines, (2011). Distribution of Mineral Resources and Mining in the Karamoja Region of Uganda. *Journal of Science and Sustainable Development, 57-76.*

50. Montgomery, M. A., & Elimelech, M, (2007). Water and sanitation in developing countries including health in the equation. *Journal of Environmental science & technology, 17-24.*

51. Mungoma, S, (1990). *The alkaline, saline lakes of Uganda: a review. Hydrobiologia, 75-80.*

52. Nagudi, B, (2011). *Status of Geological Resources in Uganda. For the Embassy of the Republic of Korea in Uganda, 10-23.*

53. Nakalembe, C., Dempewolf, J., & Justice, C, (2017). *Agricultural land use change in Karamoja region, Uganda. Land Use Policy, 2-12.*

54. Nasiru, R, (2013). Geommetry Correction in Efficiency of NaI (Tl) Detector. Pelagia Research Library. *Advances in Applied Science Research, 400-406.*

55. National Academy of Sciences (NAS), Biological Effects of Ionizing Radiation (BEIR), (2006). *Health risks from exposure to low levels of ionizing radiation: BEIR VII, Phase 2 / Committee to Assess Health Risks from Exposure to Low Levels of Ionizing Radiation, Board on Radiation Effects, Research Division on Earth and Life Studies, National Research Council of the National Academies, 239-252.*

56. Ndontchueng, M. M., Mekongtso Nguelem, E. J., Simo, A., Njinga, R. L., & Joël, G. S. C, (2014). *Gamma emitting radionuclides in soils from selected areas in Douala-Bassa zone, littoral region of Cameroon*. *ISRN Spectroscopy, 1-8.*

57. Ngoya, J. B, (2008). *Service delivery and conflict transformation: A case study of selected sub-counties in Moroto District (Masters dissertation, Makerere University), 98.*

58. Nicolet, J. P., & Erdi-Krausz, G, (2003). Guidelines for radioelement mapping using gamma ray spectrometry data. *International Atomic Energy Agency Technical Documents (IAEA-TECDOC), 1363-1387.*

59. Nsubuga, F. N., Namutebi, E. N., & Nsubuga-Ssenfuma, M, (2014). Water resources of Uganda: an assessment and review. *Journal of Water Resource and Protection, 1297-1305.*

60. Okeyode, I. C., Jibiri, N. N., Mustapha, A. O., Makinde, V., & Akinboro, F. G, (2015). Department of Physics, Federal University of Agriculture, Abeokuta, Ogun state, Nigeria 2 Radiation and Health Physics Research Laboratory, Department of Physics, University of Ibadan, Ibadan, Nigeria. *Journal of the Nigerian Association of Mathematical Physics, 379-390.*

61. Paredes, B. L., Araújo, H. M., Froborg, F., Marangou, N., Olcina, I., Sumner, T. J. & Vacheret, A, (2018). *Response of photomultiplier tubes to xenon scintillation light. Astroparticle Physics, 56-66.*

62. Parks, J. E, (2009). *The Compton Effect-Compton Scattering and Gamma Ray Spectroscopy. Department of Physics and Astronomy, University of Tennessee, 4-5*.

63. Pring, A, (2006). Rock-Forming Minerals. Volume 4B. Framework Silicates: Silica Minerals. Feldspathoids and the Zeolites. *Geological Magazine, 557-562.*

64. Reilly, D. & Grasty, N, (1991). *Gamma-ray interactions with matter. Passive nondestructive analysis of nuclear materials, 27-42.*

65. Ruettinger, L., Taenzler, D., Musana, P., & Narcisio, B, (2011). *Water, Crisis and Climate Change in Uganda: A Policy Brief. Kampala: Adelphi, 66-69.*

66. Rugumayo, A. I., Jennings, E., Linnane, S., & Misstear, B, (2006). *Water resources in Uganda. Journal of Water Resource and Protection, 129-137.*

67. Rump, A., Eder, S., Lamkowski, A., Hermann, C., Abend, M., & Port, M, (2019). A quantitative comparison of the chemo-and radiotoxicity of uranium at different enrichment grades. *Toxicology letters, 159-168.*

68. Shamsi, D. M, (2014). *Natural Radioactivity in groundwater, rocks and sediments from some areas in the UAE: Distribution, Sources and Environmental Impact, 125-133.*

69. Tchokossa, P., Olomo, J. B., & Balogun, F. A, (2011). Assessment of radionuclide concentrations and absorbed dose from consumption of community water supplies in oil and gas producing areas in Delta State, Nigeria. *World Journal of Nuclear Science and Technology, 77-89.*

70. Turner, J. E, (2007). *Atoms, Radiation and Radiation Protection. WILEY-VCH Verlag GmbH & Co. KGaA, Weinheim, 3rd Edition, 607-623.*

71. Uganda National Bureau of Standards report, (2009). *Contamination of water Resources in Uganda, 82-96.*

72. Uganda National Bureau of Standards report, (2016). *Groundwater Resources in Urban Water Management. In Groundwater Management in Uganda, 35-59.*

73. UNICEF Joint Water Supply, & Sanitation Monitoring Programme, (2012). *Progress on drinking water and sanitation: 2012 update. World Health Organization, 1-11.*

74. United Nations Scientific Committee on Effects of Atomic Radiation (UNSCEAR), (2008). United Nations Scientific Committee on the Effects of Atomic Radiation. Sources and Effects of Ionizing Radiation. *A Report to the General Assembly with Scientific Annexes, 21-222.*

75. United Nations Scientific Committee on the Effects of Atomic Radiation, & Annex, B, (2000). Exposures from natural radiation sources. *Cosmic rays, 11-44.*

76. UNSCEAR Report, (2000). Sources and effects of ionizing radiation. *Journal of Radiological Protection, 83-102.*

77. Uosif, M. A. M., Tammam, M., Issa, S. A., & Elsaman, R, (2012). Naturally Occurring Radionuclides in Sludge samples from some Egyptian Drinking water Purification Stations. *International Journal of Advanced Science and Technology, 69-82.*

78. Westfall, C, (2019). From Desire to Data: How JLab's Experimental Program Evolved Part 3: From Experimental Plans to Concrete Reality, JLab Gears Up for Research, mid-1990 through 1997. *Physics in Perspective, 108-159.*

79. WHO, (2011). *Guidelines for drinking-water quality. World Health Organization, 303-364.*

80. WHO/UNICEF, (2014). Joint Water Supply, & Sanitation Monitoring Programme*Progress on drinking water and sanitation update*. *World Health Organization, 12-21*.

81. World Water Assessment Programme (United Nations), (1999). *Water for People, Water for Life: A Joint Report by the Twenty-three UN Agencies Concerned with Freshwater*. *Unesco, 103-114.*

82. World Water Assessment Programme (United Nations), (2006). *Water: A shared responsibility, Berghahn Books, 2-33*.

83. Xiang, W., Griffin, W. L., Jie, C., Pinyun, H., & Xiang, L. I, (2011). U and Th contents and Th/U ratios of zircon in felsic and mafic magmatic rocks: *Improved zircon-melt distribution coefficients. Acta Geologica Sinica-English Edition, 164-174.*

84. Yusoff, A. H., & Mohamed, C. A. R, (2016). Mini review uranium-thorium decay series in the marine environment of the southern South China Sea. *Journal of Geophysics, 2-5.*

85. Zamora, M. L., Tracy, B. L., Zielinski, J. M., Meyerhof, D. P., & Moss, M. A, (1998). *Chronic ingestion of uranium in drinking water: a study of kidney bio effects in humans*. *Toxicological Sciences, 68-77.*

APPENDICES

APPENDIX A

BASIC DATA FOR WATER SAMPLES.

RUPA SUB COUNTY

Sample	Prominent Photo peaks	Centroid energy /keV	SD	FWHM /keV	Sum btn markers /keV	Time /s	Rate /s^{-1}	Radio-nuclide	Activity levels /Bql^{-1}
A_1	1	86.86	6.25	14.70	225	1511	0.1490	^{232}Th(Th-228)	10.57
	2	188.33	7.64	17.94	233	1511	0.1540	^{238}U(Ra-226)	72.64
	3	235.59	8.22	19.32	204	1511	0.1349	^{232}Th(Pb-212)	4.50
	4	280.65	8.45	19.85	210	1511	0.1390	^{238}U(Pb-214)	11.90
	5	498.19	10.74	41.74	484	1511	0.3200	^{232}Th(Tl-208)	64.27
	6	619.35	16.38	38.49	107	1511	0.0710	^{235}U(Bi-214)	6.86
	7	1410.33	10.84	25.41	04	1511	0.0025	^{40}K	2170
A_2	1	86.20	6.66	15.64	94	1511	0.0619	^{232}Th(Th-228)	4.21
	2	158.88	5.88	13.81	108	1511	0.0716	^{238}U(Ra-226)	32.41
	3	229.21	0.05	11.34	35	1511	0.0231	^{232}Th(Pb-212)	0.74
	4	317.93	4.55	10.70	36	1511	0.0240	^{238}U(Pb-214)	1.56
	5	911.99	7.28	17.10	19	1511	0.0123	^{60} Co	1.20
A_3	1	154.32	6.95	16.34	93	1511	0.06171	^{238}U(Ra-226)	29.29
	2	192.42	6.29	14.78	75	1511	0.0495	^{232}Th(Pb-212)	1.66
	3	232.62	10.90	25.63	112	1511	0.07418	^{232}Th(Pb-212)	2.49
	4	291.89	6.43	15.10	67	1511	0.0446	^{238}U(Pb-214)	3.84
	5	495.94	12.29	28.87	87	1511	0.0579	^{232}Th(Tl-208)	11.70
A_4	1	86.36	7.56	17.78	275	1511	0.1820	^{232}Th(Th-228)	12.39
	2	187.86	6.64	15.60	230	1511	0.1520	^{238}U(Ra-226)	68.81
	3	228.90	10.20	23.98	461	1511	0.23643	^{232}Th(Pb-212)	7.57
	4	238.27	16.88	39.66	538	1511	0.3561	^{238}U(Pb-214)	29.24
	5	490.37	6.18	14.51	108	1511	0.0715	^{232}Th(Tl-208)	13.78
	6	503.13	15.92	37.41	195	1511	0.12893	^{232}Th(Tl-208)	24.85
	7	1418.14	7.69	17.97	03	1511	0.001755	^{40}K	1460
A_5	1	86.64	7.56	17.77	83	1511	0.0550	^{232}Th(Th-228)	3.92
	2	127.71	2.86	6.73	37	1511	0.0246	^{238}U(Ra-226)	11.65
	3	160.36	4.03	9.48	84	1511	0.0556	^{238}U(Ra-226)	26.33
	4	218.27	8.34	19.61	65	1511	0.0430	^{232} Th(Pb-212)	1.44
	5	380.75	4.19	9.85	25	1511	0.01671	^{232}Th(Tl-208)	3.37
A_6	1	88.82	6.86	16.12	209	1511	0.13801	^{238}U(Ra-226)	63.68
	2	121.58	7.82	18.38	193	1511	0.12799	^{238}U(Ra-226)	59.06
	3	159.56	5.60	13.17	139	1511	0.0920	^{238}U(Ra-226)	42.45
	4	385.61	5.56	13.07	46	1511	0.0303	^{232}Th(Tl-208)	5.95
A_7	1	88.97	6.64	15.61	101	1511	0.0668	^{238}U(Ra-226)	30.59
	2	121.98	8.85	20.79	116	1511	0.0768	^{238}U(Ra-226)	35.17
	3	155.56	7.30	17.15	124	1511	0.0818	^{238}U(Ra-226)	37.46
	4	392.41	10.18	23.92	57	1511	0.0375	^{232}Th(Tl-208)	7.31

Note: SD = Standard Deviation

FWHM = Full Width at Half Maximum

KATIKEKILE SUB COUNTY

Sample	Prominent Photo peaks	Centroid energy /keV	SD	FWHM /keV	Sum btn markers /keV	Time /s	Rate /s^{-1}	Radio-nuclide	Activity levels /Bql^{-1}
B_1	1	97.46	7.20	20.43	497	1511	0.3290	^{238}U(Ra-226)	152.41
	2	121.33	8.06	18.95	264	1511	0.1750	^{238}U(Ra-226)	81.07
	3	161.74	4.50	10.57	109	1511	0.0720	^{238}U(Ra-226)	33.35
	4	218.70	18.99	44.63	378	1511	0.2503	^{232}Th(Pb-212)	8.20
	5	491.37	14.61	34.33	187	1511	0.1238	^{238}U(Pb-214)	8.23
B_2	1	86.19	6.55	15.39	147	1511	0.0965	^{232}Th(Th-228)	6.80
	2	118.82	7.95	18.68	135	1511	0.0896	^{238}U(Ra-226)	42.01
	3	158.09	7.05	16.57	98	1511	0.0647	^{238}U(Ra-226)	30.34
	4	235.17	8.11	19.05	71	1511	0.0473	^{232}Th(Pb-212)	1.57
	5	401.81	10.31	24.23	70	1511	0.0466	^{232} Th(Tl-208)	9.34
	6	963.95	5.31	12.49	25	1511	0.0164	^{60} Co	1.65
	7	1415.99	4.06	9.55	02	1511	0.0014	^{40} K	1210
B_3	1	127.50	2.43	5.71	83	1511	0.0547	^{238}U(Ra-226)	26.33
	2	233.18	6.63	15.58	94	1511	0.0620	^{232}Th(Pb-212)	2.11
	3	279.69	7.31	17.18	72	1511	0.0475	^{238}U(Pb-214)	4.15
	4	375.01	5.09	11.96	47	1511	0.0312	^{238}U(Pb-214)	2.15
	5	479.30	6.55	15.39	60	1511	0.0396	^{232}Th(Tl-208)	8.11
	6	1070.89	3.05	7.16	16	1511	0.0104	^{60} Co	1.08
	7	1553.26	2.93	6.89	07	1511	0.00493	^{40} K	4360
B_4	1	87.18	7.12	16.74	204	1511	0.1350	^{232}Th(Th-228)	9.28
	2	119.91	7.98	18.74	198	1511	0.1310	^{238}U(Ra-226)	59.89
	3	156.18	6.65	15.62	202	1511	0.1340	^{238}U(Ra-226)	61.26
	4	193.95	10.19	23.94	153	1511	0.1013	^{232}Th(Pb-212)	3.27
	5	234.28	11.31	26.58	193	1511	0.1280	^{232}Th(Pb-212)	4.14
	6	487.64	9.56	22.47	107	1511	0.0710	^{232} Th(Tl-208)	13.82
	7	1414.08	8.64	20.31	02	1511	0.0015	^{40} K	1260
B_5	1	87.66	6.00	14.10	149	1511	0.0984	^{232}Th(Th-228)	6.74
	2	119.34	9.15	21.49	139	1511	0.0921	^{238}U(Ra-226)	41.96
	3	156.64	5.46	12.82	82	1511	0.0543	^{238}U(Ra-226)	24.74
	4	186.05	4.66	24.21	54	1511	0.0359	^{238}U(Ra-226)	16.35
	5	271.54	4.68	10.99	39	1511	0.0257	^{238}U(Pb-214)	2.12
	6	374.69	5.42	12.74	51	1511	0.0339	^{232} Th(Tl-208)	6.57
B_6	1	88.29	7.32	17.19	319	1511	0.2110	^{238}U(Ra-226)	95.65
	2	119.91	9.08	21.33	416	1511	0.2750	^{238}U(Ra-226)	124.67
	3	153.89	8.17	19.21	346	1511	0.2290	^{238}U(Ra-226)	103.81
	4	227.80	9.82	23.07	310	1511	0.2049	^{232}Th(Pb-212)	6.57
	5	484.23	11.03	25.92	345	1511	0.2280	^{232} Th(Tl-208)	44.00
B_7	1	89.33	3.69	8.68	65	1511	0.0432	^{238}U(Ra-226)	19.60
	2	113.60	4.16	9.76	68	1511	0.0452	^{238}U(Ra-226)	20.48
	3	159.14	5.16	12.13	74	1511	0.0493	^{238}U(Ra-226)	22.33
	4	207.45	0.01	15.74	42	1511	0.0278	^{232}Th(Pb-212)	0.89
	5	392.60	6.48	15.23	66	1511	0.0438	^{232}Th(Tl-208)	8.46
	6	478.45	4.00	9.39	53	1511	0.0351	^{232} Th(Tl-208)	6.77

Note: SD = Standard Deviation

FWHM = Full Width at Half Maximum

NADUNGET SUB COUNTY

Sample	Prominent Photo peaks	Centroid energy /keV	SD	FWHM /keV	Sum btn markers /keV	Time /s	Rate /s^{-1}	Radio-nuclide	Activity levels /Bql^{-1}
C_1	1	91.60	5.86	13.77	123	1511	0.0813	^{238}U(Ra-226)	37.95
	2	157.39	8.86	20.39	123	1511	0.0813	^{238}U(Ra-226)	37.95
	3	230.55	0.53	10.80	65	1511	0.0433	^{232}Th(Pb-212)	1.43
	4	278.95	9.86	23.16	54	1511	0.0357	^{238}U(Pb-214)	3.02
	5	1574.42	6.13	14.41	06	1511	0.0043	^{40} K	3670
C_2	1	87.01	6.53	15.34	146	1511	0.0965	^{232}Th(Th-228)	7.61
	2	121.20	7.39	17.37	249	1511	0.1650	^{238}U(Ra-226)	86.52
	3	156.22	7.34	17.24	184	1511	0.1220	^{238}U(Ra-226)	63.97
	4	405.23	9.23	21.78	97	1511	0.0639	^{232}Th(Tl-208)	14.27
	5	491.81	18.94	44.51	181	1511	0.1200	^{232} Th(Tl-208)	26.79
	6	1188.83	4.63	10.89	06	1511	0.0043	^{40} K	4120
C_3	1	120.18	8.07	18.97	154	1511	0.1020	^{238}U(Ra-226)	43.31
	2	185.33	15.07	35.41	252	1511	0.1670	^{238}U(Ra-226)	70.91
	3	379.87	12.72	29.89	83	1511	0.0550	^{232}Th(Tl-208)	9.94
	4	495.53	9.33	21.92	69	1511	0.0458	^{232}Th(Tl-208)	8.28
	5	1476.29	4.04	9.5	07	1511	0.00463	^{40} K	3610
C_4	1	86.22	6.92	16.27	249	1511	0.1650	^{232}Th(Th-228)	11.04
	2	122.29	26.01	61.11	294	1511	0.1945	^{238}U(Ra-226)	86.58
	3	393.50	8.5	19.98	86	1511	0.0566	^{232}Th(Tl-208)	10.73
	4	499.01	4.80	48.87	408	1511	0.2700	^{232}Th(Tl-208)	51.16
	5	1170.17	6.57	15.43	22	1511	0.0148	^{60} Co	1.42
	6	1257.12	4.01	9.42	06	1511	0.0038	^{40} K	3110
C_5	1	86.78	6.91	16.24	296	1511	0.1961	^{232}Th(Th-228)	13.61
	2	119.20	8.39	19.71	366	1511	0.2420	^{238}U(Ra-226)	111.73
	3	154.83	7.78	18.28	239	1511	0.1580	^{238}U(Ra-226)	72.95
	4	191.70	7.73	18.17	157	1511	0.1041	^{232}Th(Pb-212)	3.40
	5	235.78	9.29	21.83	296	1511	0.1960	^{232}Th(Pb-212)	6.40
	6	494.96	14.13	33.20	379	1511	0.2510	^{232}Th(Tl-208)	49.34
	7	366.26	19.07	44.81	151	1511	0.1000	^{232} Th(Tl-208)	19.66
	8	326.75	14.72	34.58	115	1511	0.0763	^{235}U(Bi-214)	7.21
C_6	1	85.92	6.55	15.38	251	1511	0.1660	^{232}Th(Th-228)	11.43
	2	120.67	8.32	19.54	221	1511	0.1465	^{238}U(Ra-226)	67.08
	3	155.62	9.02	21.19	190	1511	0.1258	^{238}U(Ra-226)	57.60
	4	230.25	6.30	14.8	190	1511	0.1260	^{232}Th(Pb-212)	4.08
	5	278.36	7.43	17.45	281	1511	0.1861	^{238}U(Pb-214)	15.46
	6	390.26	15.38	36.14	243	1511	0.1610	^{232}Th(Tl-208)	31.39
	7	484.91	9.48	22.28	267	1511	0.1770	^{232}Th(Tl-208)	34.51
C_7	1	88.87	5.66	13.29	187	1511	0.1240	^{238}U(Ra-226)	58.26
	2	118.70	7.12	16.72	180	1511	0.1190	^{238}U(Ra-226)	55.91
	3	154.14	8.04	18.89	169	1511	0.1120	^{238}U(Ra-226)	52.62
	4	204.16	9.72	22.85	175	1511	0.1160	^{232}Th(Pb-212)	3.85
	5	481.64	13.25	31.13	171	1511	0.1130	^{232}Th(Tl-208)	22.60
	6	1237.10	4.20	9.87	02	1511	0.0010	^{40} K	863.00

Note: SD = Standard Deviation

FWHM = Full Width at Half Maximum

NORTHERN DIVISION

Sample	Prominent Photo peaks	Centroid energy /keV	SD	FWHM /keV	Sum btn markers /keV	Time /s	Rate /s^{-1}	Radio-nuclide	Activity levels /Bql^{-1}
D_1	1	86.30	6.45	15.16	142	1511	0.0940	^{232}Th(Th-228)	6.37
	2	120.06	7.53	17.69	186	1511	0.1231	^{238}U(Ra-226)	55.51
	3	230.47	9.99	23.49	200	1511	0.1324	^{232}Th(Pb-212)	4.22
	4	277.89	9.66	22.69	97	1511	0.0642	^{238}U(Pb-214)	11.97
	5	499.09	16.37	38.47	171	1511	0.1134	^{232}Th(Tl-208)	21.77
	6	666.99	9.67	22.72	35	1511	0.0225	^{152}Eu	1.47
D_2	1	120.63	7.19	16.88	97	1511	0.0641	^{238}U(Ra-226)	29.96
	2	157.84	4.68	11.01	67	1511	0.0443	^{238}U(Ra-226)	20.71
	3	184.51	4.12	9.68	41	1511	0.0273	^{238}U(Ra-226)	12.76
	4	230.44	8.06	18.94	71	1511	0.0466	^{232}Th(Pb-212)	1.54
	5	390.78	7.19	16.90	38	1511	0.0248	^{232}Th(Tl-208)	4.94
D_3	1	127.74	3.28	7.70	70	1511	0.0459	^{238}U(Ra-226)	21.64
	2	155.66	5.07	11.91	51	1511	0.0342	^{238}U(Ra-226)	16.13
	3	229.54	4.17	9.80	89	1511	0.0590	^{232}Th(Pb-212)	1.97
	4	383.20	10.30	24.21	44	1511	0.0289	^{232}Th(Tl-208)	5.80
	5	475.44	5.05	11.87	20	1511	0.0132	^{232}Th(Tl-208)	2.65
D_4	1	91.60	3.11	7.31	68	1511	0.0447	^{238}U(Ra-226)	21.06
	2	127.70	3.43	8.81	28	1511	0.0187	^{238}U(Ra-226)	8.81
	3	233.84	0.03	10.09	17	1511	0.0108	^{232}Th(Pb-212)	0.36
	4	397.58	6.95	16.34	39	1511	0.0260	^{232}Th(Tl-208)	5.22
D_5	1	88.13	6.96	16.36	242	1511	0.1613	^{238}U(Ra-226)	73.86
	2	118.85	8.52	20.02	322	1511	0.2128	^{238}U(Ra-226)	97.40
	3	153.95	8.08	18.98	233	1511	0.1543	^{238}U(Ra-226)	70.63
	4	235.38	9.50	22.32	396	1511	0.2622	^{232}Th(Pb-212)	8.49
	5	497.82	5.96	37.50	358	1511	0.2369	^{232}Th(Tl-208)	46.58
D_6	1	89.74	7.83	18.40	237	1511	0.1570	^{238}U(Ra-226)	72.02
	2	119.44	8.34	19.60	261	1511	0.1730	^{238}U(Ra-226)	79.35
	3	157.20	6.79	15.95	224	1511	0.1480	^{238}U(Ra-226)	67.89
	4	196.16	4.92	11.57	76	1511	0.0499	^{232}Th(Pb-212)	1.62
	5	227.15	7.31	17.17	178	1511	0.1181	^{232}Th(Pb-212)	3.83
	6	306.80	12.53	29.44	177	1511	0.1171	^{238}U(Pb-214)	7.69
	7	491.28	16.52	38.83	345	1511	0.2280	^{232}Th(Tl-208)	44.53
D_7	1	90.60	5.36	12.60	150	1511	0.0993	^{238}U(Ra-226)	40.45
	2	119.19	8.69	20.41	113	1511	0.0748	^{238}U(Ra-226)	30.48
	3	162.68	3.63	8.54	74	1511	0.0493	^{238}U(Ra-226)	20.05
	4	197.96	6.42	15.08	80	1511	0.0528	^{232}Th(Pb-212)	1.52
	5	231.99	5.15	12.11	56	1511	0.0368	^{232}Th(Pb-212)	1.06
	6	275.32	8.62	20.24	130	1511	0.0860	^{238}U(Pb-214)	6.35
	7	480.91	12.24	28.77	90	1511	0.0593	^{232}Th(Tl-208)	10.28

Note: SD = Standard Deviation

FWHM = Full Width at Half Maximum

APPENDIX B

EFFECTIVE DOSE EQUIVALENT CONVERSION FACTORS

Radionuclide	Conversion factor/mSvBq^{-1}	
	Children	Adults
^{226}Ra	6.2×10^{-7}	2.8×10^{-7}
^{232}Th	3.5×10^{-7}	2.3×10^{-7}
^{40}K	2.1×10^{-8}	6.2×10^{-9}

MASS OF WATER SAMPLES

Borehole	Mass/kg (± 0.0001)
A_1	0.4930
A_2	0.5137
A_3	0.4900
A_4	0.5137
A_5	0.4910
A_6	0.5040
A_7	0.5078
B_1	0.5020
B_2	0.4960
B_3	0.4832
B_4	0.5087
B_5	0.5105
B_6	0.5130
B_7	0.5030
C_1	0.4982
C_2	0.4435
C_3	0.5477
C_4	0.5225
C_5	0.5037
C_6	0.5078
C_7	0.4950
D_1	0.5157
D_2	0.4975
D_3	0.4932
D_4	0.4935
D_5	0.5080
D_6	0.5070
D_7	0.5710